

Spring 5-9-2016

# Chiral capillary electrophoresis-mass spectrometry: developments and applications of novel glucopyranoside molecular micelles

yijin liu  
*Georgia State University*

Follow this and additional works at: [https://scholarworks.gsu.edu/chemistry\\_diss](https://scholarworks.gsu.edu/chemistry_diss)

---

## Recommended Citation

liu, yijin, "Chiral capillary electrophoresis-mass spectrometry: developments and applications of novel glucopyranoside molecular micelles." Dissertation, Georgia State University, 2016.  
[https://scholarworks.gsu.edu/chemistry\\_diss/120](https://scholarworks.gsu.edu/chemistry_diss/120)

This Dissertation is brought to you for free and open access by the Department of Chemistry at ScholarWorks @ Georgia State University. It has been accepted for inclusion in Chemistry Dissertations by an authorized administrator of ScholarWorks @ Georgia State University. For more information, please contact [scholarworks@gsu.edu](mailto:scholarworks@gsu.edu).

CHIRAL CAPILLARY ELECTROPHORESIS-MASS SPECTROMETRY: DEVELOPMENTS  
AND APPLICATIONS OF NOVEL GLUCOPYRANOSIDE MOLECULAR MICELLES

by

YIJIN LIU

Under the Direction of Dr. Shahab A. Shamsi

by

YIJIN LIU

Under the Direction of Dr. Shahab A. Shamsi

## ABSTRACT

Micellar electrokinetic chromatography (MEKC), one of the major capillary electrophoresis (CE) modes, has been interfaced to mass spectrometry (MS) to provide high sensitivity and selectivity for analysis of chiral compounds. The research in this dissertation presents the development of novel polymeric glucopyranoside based molecular micelles ( $M_0M_s$ ) (aka. polymeric surfactants) and their application in chiral MEKC-MS.

Chapter 1 is a review of chiral CE-MS - in the period 2010-2015. In this chapter, the fundamental of chiral CE and CE-MS is illustrated and the recent developments of chiral selectors and their applications in chiral EKC-MS, CEC-MS and MEKC-MS are discussed in details.

Chapter 2 introduces the development of a novel polymeric  $\alpha$ -D-glucopyranoside based surfactants, *n*-alkyl- $\alpha$ -D-glucopyranoside 4,6-hydrogen phosphate, sodium salt. In this chapter, polymeric  $\alpha$ -D-glucopyranoside-based surfactants with different chain length and head groups have been successfully synthesized, characterized and applied as compatible chiral selector in MEKC-ESI-MS/MS. or the enantioseparation of ephedrines and  $\beta$ -blockers.

Chapter 3 continues to describe the employment of polymeric glucopyranoside based surfactants as chiral selector in MEKC-MS/MS. The polymeric  $\beta$ -D-glucopyranoside based surfactants, containing charged head groups such as *n*-alkyl  $\beta$ -D-glucopyranoside 4,6-hydrogen phosphate, sodium salt and *n*-alkyl  $\beta$ -D-glucopyranoside 6-hydrogen sulfate, monosodium salt were able to enantioseparate 21 cationic drugs and 8 binaphthyl atropisomers (BAIs) in MEKC-MS/MS, which promises to open up the possibility of turning an analytical technique into high throughput screening of chiral compounds. Physicochemical properties and enantioseparation capability of polymeric  $\beta$ -D-glucopyranoside based surfactants with different head groups and

chain lengths were compared. Moreover, the comparison of polymeric  $\alpha$ - and  $\beta$ -D-glucopyranoside 4,6-hydrogen phosphate, sodium salt were further explored with regard to enantioseparations of ephedrine alkaloids and b-blockers. The concept of multiplex chiral MEKC-MS for high throughput quantitation is demonstrated for the first time in scientific literature.

INDEX WORDS: Mass spectrometry, Micellar electrokinetic chromatography (MEKC), Chiral molecular micelles, glucopyranoside surfactants, Capillary electrophoresis-Mass spectrometry (CE-MS), Chiral separation

CHIRAL CAPILLARY ELECTROPHORESIS-MASS SPECTROMETRY: DEVELOPMENTS  
AND APPLICATIONS OF NOVEL GLUCOPYRANOSIDE MOLECULAR MICELLES

by

YIJIN LIU

A Dissertation Submitted in Partial Fulfillment of the Requirements for the Degree of

Doctor of Philosophy

in the College of Arts and Sciences

Georgia State University

2016

Copyright by

Yijin Liu

2016

CHIRAL CAPILLARY ELECTROPHORESIS-MASS SPECTROMETRY: DEVELOPMENTS  
AND APPLICATIONS OF NOVEL GLUCOPYRANOSIDE MOLECULAR MICELLES

by

YIJIN LIU

Committee Chair: Shahab A. Shamsi

Committee: Gangli Wang

Peng G. Wang

Electronic Version Approved:

Office of Graduate Studies



College of Arts and Sciences

Georgia State University

May 2016

## ACKNOWLEDGEMENTS

I would like to sincerely thank my advisor Dr. Shahab A. Shamsi for his thought advice and patient guidance in the past five years. Without him, I could never have achieved anything in my research. I would also like to thank my dissertation committee member, Dr. Gangli Wang and Dr. Peng Wang, for their kindness and patience. Moreover, I owe many thanks to all my colleagues over the years, namely, Dr. Jun He, Dr. Will Bragg, Dr. Xiaochun Wang, Yang Lu, and Ferdoushi Akter. It has been a great pleasure working with them. I'm also grateful for the financial support to carry out my research from the fellowship provided by Molecular Basis of Disease Foundation.

Finally, I would like to express my appreciations to all my family members. Without their love and encourage, none of this would have been possible.

## TABLE OF CONTENTS

ACKNOWLEDGEMENTS.....	v
LIST OF TABLES.....	viii
LIST OF FIGURES.....	ix
<b>Chapter 1.</b> Chiral Capillary Electrophoresis-Mass Spectrometry: Developments and Application in the Period 2010-2015.....	1
1.1 Introduction.....	2
1.2 Separation principles.....	7
1.3 Chiral selectors used in CE-MS.....	18
1.4 Applications in biological samples.....	35
1.5 Concluding remarks.....	41
References.....	44
<b>Chapter 2.</b> Synthesis, characterization and application of polymeric <i>n</i> -alkyl $\alpha$ -D-glucopyranoside surfactants for enantioseparation in micellar electrokinetic chromatography-tandem mass spectrometry.....	52
2.1 Introduction.....	53
2.2 Materials and methods.....	55
2.3 Results and discussion.....	62
2.4 Concluding remarks.....	75
References.....	77

**Chapter 3.** Chiral capillary electrophoresis-mass spectrometry: Turning an analytical technique into high throughput screening of chiral compounds using novel polymerized  $\beta$ -D-glucopyranoside surfactants

3.1 Introduction .....	80
3.2 Materials and methods .....	83
3.3 Result and discussion.....	89
3.4 Concluding remarks .....	114
References .....	115
APPENDICES .....	119
Appendix A. Supporting Material for Chapter 2 .....	119
Appendix B. Supporting Material for Chapter 3 .....	129

## LIST OF TABLES

<b>Table 1.1</b> Recent applications of chiral selectors in CE-MS from 2010 to 2015.....	18
<b>Table 1.2</b> Chiral separations of five positively charged compounds and two negatively charged compounds using GMA- $\beta$ -CD-AMPS monolithic column in CEC-MS.....	31
<b>Table 1.3</b> Chiral separation of acidic and basic compounds using GMA- $\beta$ -CD-VBTA monolithic column in CECMS.....	32
<b>Table 2.1</b> Fragmentor voltage, collision energy and product ion formations for the analytes from optimization experiments using flow injection ESI-MS <sup>a)</sup> .....	61
<b>Table 2.2</b> Physicochemical properties of <i>n</i> -alkenyl- $\alpha$ -D-glucopyranoside monomers and polymers.....	63
<b>Table 3.1</b> Physicochemical properties of <i>n</i> -alkenyl $\beta$ -D-glucopyranoside monomers and polymers.....	92
<b>Table 3.2</b> Optimized molar ratio and reaction time for glycosylation reactions of $\alpha$ - and $\beta$ -SUGP.....	90
<b>Table 3.3</b> Effective mobility of $\beta$ -D sugar surfactant monomers and polymers of different head group and chain length.....	93
<b>Table 3.4</b> Effect of head group on resolution ( $R_s$ ), migration time ( $tr_2$ ), selectivity ( $\alpha$ ) and efficiency ( $N_{avg}$ ) of 25 enantiomeric compounds using poly $\beta$ - <i>n</i> -undecyl glucopyranoside surfactant pseudophases.....	97
<b>Table 3.5</b> Effect of chain length on resolution ( $R_s$ ), migration ime ( $tr_2$ ), selectivity ( $\alpha$ ) and efficiency ( $N_{avg}$ ) of enantiomeric compounds using poly $\beta$ - <i>n</i> -undecyl glucopyranoside surfactant pseudophases.....	104

## LIST OF FIGURES

- Figure 1.1** Schematic of the separation principle in chiral EKC using negatively charged cyclodextrin as chiral selector. The  $\mu_{EOF}$  is the mobility of EOF;  $\mu_{PSP}$  (complexed) is the mobility of anionic cyclodextrin complexed with the analyte;  $\mu_{PSP}(\text{free})$  is the mobility of the free form of anionic cyclodextrin;  $\mu_C$  is the mobility of the cationic chiral analyte;  $\mu_1$  is the mobility of the non-polar neutral chiral analyte;  $\mu_2$  is the mobility of the polar neutral chiral analyte;  $\mu_A$  is the mobility of the anionic chiral analyte. The detector end is positioned at the electrospray end of the mass spectrometer where the flowing sheath liquid combines the effluent from the CE capillary protruding from the nebulizer (acting as an outlet vial) to complete the electric circuit.....9
- Figure 1.2** Schematic of the separation principle in chiral MEKC using high molecular-weight molecular micelle (MOM) as a pseudostationary phase. The open five-point star, open heart and open triangle represents the free form of the enantiomer of neutral chiral analytes; the solid five-point star, solid heart and solid triangle represents the complexed form of the enantiomer of neutral chiral analytes; C, C' are the complexed and free forms of enantiomers of cationic chiral analyte, respectively; A, A' are the complexed and free forms of enantiomers of anionic chiral analyte, respectively;  $\mu_{MoM}(\text{complexed})$  is the mobility of the anionic MoM complexed with the analyte;  $\mu_{MoM}(\text{free})$  is the mobility of the free form of anionic polymeric molecular micelles.....14
- Figure 1.3** Separation mechanism in chiral CEC using open-tubular column (A), packed column (B) and monolithic column (C). A and A' represent the two enantiomers of the chiral analyte.....17
- Figure 1.4** Extracted ion electropherograms obtained from the mixture of the 8 ATS (50 mg/mL

for individual enantiomers).....22

**Figure 1.5** APPI-MS spectra of the four BNZ compounds. The inset plots of HBNZ and BNZ show the signal intensity with and without 0.5% acetone. The error bar in each plot represents  $3(\sigma)$  standard deviations.....25

**Figure 1.6** Representative electropherograms showing the comparison of CMEKC-UV versus CMEKC-APPI-MS. Experimental conditions: 120 cm\_50  $\mu$ m id fused-silica capillary; 55mM  $\text{NH}_4\text{OAc}$ , pH 8.0, with 50mM poly-L,LSULV, 15mM poly-L-SUCL; +25 kV, 20°C; analyte: 1mg/mL BNZ derivatives in 50/50 MeOH/ $\text{H}_2\text{O}$ , injected at 5 mbar, 10 s; spray chamber parameters: DGF 5 L/min; nebulizer pressure 5 psi; DGT 150°C; VT 150°C; capillary voltage 2000 V; fragmentor 80 V, gain 3; SIM at  $m/z = 195,197$ ; UV absorbance at 214 nm; sheath liquid: 5mM  $\text{NH}_4\text{OAc}$  in 50/50 MeOH/ $\text{H}_2\text{O}$ , 0.5% Acetone; flow rate 7.5 mL/min.....26

**Figure 1.7** Schematic of fritless column with the New Objective PicoClear connector. The elastomeric insert of the connector ensures that the two capillaries do not grind together when joined. The arrows, at the bottom, represent the lengths of the inlet packed portion (15 cm) and outlet packed portion (35 cm) of the fritless column (not to scale).....29

**Figure 1.8** Comparison between poly-(GMA- $\beta$ -CD-co-EDMA -co-AMPS) column (A) and poly-(AADCL-co-EDMA) column (B) for simultaneous enantioseparation of ( $\pm$ )-PEP and ( $\pm$ )-EP enantiomers. The CEC column dimensions for the poly(GMA- $\beta$ -CD-co-EDMA-co-AMPS) columns are the same as described in Figure 1. Mobile phase: 50% (v/v) ACN and 50% aqueous buffer, 5 mM  $\text{NH}_4\text{OAc}$ , 0.3% (v/v) TEA (pH 4.0). Mobile phase conditions for the AADCL column are the same as described in Figure 3. Both ( $\pm$ )-PEP and ( $\pm$ )-EP (1 mg/mL) are dissolved in 50/50 ACN/ $\text{H}_2\text{O}$  (v/v); injection, 5 kV for 3 s.....34

**Figure 1.9** CEC–ESI-MS/MS of ( $\pm$ ) PEP and ( $\pm$ ) EP with AADCL column. CEC conditions: 53 cm long column, 30 cm monolithic bed length. 0.3 kV/cm (15 kV); high pressure, 5 bar applied at inlet end of the column. Other conditions are the same as in Figure 1. The ( $\pm$ ) PEP and ( $\pm$ ) EP (50  $\mu$ g/mL) were injected at 5 kV for 3 s. The MRM product ions were observed at  $m/z$  115.1 and 133.1 for ( $\pm$ ) PEP and  $m/z$  ( $\pm$ ) EP respectively; nebulizer pressure, 7 psi; drying gas flow rate, 5 L/min; drying gas temperature, 150 °C; capillary voltage, 3500 V; fragmentor, 90 V. Sheath liquid: 80/20 MeOH/H<sub>2</sub>O (v/v), 5 mM NH<sub>4</sub>OAc (pH 6.8) delivered at a flow rate of 8  $\mu$ L/min.....35

**Figure 1.10** Electropherograms obtained from studying DOPA metabolism: (A) racemic DOPA standard solution (50  $\mu$ M for each enantiomer); (B) 500  $\mu$ M racemic DOPA incubated with the culture medium for 2 h; (C) 500  $\mu$ M racemic DOPA incubated with PC-12 cells ( $2 \times 10^6$  cells/ml) for 2 h. Chiral CE–MS/MS condition were as follows: sheath liquid, 50% methanol in water containing 0.1% formic acid at 3  $\mu$ L/min; ESI spray voltage, +4 kV; capillary temperature, 220 °C; sheath gas, 20 au; auxiliary gas, 0 au.....37

**Figure 1.11** Optimized enantioseparation of WAR and its hydroxylated metabolites by CEC–ESI-MS (A–D). Conditions: 40 cm long vancomycin packed column (total long 65 cm, 375  $\mu$ m O.D. and 75  $\mu$ m I.D.). Running buffer, ACN/H<sub>2</sub>O (45/55, v/v), 10 mM NH<sub>4</sub>OAc at pH 4.0 (A) and ACN/MeOH/H<sub>2</sub>O (30/50/20, v/v/v), 10 mM NH<sub>4</sub>OAc at pH 4.0 (B). Applied voltage, +25 kV; injection, 5 kV, 3 s. Spray chamber and sheath liquid conditions nebulizer pressure: 4 psi, drying gas temp.: 200 °C, drying gas flow: 6 L/min, capillary voltage: –3000 V, fragmentor voltage, 91 V, SIM mode; sheath liquid: MeOH/H<sub>2</sub>O (80/20, v/v), 5 mM NH<sub>4</sub>OAc, pH 6.8 with flow rate of 0.5  $\mu$ L/min; and sample concentration: 10  $\mu$ g/mL in ACN/H<sub>2</sub>O (40/60, v/v).....39



**Figure 1.12** Comparison of the detection of WAR and its hydroxylated metabolites by MEKC–MS (A and C) and MEKC–MS/MS (B and D). For MEKC–MS, all the conditions are the same as in Fig.11. MEKC–MS/MS conditions: 120 cm long (375  $\mu\text{m}$  O.D. and 50  $\mu\text{m}$  I.D.) fused silica capillary. Buffer: 25 mM  $\text{NH}_4\text{OAc}$  pH 5.0, 25 mM poly-1,1-SULV with 15% (v/v) MeOH; injection: 5 mbar for 2 s; voltage: 30 kV; spray chamber parameters: drying gas temperature: 200  $^\circ\text{C}$ , drying gas flow rate: 8 L/min, nebulizer pressure: 4 psi, capillary voltage:  $-3000$  V, collision energy: 20 eV for all except 5 eV for I.S., fragmentor voltage: 125 V for all except 75 V for I.S. Sheath liquid: MeOH/ $\text{H}_2\text{O}$  (80/20, v/v) with 5 mM  $\text{NH}_4\text{OAc}$ , sheath liquid flow rate: 5  $\mu\text{L}/\text{min}$ .....39

**Figure 1.13** Total ion electrochromatograms of subject treated with O-DVX without and with indinavir therapy at 1 h and 4 h, respectively. The MEKC–MS/MS conditions: 60 cm long (375  $\mu\text{m}$  O.D., 50  $\mu\text{m}$  I.D.) fused silica capillary. Buffer: 20 mM  $\text{NH}_4\text{OAc}$  + 25 mM TEA, pH8.5, 15 mM polydipeptide surfactant. Applied voltage, +25 kV, injection, 5 mbar, 100 s. Spray chamber parameters: nebulizer pressure: 3 psi, drying gas temp.: 200 $^\circ\text{C}$ , drying gas flow: 8 L/min; capillary voltage: +3000 V; fragmentor voltage, 113 V for O-DVX and 117 V for VX; collision energy: 17 eV; MRM transition: O-DVX: 264.2  $\rightarrow$  58.1; VX: 278.2  $\rightarrow$  58.1. Sheath liquid: MeOH/ $\text{H}_2\text{O}$  (80/20, v/v), 5 mM  $\text{NH}_4\text{OAc}$ , pH 6.8 with flow rate of 0.5 mL/min; The MRM precursor to product ion transition for R-atenolol is 267.2  $\rightarrow$  145.2. The enantiomer S-O-DVX eluted first followed by the R-O-DVX. (1,1'= O-DVX). Without indinavir therapy:  $S/N_1= 118$ ,  $S/N_{1'}= 171$  at 1 h and  $S/N_1= 199$ ,  $S/N_{1'}= 210$  at 4 h. With indinavir therapy:  $S/N_1= 207$ ,  $S/N_{1'}= 210$  at 1 h and  $S/N_1= 367$ ,  $S/N_{1'}= 630$  at 4 h for S- and R-enantiomer of O-DVX, respectively.....41

**Scheme 2.1** Synthesis of poly-*n*-alkyl  $\alpha$ -D-glucopyranoside 4,6-hydrogen phosphate, sodium salt ( $\alpha$ -SUGP) and poly-*n*-alkyl  $\alpha$ -D-glucopyranoside 6-hydrogen sulfate, monosodium salt ( $\alpha$ -SUGS).....57

**Figure 2.1** Comparison of ESI-MS signal of dansylated phenylalanine (DNS-PA) obtained by direct infusion positive ion ESI-MS in the presence of (A) no surfactant, (B) 50 mM unpolymerized *n*-undecenyl  $\alpha$ -D-glucopyranoside 4,6-hydrogen phosphate, sodium salt ( $\alpha$ -SUGP) salts, and (C) 50 mM polymeric *n*-undecyl  $\alpha$ -D-glucopyranoside 4,6-hydrogen phosphate, sodium salt (poly- $\alpha$ -SUGP).....65

**Figure 2.2** Effect of polymerization concentrations of UGP surfactant monomers on chiral *Rs* of zwitterionic compound (dansyl phenylalanine) and anionic compound (BNP) in MEKC. Conditions: Panel (A): 56 cm effective length (375  $\mu$ m O.D., 50  $\mu$ m I.D.) fused silica capillary; sample concentration: 1.0 mg/mL in MeOH/-H<sub>2</sub>O (50/50). Buffer: 12.5 mM NaH<sub>2</sub>PO<sub>4</sub> +12.5 mM Na<sub>2</sub>HPO<sub>4</sub>, pH 7.0, 45 mM poly- $\alpha$ -SUGP. Applied voltage: +20 kV, injection: 5 mbar, 10 s. Panel (B) sample concentration: 1.0 mg/mL in MeOH/H<sub>2</sub>O (50/50). Buffer: 20 mM NH<sub>4</sub>OAc, pH 10.8, 15 mM poly- $\alpha$ -SUGP. Conditions for applied voltage, injection and capillary dimensions are the same as panel A. Peak identification: 1 = *R*- DNS-PA, 1' = *S*-DNA-PA, 2 = *R*-BNP, 2' = *S*'-BNP ..... 66

**Figure 2.3** Comparison of MEKC-UV (A), and MEKC-MS/MS (B) for chiral separation of BNP. Conditions: (A) 56 cm effective length (375  $\mu$ m O.D., 50  $\mu$ m I.D.) fused silica capillary. BNP concentration: 1.0 mg/mL in MeOH/H<sub>2</sub>O (50/50). Buffer: 20 mM NH<sub>4</sub>OAc, pH 10.8, 15 mM poly- $\alpha$ -SUGP. Applied voltage: +20 kV, injection: 5 mbar, 10 s. The capillary dimension in (B) are the same as (A) except for 60 cm effective length fused silica capillary. BNP concentration: 0.1 mg/mL in MeOH/H<sub>2</sub>O (50/50, v/v). Spray chamber parameters: nebulizer

pressure: 3 psi; drying gas temp: 250 °C, drying gas flow rate: 6 L/min; capillary voltage: -3000 V; fragmentor voltage: 200 V, collision energy: 41 eV, MRM transition: 347.1 → 79.1. Sheath liquid: MeOH/H<sub>2</sub>O (80/20, v/v), 5 mM NH<sub>4</sub>OAc, pH 6.8 with a flow rate of 0.5 mL/min. Peak identification: *I* = *R*-BNP, *I*' = *S*'-BNP. .... 69

**Figure 2.4** Bar plots illustrating the effect of chain length and head groups of sugar surfactants on chiral *R*s of ephedrine alkaloids in MEKC-MS/MS. Conditions: 75 cm long (375 μm O.D., 50 μm I.D.) fused silica capillary. Buffer: 25 mM NH<sub>4</sub>OAc, pH 5.0, 30 mM polymeric UGP, UGS, OGP and OGS. Applied voltage, +20 kV, injection, 5 mbar, 10 s. Spray chamber and sheath liquid conditions are the same as Fig. 2.3. Sample concentration: 10 μg/mL in MeOH/H<sub>2</sub>O (10/90, v/v). (B) Bar plots illustrating the effect of chain length and head groups of sugar surfactants on chiral *R*s of β-blockers in MEKC-MS/MS. Conditions and spray chamber parameters are the same as Fig. 2.2 except 25 mM NH<sub>4</sub>OAc adjusted to pH 7.0 by NH<sub>4</sub>OH. Fragmentor voltage, collision energy and product ion formations of ephedrine and β-blockers are listed in Table 2 ..... 71

**Figure 2.5** (A) Bar plots illustrating the effect of pH on chiral *R*s of ephedrine alkaloids in MEKC-MS/MS. Buffer conditions and spray chamber parameters are the same as in Fig. 2.3 (A) except 30 mM poly-α-SUGP was used at pH 5.0, 5.5 and 6.0. (B) Bar plots illustrating the effect of pH on chiral *R*s of β-blockers in MEKC-MS/MS. Conditions and spray chamber parameters are the same as in Fig. 2.4 (B) except 30 mM poly-α-D-UGP was used in the pH range of 6.0 to 9.5. .... 73

**Figure 2.6** Electropherograms for enantioseparation of ephedrine alkaloids using sugar surfactant with optimum head group and chain length at optimum pH 5.0 in MEKC-MS/MS. Conditions and spray chamber parameters are the same as Fig.2.5 (A) except 30 mM poly-α-D-

UGP was employed. Peak identifications: 1 = (*1R,2S*)-(-)norephedrine, 1' = (*1S,2R*)-(+)-norephedrine, 2 = (*1R, 2R*) (-)pseudoephedrine, 2' = (*1S,2S*)(+) pseudoephedrine; 3 = (*1R,2S*)-(-)ephedrine, 3' = (*1S,2R*)-(+)-ephedrine; 4 = (*1R,2S*)-(-)*N*-methylephedrine, 4' = (*1S,2R*)-(+)*N*-methylephedrine ..... 75

**Figure 2.7** Electropherograms for enantioseparation of  $\beta$ -blockers using sugar surfactant with optimum head group and chain length at optimum pH 7.0 in MEKC-MS/MS. Conditions and spray chamber parameters are the same as Fig.2.5 (B) except 30 mM poly- $\alpha$ -D-UGP was employed. Peak identifications: 1,1' = atenolol, 2,2' = carteolol, 3,3' = metoprolol, 4,4' = talinolol. For each  $\beta$ -blocker the *R*-enantiomer always eluted first than *S*-enantiomer.....75

**Scheme 3.1** Synthesis scheme for poly(*n*-undecyl  $\alpha$ -D-glucopyranoside 4,6-hydrogen phosphate, sodium salt **16**) (poly- $\alpha$ -SUGP), poly(*n*-undecyl  $\beta$ -D-glucopyranoside 4,6-hydrogen phosphate, sodium salt **17**) (poly- $\beta$ -SUGP), poly(*n*-octyl  $\beta$ -D-glucopyranoside 4,6-hydrogen phosphate sodium salt **19**) (poly- $\beta$ -SOGP), poly-(*n*-undecyl  $\beta$ -D-glucopyranoside 6-hydrogen sulfate, monosodium salt **18**), (poly- $\beta$ -SUGS), poly(*n*-octyl  $\beta$ -D-glucopyranoside 6-hydrogen sulfate, monosodium salt **20**) (poly- $\beta$ -SOGS).....86

**Fig. 3.1** Plot comparing the surface tension versus concentration of monomers and polymers of (A) phosphated surfactants ( $\beta$ -SOGP and  $\beta$ -SUGP); and (B) sulfated surfactants ( $\beta$ -SOGS and  $\beta$ -SUGS).....95

**Fig. 3.2** Electropherograms comparing the effect of head group of polymeric sugar surfactants on chiral separation of atropine and homatropine in MEKC-MS/MS. Conditions: 25 mM NH<sub>4</sub>OAc, pH 5.0, using 15 mM poly- $\beta$ -SUGS (left) and poly- $\beta$ -SUGP (right). Sample

concentration: 100  $\mu\text{g/mL}$  in MeOH/H<sub>2</sub>O (10/90, v/v). Other conditions are the same as discussed in section 3.2.3.1.....101

**Fig. 3.3** Electropherograms comparing the effect of chain length of polymeric sugar surfactants on chiral separation of nadolol in MEKC-MS/MS. Conditions: 25 mM NH<sub>4</sub>OAc, pH 5.0, using 30 mM (A) poly- $\beta$ -SOGS, (B) poly- $\beta$ -SUGS, (C) poly- $\beta$ -D-SOGP and (D) poly- $\beta$ -SUGP. Sample concentration: 100  $\mu\text{g/mL}$  in MeOH/H<sub>2</sub>O (10/90, v/v). Other conditions are the same as discussed in section 3.2.3.1.....102

**Fig. 3.4** MEKC-MS of (A) 21 resolved cationic compounds and (B) 8 binaphthyl derivatives using four sugar surfactants using the optimum head group and optimum chain length of polymeric sugar surfactants. Buffer conditions: 25 mM NH<sub>4</sub>OAc was used as BGE in all separations, pH 5, 30 mM poly- $\beta$ -SUGP (A1); pH 7, 30 mM poly- $\beta$ -SUGP (A2); pH 5, 15 mM poly- $\beta$ -SUGP (A3) pH 6, 15 mM poly- $\beta$ -SUGP (A4) pH 7, 15 mM poly- $\beta$ -SUGP (A5); pH 5, 30 mM poly- $\beta$ -SUGS (C1); pH 5, 15 mM poly- $\beta$ -SUGS (C2); pH 5, 15 mM poly- $\beta$ -SOGS (D); pH 10.8 with 15 mM poly- $\beta$ -SOGP (B); pH 10.8, 15 mM poly- $\beta$ -SOGS (D2); Sample concentration: 100  $\mu\text{g/mL}$  in MeOH/H<sub>2</sub>O (10/90, v/v), Other conditions are the same as in Fig. 3.2.....110

**Fig.3.5** Bar plots showing the chiral resolution values from the chiral screening using sugar surfactant polymers with different head groups and chain lengths. The  $R_s$  values are classified as poor ( $R_s = 0$ ), fair-to-good ( $0 < R_s < 1.5$ ), and excellent ( $R_s > 1.5$ ).....112

**Fig. 3.6** Electropherograms comparing the effect of anomeric configuration of 30 mM polymeric phosphated sugar on the enantioseparation of (A-B) pseudoephedrine and (C-D) metoprolol in MEKC-MS/MS. Buffer: 25 mM NH<sub>4</sub>OAc, pH 5.0 and 7.0 for pseudoephedrine and metoprolol, respectively. Sample concentration: 100  $\mu\text{g/mL}$  in MeOH/H<sub>2</sub>O (10/90, v/v). Other conditions

are the same as Fig.2. The bar plots in (E) showing the chiral resolution values from the chiral screening using sugar surfactant polymers with different anomeric configurations. The  $R_s$  values are classified as poor ( $R_s = 0$ ), fair-to-good ( $0 < R_s < 1.5$ ), and excellent ( $R_s > 1.5$ ).....112

**Fig. 3.7** Multiplexed enantioseparation of 1, 1'-binaphthyl phosphate (BNP) using serial dilution of four discrete sample segments with concentrations of 1,1'= 100 ug/mL, 2,2' = 200 ug/mL , 3,3'= 300 ug/mL and 4,4' = 500 ug/mL (bottom electropherogram) at fixed concentration (250 ug/ml) of *R*-binaphthol as an internal standard (top electropherogram) in a single run using an optimum micelle spacer of 5mbar, 120s. Buffer: 25 mM NH<sub>4</sub>OAc, pH 5.0, 15 mM SUGS. The Fig 6 inset shows a calibration curve for a single step acquisition of four point calibration linear over the range of 100 µg/mL to 500 µg/mL. Other conditions are the same as discussed in section 3.2.3.1.....114

## **Chapter 1**

# **A Review: Chiral Capillary Electrophoresis-Mass Spectrometry: Developments and Applications in the Period 2010-2015**

The sensitive detection of chiral compounds in biological samples represents a significant challenge and is currently considered a bottleneck in many chiral analysis projects. The use of a of chiral selectors such as modified cyclodextrins (CDs) and amino acid based polymeric surfactants (a.k.a. molecular micelles, MoMs) in electrokinetic chromatography (EKC), micellar electrokinetic chromatography (MEKC) and capillary electrochromatography (CEC) have shown to be successful for various enantioseparation modes in capillary electrophoresis (CE). Chiral CE with mass spectrometry (MS) detection can largely improve the limit of detection. Therefore, in chiral CE-MS chiral compounds are not only enantioseparated with high efficiency and high chiral selectivity but also high sensitivity. In this review, major chiral CE-MS modes, separation and detection principles as well as a brief history are introduced. Next, recent developments and progress of chiral CE-MS dating from Jan. 2010 to Sep. 2015 are described. The various achievements, biomedical and clinical applications of CDs and MoMs in EKC-MS, MEKC-MS and CEC-MS are discussed. Finally, conclusions and future prospects of CE-MS in chiral analysis are drafted.

## **1.1. Introduction**

Although non-chromatographic methods (e.g., polarimetry, nuclear magnetic resonance, isotopic dilution, calorimetry and enzyme techniques) could be used for enantiomeric analysis, these methods need pure samples. Chromatographic techniques such as gas chromatography (GC), high performance liquid chromatography (HPLC), and capillary electrophoresis (CE) does not require pure samples and efficiently quantitate multiple chiral compounds. Chiral HPLC and CE have proven to be better methods than chiral GC for enantiomeric analysis of non-volatile compounds. Separation systems such as HPLC or SFC may rival or complement CE but the



options are available through numerous modes of CE [e.g., micellar electrokinetic chromatography, (MEKC) and capillary electrochromatography, (CEC)]. These modes if properly tuned provide high efficiency and resolution like capillary zone electrophoresis (CZE) and high selectivity like HPLC. Furthermore, it is much easier and cost effective to employ expensive and exotic chiral selectors (either added as pseudophase in the CE buffer or as a real stationary phase in a capillary column).

Chiral separations in CE was first performed in 1985 using ligand exchange systems [1]. Currently, chiral CE is considered equally competitive to chiral HPLC and chiral SFC techniques. However, the development of sensitive detection methodologies for CE for trace levels detection of chiral compounds is currently one of the most challenging issue in chiral CE. This is because there is a growing need to measure changes at nanomolar to picomolar levels of a parent chiral drug and its metabolites (aka. chiral metabonomics) in biological fluids and tissues for therapeutics and early disease diagnostics.

As mentioned above, despite of the attractive properties of CE, sensitivity is the critical point in chiral analysis by UV detection as it hardly meets the requirements for trace analysis of chiral compounds in biological samples due to short optical path-length of the capillary. Laser induced fluorescence might offer enhanced detection, but is limited to only few chiral compounds. Recent emergence of chiral CE-MS offer new perspectives into the analysis of chiral molecules important in human diets, drugs and diseases. Thus, the technical marriage between CE and MS particularly for sensitive and routine analysis of chiral compounds in real biological matrices could provide major breakthrough for several important reasons: (i) solve the identification problems of unknown chiral non-chromophoric or chromophoric compounds in real samples, (ii) development of modern MS, MS-MS and MS<sup>n</sup> instruments provide better

accuracy, mass resolution, structural information about the unknown metabolites of a parent drug, (iii) reduce matrix effects of biological samples when the co-migrating peaks are baseline resolved, (iv) provide high throughput for analysis of multiple chiral compounds. In addition, not only selective, sensitive and specific CE-MS schemes are needed but also high purity chiral reagents and rugged capillary columns, will provide better RSD for run-to-run and batch to batch reproducibility of chiral pseudophases and stationary phases, respectively. Multiplex capability will allow high throughput quantitation, which is very much needed to advance the field.

### **Various Modes of CE-MS**

Chiral CE-MS is a generic term and depending on format and type of chiral selectors used, the technology of CE-MS is segmented into several separation techniques. Examples of chiral CE-MS modes includes: (a) chiral capillary zone electrophoresis (CCZE)-MS; [2-4] (b) chiral electrokinetic chromatography (CEKC)-MS; [5-7] (c) chiral micellar electrokinetic chromatography (CMEKC)-MS; [8-9] and (d) capillary electrochromatography (CEC)-MS [10].

The first mode of CCZE separate enantiomeric ions based on the same principle as conventional CE upon application of applied voltage except that the volatile buffer contains chiral selectors such as native [ $\alpha$ -,  $\beta$ -,  $\gamma$ - CDs] or derivatized (dimethyl-, trimethyl-, hydroxypropyl- $\beta$ -CDs) at very low concentrations [1]. The aforementioned neutral chiral selectors, which moves at the rate of electroosmotic flow (EOF) are only useful for separation and detection of charged chiral enantiomers. It should be noted that there is no electrophoretic mobility difference between the two enantiomers, only the difference in enantioselective interactions with the chiral selector may create a difference in apparent effective mobility between complexed and the uncomplexed form of the enantiomer with the neutral chiral selectors. Because efficiencies are higher, even small difference in mobility leads to

enantioseparation. If we have a mixture of cation and anionic enantiomeric compounds then the two chiral cations with the largest charge to mass ratio ( $q/m$ ) will elute first, followed by chiral cations with reduced ratios, anions with smaller  $q/m$  and finally anions elutes with greater ratios before their ionization in the electrospray.

The CEKC-MS mode is similar to CCZE-MS except charged chiral reagents (positively and negatively charged CDs, crown ethers, macrocyclic antibiotics and proteins) now act as moving pseudostationary phase (PSP), which can be used to separate and detect both neutral and charged chiral analytes by MS. In CMEKC, unpoloymerized micelles or polymerizable charged surfactants forming molecular micelles (MoMs) are added to the volatile buffer to achieve chiral separations. Nevertheless, the general requirements for the use of neutral or charged chiral reagents for all three modes (i.e., CCZE-MS, CEKC-MS and CMEKC-MS) are: (a) sufficient solubility in the buffer without generating too much background current i.e.,  $< 50 \mu\text{m}$ ; (b) compatibility with MS detection ; (c) high molecular weight but low viscosity allowing faster elution of enantiomers and; (d) less spectral clutter do not produce interfering MS signal in  $m/z$  range of interest.

The fourth and final mode is CCEC in which retention occurs due to combination of electrophoretic and chromatographic separation principles. The three different fabrication formats of stationary phase in CCEC are: (a) packed, (b) open tubular and (c) monolithic columns. In packed column CEC, the separation capillary is homo-geneously packed with chiral particles under high pressures and frits or fritless columns can be fabricated to retain the chiral particles inside the column. In open tubular CEC, the chiral selector is chemically bonded or physically coated to the inner core of the capillary tube, whereas in monolithic format a single piece of polymerized chiral monolith is formed inside the pretreated capillary. Notably, all three

version of CCEC avoids the introduction of low molecular weight chiral selector for MS detection.

The MS coupled to CE provides not only very sensitive analysis but also structural information. Since its first successful application for chiral separation in 1995 [11], the development of chiral CE-MS has continued to expand and grow. Although the application of chiral CZE-MS and EKC-MS is still not widely used due to the interference caused by relatively large concentrations of nonvolatile chiral selectors entering the MS, considerable progress has been made to circumvent these disadvantages in the past few years through instrumentation development and interface design. Thus, hyphenation of CE to MS has been attempted with at least four interface designs: (a) sheath flowing through a triple tube nebulizer, (b) porous tip sheathless, (c) micro flow through vial, and (c) EOF driven sprayer using borosilicate glass combined with sheath flow. In addition to conventional ESI ionization source, atmospheric pressure photoionization (APPI) has been used to detect neutral chiral compounds in the gas phase. The type of mass analyzers (QTOF, TOF, ion trap, single and triple quadrupoles have been used [12-15]. Among them, sheath flow interface with electrospray ionization (ESI), and quadrupole MS have been reported for majority of enantioselective analysis.

In this review, we focused our critiques on recent developments and applications of chiral separation using chiral EKC-MS, MEKC-MS and CEC-MS from 2010 up to 2015. This review first presents the separation principle in various modes of chiral CE-MS. Next, chiral selectors used in chiral EKC-MS, chiral MEKC-MS and chiral CEC-MS are reviewed in details that cover analysis of chiral compounds important in pharmaceutical, agricultural and environmental fields. The application at low levels of chiral drugs in biological samples is discussed. Finally, the

review ends with some general concluding remarks and future prospects of these hyphenated modes for various applications related to enantiomeric analysis.

## 1.2. Chiral CE-MS

### 1.2.1 A Brief Theory of CE

The separation of different charged compounds with various charge to mass ratio in capillary zone electrophoresis (CZE) is based on the electrophoretic mobility ( $\mu_e$ ) difference under a given electric field ( $E$ ). The relationship of the solute velocity ( $v$ ) and its  $\mu_e$  can be expressed as:

$$v = \mu_e E \quad (1)$$

In CE,  $v$  can be replaced by  $l/t$ , where  $l$  is the effective capillary length,  $t$  is the migration time. Similarly,  $E$  can be replaced by  $V/L$ , where  $V$  is applied voltage and  $L$  is the total length of the capillary. Therefore, equation (1) can be described as following equation (2) to calculate experimental apparent mobility  $\mu_a$ .

$$\mu_a = lL/(tV) \quad (2)$$

### 1.2.2 Separation principles in CEKC-MS

The coupling of EKC to MS was first introduced by Schulte *et al.* for chiral separations [16]. In CEKC-MS, the enantioseparation is achieved by adding the chiral selectors (aka.PSP) into the volatile background electrolyte (BGE). The difference of enantioselective noncovalent interactions between enantiomers and chiral PSP leads to the differences in apparent electrophoretic mobility, consequently enantioseparation. In contrast to the most basic mode of

CE-MS, charged CDs, macrocyclic antibiotics or crown ethers have been used to separate both charged and neutral chiral compounds in EKC-MS. The major intermolecular interactions between analyte and chiral selector are inclusion, hydrophobic, hydrogen bonding, electrostatic and van der Waals interactions with the moving charged PSP.

Fig. 1.1 illustrates the separation principle of CEKC with anionic charged CDs. In this case, the capillary wall is negatively charged due to almost complete deprotonation of the silanol groups. The EOF, which is the major pulling force for the solute, is toward cathodic end. When the capillary is filled with a negatively charged chiral selector (e.g., sulfated- $\beta$ -CD), the mobility of PSP ( $\mu_{\text{PSP}}$ ) is typically high towards anodic end, and is fairly large because of low molecular weight. If the mobility of EOF ( $\mu_{\text{EOF}}$ ) is larger than  $\mu_{\text{PSP}}$ , the chiral selector will elute at the time  $t_{\text{PSP}}$  at the MS detection end. However, if  $\mu_{\text{EOF}}$  is smaller than  $\mu_{\text{PSP}}$ , the chiral selector will never elute at the MS end. The neutral chiral analytes partition between the PSP and the surrounding aqueous phase, depending on hydrophobicity, hydrogen bonding and van der Waals etc. Very non-polar neutral chiral analyte ( $N_1$ ) with mobility  $\mu_1$  partition into the chiral selector and will elute at or near the  $t_{\text{PSP}}$ . On the other hand, very polar neutral chiral analyte ( $N_2$ ) with mobility  $\mu_2$  stays in the surrounding phase and will co-elute with EOF or sometimes elute before EOF. Cationic chiral analyte (C) with mobility  $\mu_c$  will elute later than the neutral chiral analyte due to the strong electrostatic attraction with the negatively charged PSP. Since anionic chiral analyte (A) with mobility  $\mu_A$  has the least interaction with the negatively charged PSP, it will remain mostly in the bulk solution resulting in fastest elution.

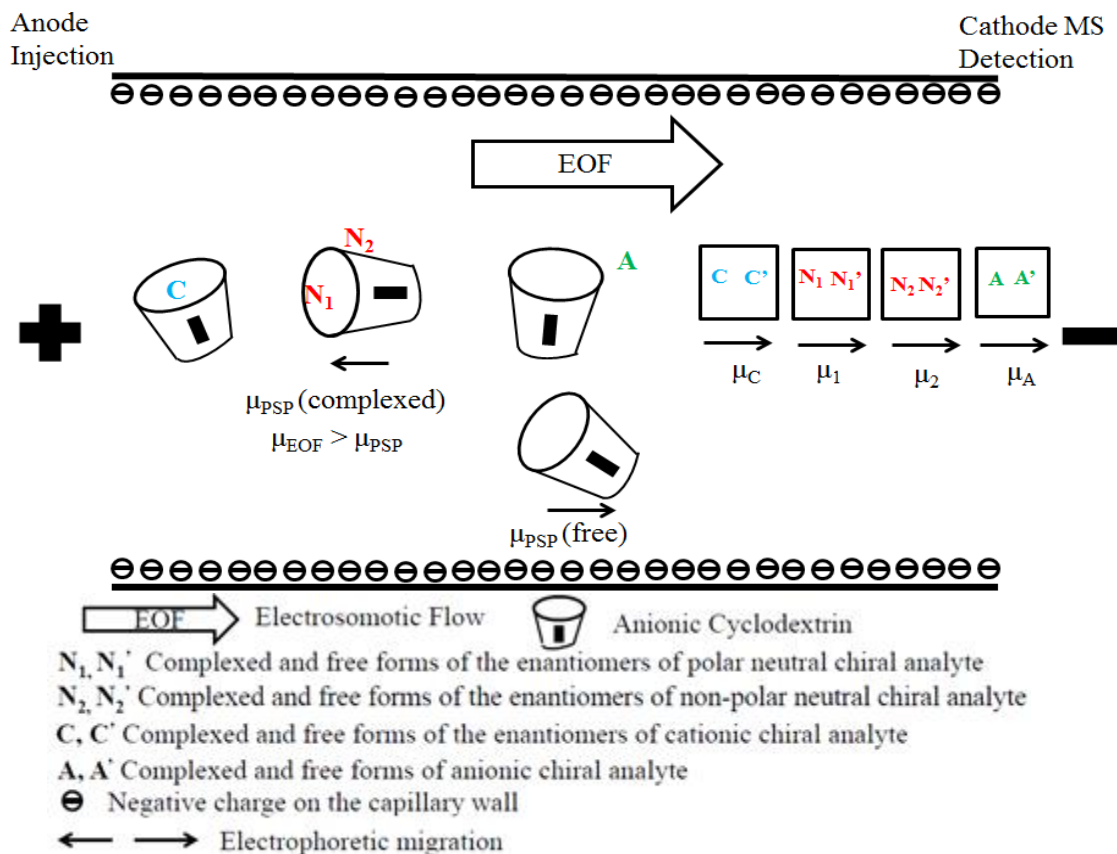


Fig.1.1 Schematic of the separation principle in chiral EKC using negatively charged cyclodextrin as chiral selector. The  $\mu_{\text{EOF}}$  is the mobility of EOF;  $\mu_{\text{PSP}}(\text{complexed})$  is the mobility of anionic cyclodextrin complexed with the analyte;  $\mu_{\text{PSP}}(\text{free})$  is the mobility of the free form of anionic cyclodextrin;  $\mu_{\text{C}}$  is the mobility of the cationic chiral analyte;  $\mu_1$  is the mobility of the non-polar neutral chiral analyte;  $\mu_2$  is the mobility of the polar neutral chiral analyte;  $\mu_{\text{A}}$  is the mobility of the anionic chiral analyte. The detector end is positioned at the electrospray end of the mass spectrometer where the flowing sheath liquid combines the effluent from the CE capillary protruding from the nebulizer (acting as a outlet vial) to complete the electric circuit.

As mentioned earlier, EKC utilizes charged chiral selector as PSP. Therefore, EKC is fundamentally a type of pseudo-chromatography and it has almost the same theory as traditional chromatography [17]. The retention factor ( $k'$ ) in CEKC is given by the following equation (3) as the moles ( $n$ ) of solutes in PSP divided by the moles of solutes ( $n$ ) in the mobile phase:

$$k' = n_{\text{psp}}/n_{\text{aq}} \quad (3)$$

The  $k'$  relates to the migration time of the analyte and PSP, which can be described by the following equation (4):

$$k' = \frac{(t_R - t_0)}{t_0 \left( 1 - \frac{t_R}{t_{PSP}} \right)} \quad (4)$$

Where  $t_R$  is the migration time of the analyte,  $t_0$  is the migration time of EOF marker,  $t_{PSP}$  is the migration time of the PSP. When the mobility of PSP is very large and is in direction opposite to EOF, i.e., when  $t_{PSP}$  is equal to infinity, equation (4) can be simplified as follows:

$$k' = \frac{(t_R - t_0)}{t_0} \quad (5)$$

In CEKC, only the difference in enantioselective interactions with the chiral selector may create a difference in apparent effective mobility, which leads to the enantioseparation. The  $R_s$  of two enantiomeric peaks in CEKC is related to selectivity ( $\alpha$ ), capacity factor ( $k'$ ) and efficiency ( $N$ ) by the following fundamental equation [18,19]:

$$R_s = \frac{\sqrt{N}}{4} \left( \frac{\alpha - 1}{\alpha} \right) \left( \frac{k_2}{1 + k_2} \right) \left( \frac{1 - t_0 / t_{PSP}}{1 + (t_0 / t_{PSP})k_1} \right) \quad (6)$$

While the first three parenthetical terms in equation (6) are the same as those expressed in conventional chromatography, the fourth parenthetical term accounts for the effect of limited



migration range, and is unique to EKC. If the mobility of anionic PSP reaches infinite, it will never elute at the cathodic end, allowing equation (6) to be modified as follows:

$$R_s = \frac{\sqrt{N}}{4} \left( \frac{\alpha - 1}{\alpha} \right) \left( \frac{k_2}{1 + k_2} \right) \quad (7)$$

When CEKC is hyphenated to MS detection, combination of volatile BGE and low concentration of chiral selector is employed. Alternatively, partial filling technique and counter current migration can be used to avoid the contamination of the ion source in ESI-MS.

### 1.2.3 Principles of CMEKC-MS

The separation mechanism of CMEKC is the same as CEKC, which is discussed in section 1.2.2 except that high molecular weight micelles (aka. molecular micelles, M<sub>0</sub>M) are used as PSP. In CMEKC, the capacity factor ( $k'$ ) can also be related to the phase ratio, which is the distribution of the enantiomers between micellar phase and the aqueous phase:

$$k' = K (V_m/V_{aq}) \quad (8)$$

where  $K$  is the distribution coefficient and  $V_m/V_{aq}$  is the phase ratio of the micellar phase over the surrounding aqueous phase. The  $V_m/V_{aq}$  ratio can be calculated by following equation (9):

$$V_m / V_{aq} = \frac{\bar{v}(C_{psp} - CMC)}{1 - \bar{v}(C_{psp} - CMC)}$$

where  $K$  is the partial specific volume of the molecular micelles and  $C_{psp}$  represents the concentration of PSP; CMC is the critical micellar concentration. Replacing the  $V_m/V_{aq}$  ratio

with equation (9), the capacity factor can be related to the micellar concentration in the following equation (10):

$$k' = K \frac{\bar{v}(C_{psp} - CMC)}{1 - \bar{v}(C_{psp} - CMC)} \quad (10)$$

Because the CMC of M<sub>o</sub>M is zero, above equation (10) can be simplified as follows:

$$k' = K \frac{\bar{v} \times C_{psp}}{1 - \bar{v} \times C_{psp}} \quad (11)$$

Since  $\bar{v}$  is a very small number, the denominator is usually negligible. For example, if  $\bar{v}$  of SDS is 0.247 L/mol and the concentration of SDS used is usually 0.1 mol/L, the denominator is 0.9753. Therefore, above equation can be described as below:

$$k' = K \times \bar{v} \times C_{psp} \quad (12)$$

Fig. 1.2 shows the separation principle of CMEKC with anionic chiral M<sub>o</sub>M. The molecular weight and the mobility of the M<sub>o</sub>M ( $\mu_{M_oM}$ ) is typically much higher compared to small molecular weight chiral selectors (e.g., charged CDs and crown ethers). Therefore, detection of  $\mu_{M_oM}$  toward cathodic end is rather difficult. When  $\mu_{EOF} \gg \mu_{M_oM}$ , the chiral M<sub>o</sub>M will finally elute but at a much longer time than a typical  $t_{mc}$  observed with unpolymerized low molecular weight chiral selectors, or the chiral M<sub>o</sub>M will never elute at the cathodic end of the capillary depending on the type of the chiral M<sub>o</sub>M used.

The very polar and hydrophilic neutral chiral analyte (★) with mobility  $\mu_1$  only interacts with the micellar surface through dipole interactions and therefore co-elute with EOF or sometimes elutes before EOF. This is followed by the moderately hydrophobic solutes (containing both polar and hydrophobic groups), which will interact at the palisade layer of the micelle (▲) and elutes with mobility  $\mu_2$ . Finally, hydrophobic neutral compounds, which do not contain any polar groups interacts with the core of the micelles (♥) and elute last with a mobility  $\mu_3$ . Thus, in CMEKC, analytes with different polarities will be separated according to the combination of dipole-dipole, hydrophobic and hydrogen bonding interactions with the M<sub>o</sub>M. Cationic chiral analyte (C<sup>+</sup>)-type containing hydrophobic and hydrogen bonding groups with mobility  $\mu_{c^+}$  will elute the very last because of the strong electrostatic binding with the negatively charged M<sub>o</sub>M. In addition, dipole-dipole interactions and hydrophobic interactions will also occur with C<sup>+</sup> type chiral analytes. The anionic chiral analyte (A<sup>-</sup>)-type with mobility  $\mu_{A^-}$  will elute faster than the moderately hydrophobic or highly hydrophobic neutral compounds and may enantioseparate only if the combined effect of hydrogen bonding and hydrophobic interactions are strong enough to overcome the electrostatic repulsions with the negatively charged M<sub>o</sub>M.



metabolites. Therefore, when CMEKC is hyphenated to MS, high molecular weight M<sub>o</sub>M having zero CMC are always considered as the best option. In addition, high concentration of organic solvent (e.g., up to 60% of methanol and 40% acetonitrile) could be used without any concerns on micellar destruction or decrease in separation selectivity of highly hydrophobic and neutral polyaromatic hydrocarbons [20]. Recent studies indicated that covalently bonded M<sub>o</sub>M can be used conveniently at concentrations as high as 50 mM without any ESI-MS signal suppression for multiple chiral separation of complex mixtures [21].

#### 1.2.4 Principles of CCEC-MS

Besides MEKC-MS, the other major CE-MS mode is CCEC-MS, which has been extensively used in the separation and detection of chiral compounds. CCEC-MS is a hybrid technique combining high selectivity of HPLC and high efficiency of CZE. There are three different types of CCEC. In open tubular (OT)-CEC-MS, a chiral stationary phase (CSP) is formed by either physically or chemically coating or bonding the chiral selector to the capillary wall. In packed column CCEC-MS, a separation capillary is slurry packed with particles using externally [22] or internally tapered [23] column or simply using a fritless column [24] with an inert packing material containing as chiral selector. In the third type of chiral CEC, a continuous rod or chiral monolith is formed inside the coated capillary by in-situ polymerization methods. Nevertheless, all of these three aforementioned formats of chiral CEC avoid the introduction of chiral selector in MS making this mode a promising technique for analysis of trace levels of chiral drugs and metabolites in biological samples.

As shown in Fig.1.3A, the EOF in coated capillaries of OT-CEC column depends strongly on the negative charges on the covalently attached bonded groups. The separation of two enantiomers A and A' occurs due to difference in distribution equilibria of the enantiomer

pair between the mobile phase and chemically bonded CSP. In packed-column CCEC, the chiral selector is bonded to a silica support which is packed into the capillary (Fig.1.1.3B). A single frit internally tapered column is packed with chiral particles and the two enantiomers A and A' are separated according to their intermolecular interactions such as  $\pi$ - $\pi$  interaction, hydrogen bonding with the chiral packing. Within monolithic capillary column, the anionic CSP forms a porous polymer network anchored to the capillary walls (Fig.1.1.3C). After the generation of EOF by the anionic crosslinked monomers of the CSP, the two enantiomers of the chiral analyte, A and A' are separated based on the combination of electrostatic, ion-pairing and hydrophobic interactions between CSP and the analytes.

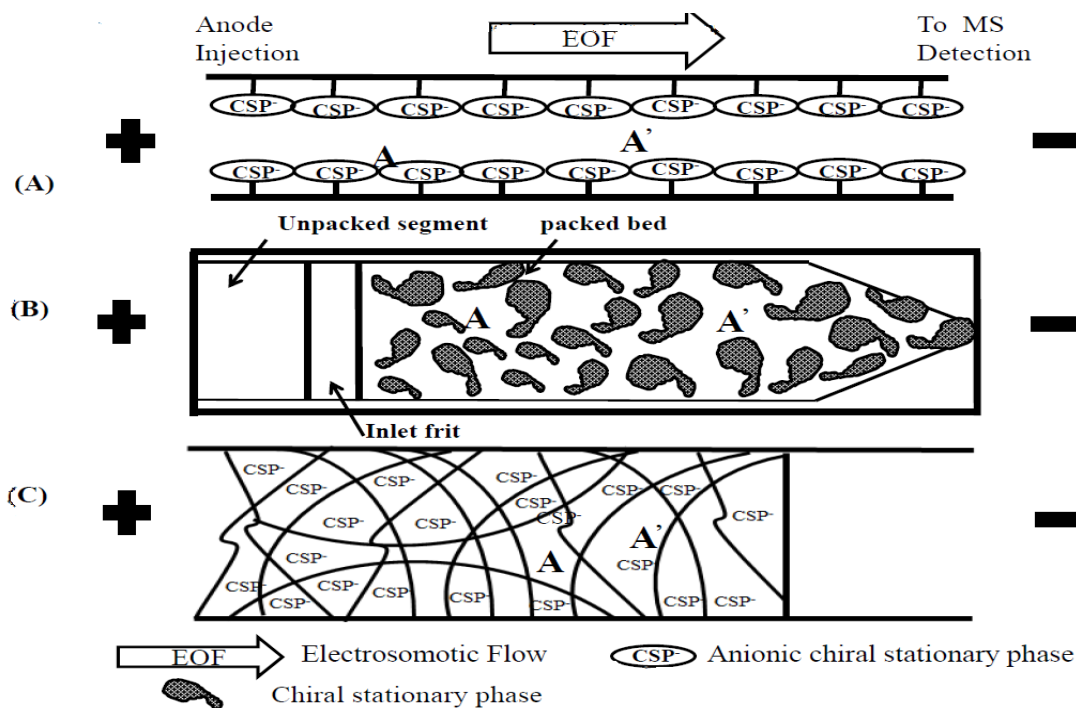


Fig.1.3 Separation mechanism in chiral CEC using open-tubular column (A), packed column (B) and monolithic column (C). A and A' represent the two enantiomers of the chiral analyte

### **1.2.5 Comparison of chiral OT-CEC-MS, packed column CEC-MS and monolithic CEC-MS**

OT-CEC columns have much simpler and less time-consuming coating procedures than packed columns but they suffer from small sample capacity and limited resolution due to the small surface area of the coating. When OT-CEC is hyphenated to MS detection, the MS source is likely to be contaminated if the coating of fused silica capillary is unstable over time. Tapered packed columns provide better enantiomeric selectivity and higher sample loading capacity compared to conventional OT-CEC. However, when such columns, in particular externally tapered column is coupled to MS, the outlet end of the CEC column exposed to the nebulizing end of the MS instrument will cause bubble formation, which results in several drawbacks such as irreproducible retention times and even current breakdown. The major advantage of monolithic CCEC is that it can be interfaced to MS easily without limitations of packing procedure and less prone to bubble formations. The main issue is to find the appropriate polymerization conditions, leading to good porosity and permeability without compromising chiral selectivity.

### **1.3. Applications of chiral selectors in CE-MS**

The applicability of chiral selectors for CE-MS in analysis of various chiral compounds was demonstrated in 15 publications in the period from Jan 2010 to July 2015. A summary of these studies listed in Table 1 provides information about the type of chiral selector and enantiomers analyzed, the type of background electrolyte and MS conditions as well as the type of capillary used. In the following sections, the applications of modes of CE-MS using the various types and formats of chiral selectors are discussed.

Table 1.1 Recent applications of chiral CE-MS from 2010 to 2015

Analyte enantiomers	chiral selector used	BGE	MS conditions	capillary used	Refs
duloxetine	(2-hydroxypropyl)- $\beta$ -CD	150 mM $\text{NH}_4\text{CO}_2\text{H}$ , pH 3.0	sheath liquid: 80:20 (v/v) MeOH/H <sub>2</sub> O with 0.1% (v/v) of HCOOH at 3.3 $\mu\text{L}/\text{min}$ . Nebulizer and the drying gas :3 psi and 5 L/min at 200 °C. ESI source in the positive ion mode at -4.5 kV with an end plate of -500 V.	fused-silica capillary	1
glutethimide, aminoglutethimide, warfarin and 2,2,2-trifluoro-1-(9-anthryl) ethanol, benzoin	CDMPC and CDMPC-SO <sub>2</sub>	70% ACN, 5 mM $\text{NH}_4\text{COOH}$ , pH 3.5	sheath liquid, MeOH/H <sub>2</sub> O (90:10, v/v) with 50 mM $\text{NH}_4\text{OAc}$ at 5.0 $\mu\text{L}/\text{min}$ ; capillary voltage, +3000 V; fragmentor voltage, 80 V; drying gas flow rate, 5 L/min; drying gas temperature, 130 °C; nebulizer pressure, 4 psi.	single inlet frit packed column	23
aminoglutethimide, derivatized methylamine and dimethylamine, Brij 30 and Brij 56 non-ionic surfactant	sulfated cellulose dimethylphenylcarbamate; mixed mode hydrophobic and anion exchange C6/SAX stationary phase; C18 stationary phase	70% ACN 5 mM $\text{NH}_4\text{CO}_2\text{H}$ , pH 3.5; 5 mM $\text{NH}_4\text{COOH}$ , pH 3.0; 80% ACN, 5 mM Tris, pH 8.0	sheath liquid : 90% MeOH 50 mM $\text{NH}_4\text{OAc}$ at 5 $\mu\text{L}/\text{min}$ . nebulizer pressure: 6 psi, drying gas flow rate: 5 L/min drying gas temperature: 250 °C.; sheath liquid: 70% MeOH 10 mM $\text{NH}_4\text{OAc}$ at 7 $\mu\text{L}/\text{min}$ . nebulizer pressure: 5 psi, drying gas flow rate: 5 L/min, drying gas temperature: 200 °C.; sheath liquid: 80% MeOH with 1 mM $\text{NH}_4\text{COOH}$ at 5 $\mu\text{L}/\text{min}$ . nebulizer pressure: 5 psi, drying gas flow rate: 5 L/min, drying gas temperature: 200 °C.	fritless packed column	24
6,7-dihydroxy-1-methyl-TIQ, 1-benzyl-TIQ, and N-methylsalsolinol	sulfated $\beta$ -cyclodextrin	20 mM acetic acid/ammonium acetate, pH 5.5	sheath liquid: 50% MeOH in H <sub>2</sub> O containing 0.1% acetic acid at 2 $\mu\text{L}/\text{min}$ ; spray voltage: 4 kV; capillary temperature: 220 °C; sheath gas: 20 au; auxiliary gas: 0 au.	fused-silica capillary	32
12 cathinone analogs	highly sulfated- $\gamma$ -cyclodextrin	50 mM phosphate, pH 2.5	source temperature: 250 °C, drying gas: 5 mL/min, nebulizer pressure: 10 psi, capillary: 3000 V, fragmentor: 125 V, skimmer: 40 V.	fused-silica capillary	33
8 cathinone derivatives	highly sulfated- $\gamma$ -cyclodextrin and (+)-(18-crown-6)-2,3,11,12-tetracarboxylic acid	0.5% formic acid	Electrospray voltage: 1.2 kV, the heated capillary of the mass spectrometer: 150 °C.	fused-silica capillary	34
8 amphetamine-type stimulants	highly sulfated- $\gamma$ -cyclodextrin	10 mM HCOOH, pH 2.5	coaxial sheath liquid: 10 mM ammonium formate-methanol (50:50, v/v) at 5 $\mu\text{L}/\text{min}$ . ESI voltage: 4.5 kV; nebulizer gas: 5.0 au; ion transfer capillary temperature : 200 °C ; voltage: 17 V.	sulfonated capillary	35
mephobarbital, pentobarbital, secobarbital	poly-L-SUCIL	25.0 mM $\text{NH}_4\text{OAc}$ , pH 7.0	Sheath liquid: 5.0 mM $\text{NH}_4\text{OAc}$ in MeOH/H <sub>2</sub> O 80:20 (v/v), 5 $\mu\text{L}/\text{min}$ . NP: 5 psi, DGF 4.0 mL/min, DGT 310 °C.	fused-silica capillary	40
Hydrobenzoin, benzoin, benzoin methyl ether, and benzoin ethyl ether	15% poly-L-SUCL and 85% of poly-L,L-SULV	40 mM $\text{NH}_4\text{OAc}$ , pH 10	Sheath liquid: 50% MeOH, 5 mM $\text{NH}_4\text{OAc}$ , 0.5% acetone at 10 $\mu\text{L}/\text{min}$ , DGF: 5.0 L/min, DGT: 100 °C, VT: 176 °C.	fused-silica capillary	44
ephedrine, pseudoephedrine, norephedrine, methylephedrine, atenolol, metoprolol, talinolol, carteolol	undecylenic $\alpha$ -D-glucopyranoside 4,6-hydrogen phosphate, sodium Salt	25.0 mM $\text{NH}_4\text{OAc}$ , pH 7.0 and 5.0	Sheath liquid: 5.0 mM $\text{NH}_4\text{OAc}$ in MeOH/H <sub>2</sub> O 80:20 (v/v), 5 $\mu\text{L}/\text{min}$ . NP: 3 psi, DGF 6.0 mL/min, DGT 200 °C.	fused-silica capillary	45
30 neutral and basic chiral compounds and two acidic compounds	glycidyl methacrylate-bonded $\beta$ -cyclodextrin	variable ACN concentration was combined with 5 mM $\text{NH}_4\text{OAc}$ containing 0.3% (v/v) TEA	sheath liquid, MeOH/H <sub>2</sub> O (80:20, v/v) containing 5 mM $\text{NH}_4\text{OAc}$ , at 5.0 $\mu\text{L}/\text{min}$ ; capillary voltage, +2000 V; drying gas flow rate, 5 L/min; drying gas temperature, 200 °C; nebulizer pressure, 5 psi.	monolithic column	51
acidic compounds (2-Phenoxypropionic Acid, 2,2-(Chlorophenoxy) propionic acid; BNP etc.	The GMA/ $\beta$ -CD-VBTA	75/25 ACN/H <sub>2</sub> O, 5 mM $\text{NH}_4\text{COOH}$ , pH 3.0	drying gas temperature, 150 °C; drying gas flow rate, 3 L/min; nebulizer pressure, 20 psi; capillary voltage, -3500 V; fragmentor voltage, 84 V	monolithic column	52
ephedrine and pseudoephedrine	poly-SAAOCL, poly-SAADCL and poly-SAADoCL	70% (v/v) ACN and 30% (v/v) aqueous buffer containing 5 mM $\text{NH}_4\text{OAc}$ , pH 5.0.	nebulizer pressure, 7 psi; drying gas flow rate, 5 L/min; drying gas temperature, 150 °C; capillary voltage, 3500 V; fragmentor, 90 V. Sheath liquid: 80/20 MeOH/H <sub>2</sub> O (v/v), 5 mM $\text{NH}_4\text{OAc}$ (pH 6.8), 8 $\mu\text{L}/\text{min}$ .	monolithic column	53
3,4-dihydroxyphenylalanine and its precursors, phenylalanine and tyrosine	sulfated $\beta$ -CD	0.2 M formic acid	sheath liquid, 50% MeOH in water containing 0.1% formic acid at 3 $\mu\text{L}/\text{min}$ ; spray voltage, 4 kV; capillary temperature, 220 °C; sheath gas, 20 au; auxiliary gas, 0 au.	fused-silica capillary	54
venlafaxine and O-desmethylvenlafaxine	poly-L,L-SULA	20 mM $\text{NH}_4\text{OAc}$ + 25 mM TEA, pH 8.5	sheath liquid: 80/20 MeOH/H <sub>2</sub> O (%v/v) containing 5 mM $\text{NH}_4\text{OAc}$ at 5 $\mu\text{L}/\text{min}$ , Capillary voltage, +3000 V, drying gas flow rate: 8.0 L/min; drying gas temperature: 200 °C; nebulizer pressure: 3 psi.	fused-silica capillary	55



### 1.3.1 Charged Cyclodextrins (CD) in CEKC-MS

Charged CDs are the most commonly used chiral selector in CEKC-MS applications. This class of chiral reagent is predominantly used in drug development, quality control, pharmacokinetic and pharmacodynamic studies owing to their remarkable enantioselectivity, special physicochemical properties and ease of commercial availability [25-29]. As mentioned earlier in section 2.2, charged CDs or their derivatives when added to the BGEs work as a PSP for the enantioseparation in EKC-MS buffers. However, introduction of even small amount of this class of nonvolatile chiral selector was reported to cause serious contamination of the ion source [30] resulting in the suppression of MS analyte signal [31]. Therefore, two different approaches such as counter-current migration (i.e., chiral selector migrating opposite to EOF) and partial filling technique (PFT) have been employed in CEKC-MS to minimize the contamination of the electrospray chamber with CDs. Both of these two approaches have shown to improve the sensitivity and the stability of the ESI-MS signal but the later technique decreases the enantioselectivity.

Wu *et al.* [32] developed a partial-filling CEKC-MS/MS method to separate and detect the enantiomers of tetrahydroisoquinoline derived neurotoxins including (*R/S*)-6,7-dihydroxy-1-methyl-TIQ (salsolinol, Sal), (*R/S*)-1-benzyl-TIQ (BTIQ), and (*R/S*)-*N*-methylsalsolinol (NMSal). Only 1.0mM sulfated  $\beta$ -CD was used as chiral selector and added to the BGE of 20 mM acetic acid/ammonium acetate at pH 5.5 to provide the 1,2,3,4-tetrahydroisoquinoline derivatives with chiral *Rs* ranging from 3 to 4.5. The resolutions reported by EKC -MS were much higher than those reported previously by HPLC methods. Moreover, the LOD of this method was only as low as 1.2 $\mu$ M for Sal enantiomers. The developed assay was successfully applied to study *in vitro* formation of NMSal, a Parkinsonian neurotoxin. The four isomers of NMSal were

separated, detected in the incubation solution and were identified as (*R*)-*e.e*-NMSal, (*R*)-*e.a*-NMSal, (*S*)-*e.e*-NMSal, and (*S*)-*e.a*-NMSal. The authors claimed this to be the first study identifying the multiple enantiomeric form of NMSal.

Recently, PFT have been effectively used in CEKC-MS especially in seized drug analysis [33]. Using 0.6% v/v highly sulfated- $\gamma$ -cyclodextrin (HS- $\gamma$ -CD) at pH 2.5, 9 out of 12 cathinone analogs were enantioseparated and detected with TOF-MS. The authors reported that the use of PFT not only successfully prevented the nonvolatile portion of the buffer from entering the MS but also greatly reduced the baseline noise on the MS by 45%. Initially, the separation parameters such as buffer pH and concentration of the chiral selector were optimized in UV detection before applying to the MS detection but the use of length of the chiral selector was optimized with CE-MS. The limit of detection as low as 1.2 ng/mL was reported for cathinone analog [( $\pm$ ) ethcathinone]. The method was validated in terms of linearity, sensitivity and limit of quantitation and was applied to the identification of methylone in seized drug samples.

In a very recent study [34], enhanced resolution was observed when 0.125 % HS- $\gamma$ -CD and 15 mM(+)-(18-crown-6)-2,3,11,12-tetracarboxylic acid (18-C-6-TCA) was investigated using an online sheathless CE/MS with low flow rates of nanoliters/minute to separate and detect eight cathinones along with their positional and optical isomers. The authors took advantage of the separation capability of both HS- $\gamma$ -CD and (+)-18-C-6-TCA to achieve the baseline enantioseparations of all cathinones derivatives except for ( $\pm$ )-4-methylethcathinone, which was partially resolved. In addition, the low flow rate (~10 nL/min) sheathless CE/MS was compared with PFT for the enantioseparations of cathinones derivatives. It was found that the relative and absolute sensitivity of detection of cathinones were almost the same in both techniques, indicating that the low flow rates CE-MS system using a sheathless interface in conjunction with

a narrow capillary (20  $\mu\text{m}$  i.d.) provides no significant suppression when HS- $\gamma$ -CD was introduced into the ESI process.

Besides PFT and sheathless CE/MS with low flow rates, chemically modified capillary can also be used to prevent the MS ion source contamination [35]. Mikuma and coworkers recently reported an EKC-MS/MS method for 8 amphetamine-type stimulants using sulfonated capillary and HS- $\gamma$ -CD as chiral selector in 10 mM formic acid at pH 2.5 in EKC-MS/MS. Fig. 1.4 shows the extracted ion electropherograms for simultaneous chiral separations of 8 amphetamine-type stimulants. Baseline separations were achieved for all enantiomers within 60 min. When chemically modified sulfonated capillary is used, the chiral selector, HS- $\gamma$ -CD counter migrates to the detector and avoided migration towards the ion source. In addition, such modified capillary also improves the repeatability of migration times with % RSD of intraday and interday to be not higher than 0.3% and 1.02 %, respectively. Although these results are excellent but a rather low number of runs were performed to truly evaluated the feasibility of run time repeatability.

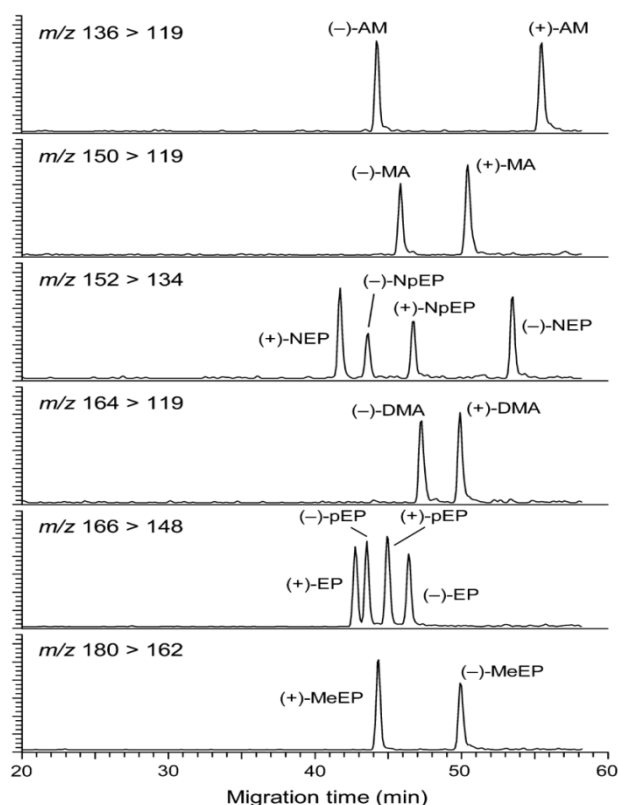


Fig.1.4 Extracted ion electropherograms obtained from the mixture of the 8 ATS (50 mg/mL for individual enantiomers). Taken from ref [35] with permission.

### 1.3.2 Molecular micelles in CMEKC-MS

Identifying novel chiral selectors providing high separation selectivity and are MS compatible has become a major effort in developing sensitive MEKC-MS approaches. High molecular mass polymeric chiral surfactants [aka. molecular micelles (MoM)] are usually beneficial for MEKC-MS because of three major advantages. First, MoMs are covalently stabilized high molecular weight micellar aggregates, which cannot be fragmented in the gas phase of ESI-MS resulting in no interference with the analyte signals. Second, MoMs are stable over a wide range of pH and are fully compatible with the use of water soluble organic solvents. Third, because of zero critical micellar concentration (CMC), very low concentration of MoMs

can be used without sacrificing the chiral  $R_s$  [36-38]. In recent years, there has been rapid growth in the development of CMEKC-MS using MoMs [39-43].

Until now, the potential applications of MEKC-MS for chiral analysis has been established mainly for the simultaneous separation and identification of various chiral pharmaceuticals and its metabolites (i.e., chiromics), interfacing to other ionization sources, search for new classes of MS compatible chiral MoMs and studies involving drug-drug interactions.

Wang and co-workers [40] developed a CMEKC-MS approach using poly sodium *N*-undecenoxy carbonyl-L-isoleucinate (poly-L-SUCIL) as a chiral selector to simultaneously separate and detect the enantiomers of three barbiturates in 32 min. A careful screening of various polymeric chiral surfactants was first performed to select the best chiral selector. Next, separation parameters such as chiral  $R_s$ , total analysis time and  $S/N$  ratio were optimized by multivariate central composite design (CCD) to obtain the highest overall chiral  $R_s$  and  $S/N$  ratio under the shortest possible run times. The optimum MEKC-MS conditions were tested by a series of experimental runs and it was found that the results were in good agreement with the predicted results. Finally, the optimized MEKC-MS method was applied to the analysis of barbiturates in human serum samples.

When the chiral analytes are highly non-polar or neutral in solution, they can only be separated using a charge chiral MoM but still could be ionized in the gas phase as charged species by atmospheric pressure photoionization (APPI-MS). In a recent report, CMEKC was coupled to APPI-MS for the first time for analysis of four benzoin derivatives [i.e., hydrobenzoin (HBNZ), benzoin (BNZ), benzoin methyl ether (BME) and benzoin ethyl ether (BEE)] [44]. Before carrying out the separation experiments, direct infusion APPI-MS experiments for the

four benzoin derivatives in both positive and negative ion modes were conducted to determine the fragmentation pathway. In positive ion mode, the protonated molecular ion of benzoin derivatives were not found to be the most abundant fragment ions. Instead  $[M+H-H_2O]^+$ ,  $[M+H-CH_3OH]^+$  and  $[M+H-C_2H_5OH]^+$  were observed as most abundant species for BNZ /HBNZ as well as benzoin methyl ether and benzoin ethyl ether, respectively (Fig.1.5). The inserted bar plots in Fig. 1.5 shows that the addition of acetone as dopant increases the sensitivity of BNZ and HBNZ but not for BME and BEE. The trends clearly suggested that the proton affinity for BNZ and HBNZ is greater than that of the solvent (methanol) as well as the dopant (acetone). Therefore, proton transfer reaction was possible through formation of solvent clusters.

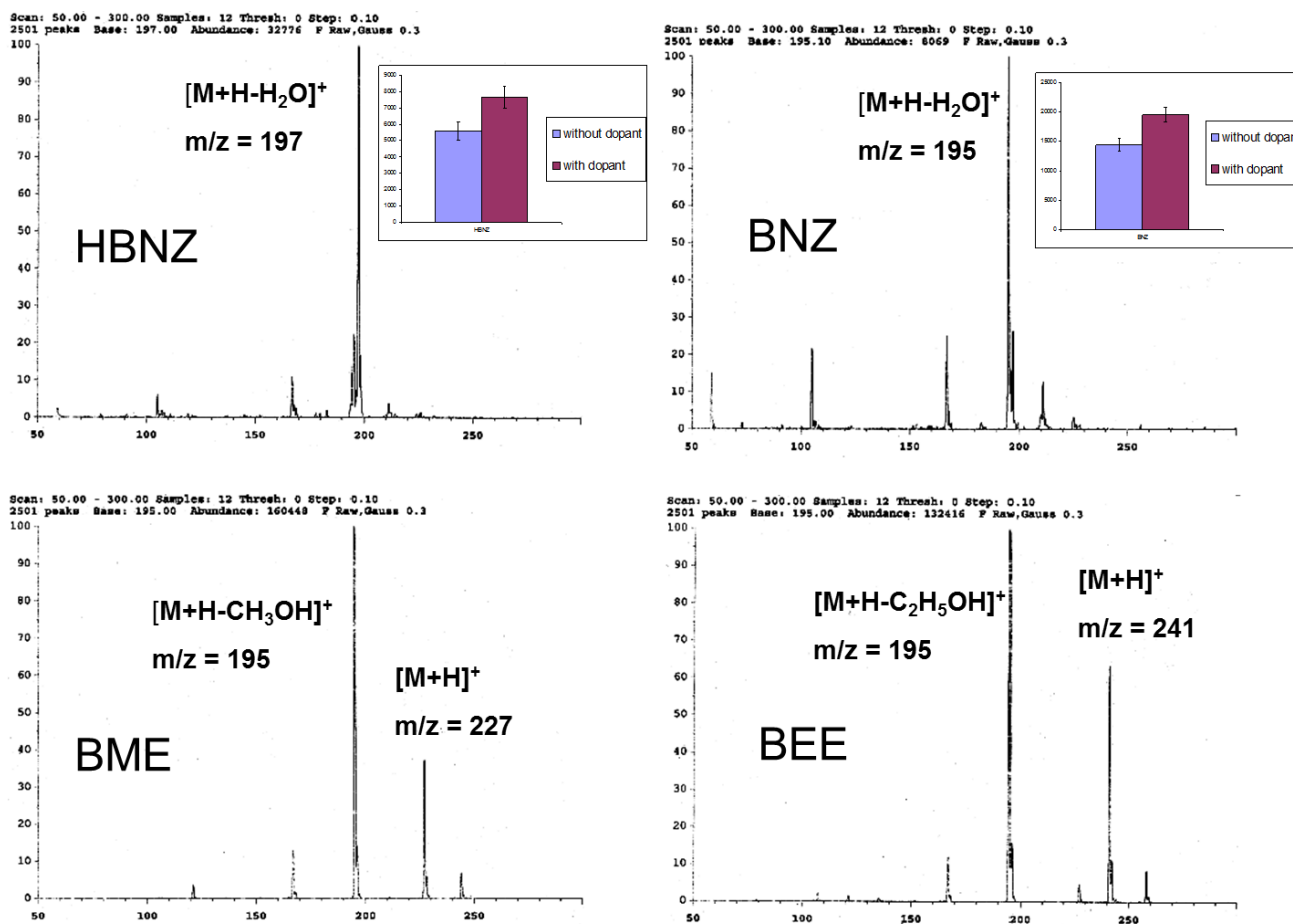


Fig.1.5 APPI-MS spectra of the four BNZ compounds. The inset plots of HBNZ and BNZ show the signal intensity with and without 0.5% acetone. The error bar in each plot represents  $3(\sigma)$  standard deviations. Taken from ref [44] with permission.

Using a binary mixture of two MoMs [poly sodium *N*-undecenoxy carbonyl-L-leucinate (poly-L-SUCL) and poly sodium *N*-undecenoyl-L,L-leucylvalinate (poly-L,L-SULV)] simultaneous enantioseparation and APPI-MS detection of all four neutral benzoin derivatives were achieved. Next, the MEKC parameters such as total surfactant concentration, voltage, buffer pH and etc. were optimized to obtain highest  $R_s/t_R$  using multivariate central composite design (CCD) and the models were validated by ANOVA. Similarly, the sheath liquid composition (methanol composition, dopant concentration and flow rate) and spray chamber parameters (drying gas flow rate, drying gas temperature and vaporizer temperature) were also optimized by CCD to achieve the maximum value of MS sensitivity (measure as peak area). Under the overall optimum multivariate conditions the MEKC-APPI-MS for the four benzoin derivatives was compared to MEKC-UV (Fig. 1.6). The comparison suggested that MEKC-APPI-MS offered much higher sensitivities up to 11 times higher than MEKC-UV for benzoin derivatives. Overall, higher  $R_s$  were obtained in MEKC-APPI-MS but at the cost of longer retention time.

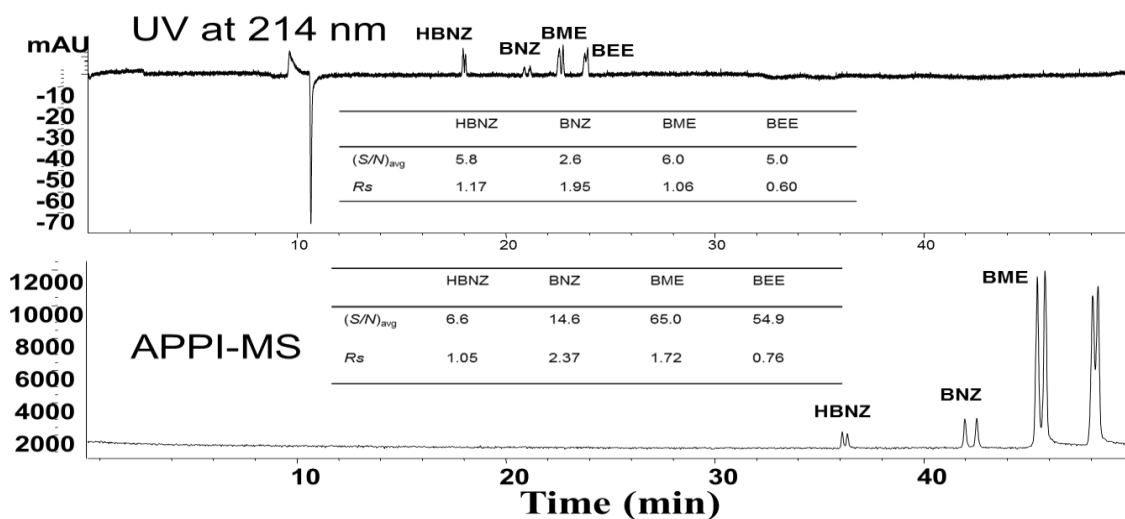


Fig.1.6 Representative electropherograms showing the comparison of CMEKC-UV versus CMEKC-APPI-MS. Experimental conditions: 120 cm 50  $\mu$ m id fused-silica capillary; 55Mm NH<sub>4</sub>OAc, pH 8.0, with 50mM poly-L,LSULV, 15mM poly-L-SUCL; 1 25 kV, 201C; analyte: 1mg/mL BNZ derivatives in 50/50MeOH/H<sub>2</sub>O, injected at 5mbar, 10 s; spray chamber parameters: DGF 5 L/min; nebulizer pressure 5 psi; DGT 150oC; VT 150°C; capillary voltage 2000 V; fragmentor 80 V, gain 3; SIM at m/z = 195,197; UV absorbance at 214 nm; sheath liquid: 5mM NH<sub>4</sub>OAc in 50/50 MeOH/H<sub>2</sub>O, 0.5% Acetone; flow rate 7.5 mL/min. Taken from ref [44] with permission.

Very recently, a novel polymeric glucose based surfactant such as *n*-alkyl- $\alpha$ -D-glucopyranoside surfactants for enantioseparation of various chiral pharmaceuticals in MEKC-MS/MS was evaluated. [45] The polymerization conditions for the formation of MoMs of *n*-undecenyl  $\alpha$ -D-glucopyranoside 4,6-hydrogen phosphate, sodium salt was first characterized by varying the polymerization concentration and profiling the chiral resolution of one anionic and one cationic compound. Next, the influence of polymeric glucopyranoside-based surfactants head groups and carbon chain length were optimized over a wide range of pH for chiral resolution of ephedrine alkaloids and  $\beta$ -blockers. The studies indicated that enantioseparations of ephedrine alkaloids and  $\beta$ -blockers could be achieved at optimum pH 5.0 and 7.0, respectively using ammonium acetate buffer, 25 mM polymeric *n*-undecyl  $\alpha$ -D-glucopyranoside 4,6-hydrogen phosphate, sodium salt. The LODs were as low as 10 ng/mL and 50 ng/mL for enantiomers of ephedrines and  $\beta$ -blockers, respectively.



### 1.3.3 Stationary phases in CCEC-MS

Historically, three main types of chiral stationary phase are commonly used in CEC: column packed with particles, monolithic columns and open tubular (OT) capillary columns. Chiral stationary phases used in HPLC have been successfully transferred to packed column and OT-CEC-MS. However, in the last five years no application was reported for OT-CEC-MS. Perhaps, this could be attributed to low sample capacity of OT columns. On the other hand, there have been publications on the development of fritless packed columns and monolithic columns for CCEC-MS applications.

The traditional approach for packing particle based chiral stationary phase in packed columns for CEC-UV requires two frits to hold the packing material. Unfortunately, this method presents many drawbacks for CEC-MS. First, irreproducible retention times and frequent current breakdown occurs due to extensive bubble formation at the outlet end exposed to the sprayer end of the MS instrument. Second, the frit formation itself is prone to changes in EOF due to difference in physical and chemical nature of the sintered frit. Although better performance were achieved using single frit internal tapered columns [46-49], the possibility of bubble formation caused by the inlet frit still remains exclusive problem for external tapered columns.

The development of fritless column for chiral CEC-MS was first reported in 2011 by Bragg and Shamsi [24]. The fritless packed column for CEC-MS was fabricated by using two internally tapered packed columns joined together by a commercially available New Objective PicoClear connector (Fig.1.7). The design of fritless column overcomes the drawbacks of traditional two fritted capillary columns while maintaining the benefits of broader compatibility with a variety of chiral packing materials and easy conditioning protocols in the CE-MS instrument. To test the robustness of fritless column, 90 consecutive runs were performed for

chiral separation of (+/-) aminoglutethimide with intraday and interday % RSD in the range of 3.2-3.7. Furthermore, the chiral CEC-MS, fritless column was reported to have better efficiency with equally good sensitivity and chiral resolution as single column packed with the same chiral stationary phase. In addition, the fritless column proved its compatibility with a variety of commercially available packing material for achiral separations with very good column-to-column and operator-to-operator reproducibility.

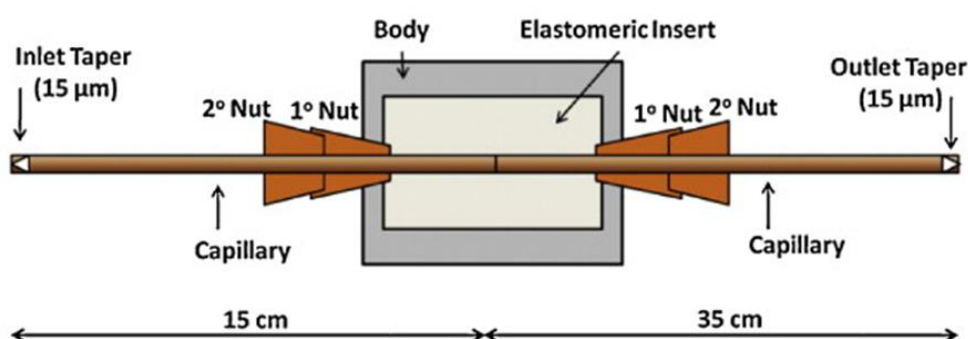


Fig.1.7 Schematic of fritless column with the New Objective PicoClear connector. The elastomeric insert of the connector ensures that the two capillaries do not grind together when joined. The arrows, at the bottom, represent the lengths of the inlet packed portion (15 cm) and outlet packed portion (35 cm) of the fritless column (not to scale). Taken from ref [50] with permission.

Although many of the problems associated with particle based packed chiral stationary phase in CEC are resolved today, the longer run times obtained in CEC-MS still remains the bottleneck for analysis of chiral compounds. Recently, only seven cm long single frit column packed with cellulose based chiral stationary phases was reported to provide high throughput analysis of chiral compounds in CEC-MS [24]. Bragg and Shamsi compared the performance of the two cellulose-based packed columns, cellulose tris (3,5-dimethyl-phenyl-carbamate) (CDMPC) and sulfonated cellulose tris (3,5-dimethylphenylcarbamate) (CDMPC-SO<sub>3</sub>) CSP for rapid enantioseparation in CEC-MS. The column packed with the charged chiral stationary

phase such as CDMPC-SO<sub>3</sub>CSP provided much faster analysis time with baseline *R<sub>s</sub>* when compared to the neutral chiral stationary such as CDMPC for the enantioseparation of glutethimide, aminoglutethimide, warfarin and 2,2,2-trifluoro-1-(9-anthryl) ethanol. Therefore, this promising research has opened the possibility of packing short chiral columns to perform high throughput screening in CEC-MS.

### 1.3.3.2 Monolithic column in CCEC-MS

Because the use of monolithic columns provides all the benefits of tapered packed columns and is less prone to bubble formation, a recent trend is the development of monolithic chiral columns for CEC-MS. Chiral monoliths developed for CEC-MS requires no end frits and the polymer forms a single continuous rod of porous material. In contrast to particle based column, the chiral monolithic columns have abundance of mesopores.

Recently, the use of methacryloyl-bonded  $\beta$ -CD to prepare monolithic column in few hours has attracted interests [50]. In this work, the author reported a versatile chiral monolithic column prepared by polymerization of glycidyl methacrylate-bonded  $\beta$ -cyclodextrin (GMA- $\beta$ -CD) with ethylene dimethacrylate (EDMA), in the presence of commonly used porogens and a negatively charged achiral monomer. This GMA- $\beta$ -CD-AMPS monolithic column was applied for CCEC-MS for the first time. While at least 30 compounds were enantioresolved by CEC-UV, in case of CEC-MS chiral separation of five positively charged chiral compounds and two acidic compounds was reported as summarized in Table 1.2. Although the preparation of monolithic column for CEC-MS was not fully optimized, a general comparison of CEC-UV with CEC-MS showed higher *S/N* ratio but slightly lower chiral *R<sub>s</sub>* with the later. The presence of an empty segment of 20 cm at the inlet end of the CEC-MS column might have contributed to some band broadening and *R<sub>s</sub>* loss in CEC-MS. However, the effective length of the monolithic bed in

CEC-UV was the same as in CEC-MS. Nevertheless, the monolithic column demonstrated excellent stability and reproducibility of retention times and enantioresolution using hexobarbital as the model chiral analyte.

Table 1.2 Chiral separations of five positively charged compounds and two negatively charged compounds using GMA- $\beta$ -CD-AMPS monolithic column in CEC-MS. Taken from ref [50] with permission.

Analytes	$R_s$	$\alpha$	$S/N$
hexobarbital	1.61	1.04	177
catechin	1	1.03	118
flavanone	0.86	1.03	80
pseudoephedrine	2.53	1.14	320
Troger's Base	1.39	1.07	115
aminoglutethimide	1.51	1.05	75
prilocaine	1.34	1.07	520

The same strategy was employed by polymerization of glycidyl GMA- $\beta$ -CD with EDMA and porogens but in the presence of positively charged achiral monomer [(vinylbenzyltrimethyl ammonium chloride, VBTA) [51]. The use of VBTA monomer provided abundance of anion exchange sites with reversed EOF. In contrast to GMA- $\beta$ -CD-AMPS, the use of GMA- $\beta$ -CD-VBTA column separated significantly more acidic compounds. (Table 1.3) Furthermore, the GMA- $\beta$ -CD-VBTA monolithic column provided two orders of magnitude higher sensitivity when coupled to triple quadrupole mass spectrometer compared to single quadrupole mass

spectrometer for several chiral compounds. Further studies are warranted to fully explore the potential of this  $\beta$ -CD based chiral monolithic column with a variety of charged monomers and crosslinkers for CEC-MS.

Table 1.3 Chiral separation of acidic and basic compounds using GMA- $\beta$ -CD-VBTA monolithic column in CEC-MS. Taken from ref [51] with permission.

Chiral Compounds	R <sub>s</sub>
2-Phenoxypropionic acid	1.5
2,3-(Chlorophenoxy)propionic acid	1.5
2,4-(Chlorophenoxy)propionic acid	1.3
2,2,4-(Dichlorophenoxy)propionic acid	0.5
2,2,4,5-(Trichlorophenoxy)propionic acid	0.5
2-Phenylbutyric acid	1.2
DNS-Valine	2
DNS-Leucine	1.3
DNS-Threonine	2.9
DNS-Serine	2.2
2,4-DNP-Methionine sulfone	1.1
2,4-DNP-Norleucine	0.9
2,4-DNP-Norvaline	2.4
2,4-DNP-Threonine	2.4
3,5-(Dinitrobenzoyl)phenylglycine	0.5
3,5-(Dinitrobenzoyl)leucine	1.5

Mandelic acid	0.1
Acetylmandelic acid	0.5
Atrolactic acid	2.1
4-Chloromandelic acid	1
3,4-(Methylenedioxy)mandelic acid	1.1
$\alpha$ -Bromophenyl acetic acid	0.8
$\alpha$ -Methoxyphenyl acetic acid	1.3
Ibuprofen	0.5
Warfarin	1.4
Coumachlor	1.4
BNP	0.5

---

Besides the CDs, other popular chiral selectors such as chiral surfactants have been used to prepare CSPs for chiral monolithic CEC. Shamsi's group developed a novel amino-acid surfactant bound chiral polymeric monolith [52]. In this latest study, chiral separations were realized in CEC and CEC-MS using surfactant bound chiral polymeric monolith derived from an acryloylamide tail, a carbamate linker, and an amino acid head group. When preparing the monolithic phase, the composition of polymerization mixture including the acid form of the chiral surfactant monomer, porogen, cross-linker was optimized to yield the best monolithic CSPs for CEC. Compared to the use of  $\beta$ -CD based chiral monolithic column, the surfactant based monolithic column was found to be superior (Fig.1.8) in terms of simultaneously resolving structurally similar analytes (EP and PEP). Three surfactant-bound monolithic columns prepared

by polymerizing leucine-based carbamate chiral surfactants with different alkyl chain length [namely, sodium 8-acrylamidoctenoxy carbonyl-L-leucinate (SAAOCL), sodium 10-acrylamidodecenoxy carbonyl-L-leucinate(SAADCL), and sodium 12-acrylamidododecenoxy carbonyl-L-leucinate (SAADoCL)] were successfully synthesized and characterized. The enantiomers of ( $\pm$ )PEP was used as a model chiral cationic analyte to investigate the effect of the mobile phase parameters on the retention factors. Under the optimized conditions, SAADCL monolithic column simultaneous separated EP and PEP isomers by CCEC-MS/MS with a run time of 44 min (Fig.1.9). Although the electrospray parameters were not extensively optimized, higher  $S/N$  ratio observed in MRM mode suggests LOD in low ng/mL range. To decrease the analysis time for CEC-MS, it is important to screen various surfactant head groups, and a range of crosslinkers to test the compatibility of this surfactant-bound monolith column in the CEC-MS/MS mode.

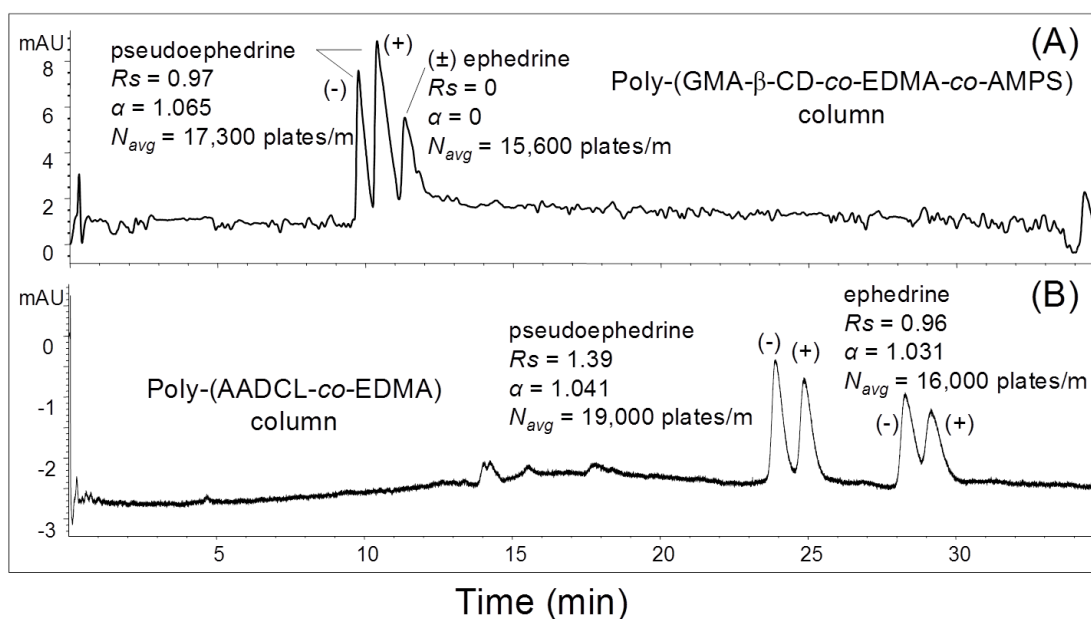


Fig. 1.8 Comparison between poly-(GMA- $\beta$ -CD-co-EDMA-co-AMPS) column (A) and poly-(AADCL-co-EDMA) column (B) for simultaneous enantioseparation of ( $\pm$ )-PEP and ( $\pm$ )-EP

enantiomers. The CEC column dimensions for the poly(GMA- $\beta$ -CD-co-EDMA-co-AMPS) columns are the same as described in Figure 1.1. Mobile phase: 50%(v/v) ACN and 50% aqueous buffer, 5 mM NH<sub>4</sub>OAc, 0.3% (v/v) TEA (pH 4.0). Mobile phase conditions for the AADCL column are the same as described in Figure 1.3. Both ( $\pm$ )-PEP and ( $\pm$ )-EP (1 mg/mL) are dissolved in 50/50 ACN/H<sub>2</sub>O (v/v); injection, 5 kV for 3 s. Taken from ref [52] with permission.

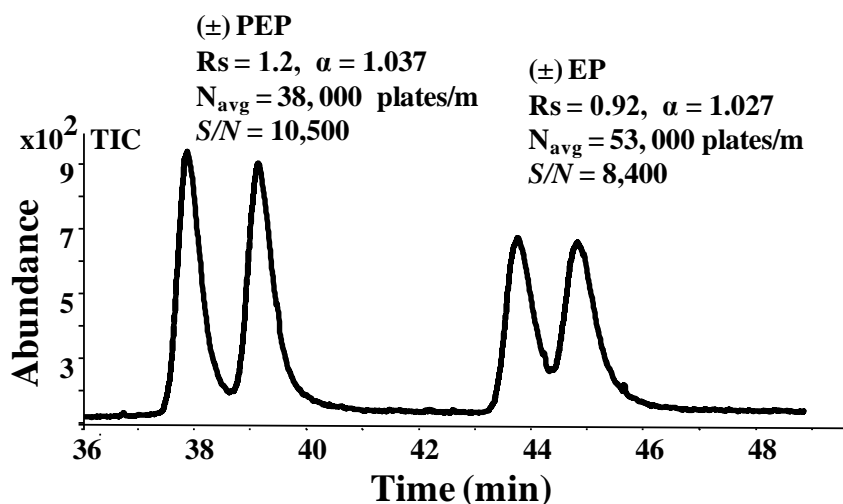


Fig.1.9 CEC-ESI-MS/MS of ( $\pm$ ) PEP and ( $\pm$ ) EP with AADCL column. CEC conditions: 53 cm long column, 30 cm monolithic bed length. 0.3 kV/cm (15 kV); high pressure, 5 bar applied at inlet end of the column. Other conditions are the same as in Figure 1.1 The ( $\pm$ ) PEP and ( $\pm$ ) EP (50  $\mu$ g/mL) were injected at 5 kV for 3 s. The MRM product ions were observed at m/z 115.1 and 133.1 for ( $\pm$ ) PEP and m/z ( $\pm$ ) EP respectively; nebulizer pressure, 7 psi; drying gas flow rate, 5 L/min; drying gas temperature, 150 °C; capillary voltage, 3500 V; fragmentor, 90 V. Sheath liquid: 80/20 MeOH/H<sub>2</sub>O (v/v), 5 mM NH<sub>4</sub>OAc (pH 6.8) delivered at a flow rate of 8  $\mu$ L/min. Taken from ref [52] with permission.

#### 1.4 Biomedical and clinical applications

Chiral CE-MS is slowly establishing as an efficient tool for drugs and metabolites analysis in biological matrices due to its high efficiency, high chiral selectivity, and high sensitivity. Though biological samples analyzed by chiral CE-MS are not as routinely used as in HPLC-MS, yet CE-MS has distinguished advantages over HPLC-MS for drug analysis in biological samples. For example, HPLC-MS requires expensive special chiral column while CE-



MS only needs few mg of exotic chiral selector, which is either added to the background electrolyte in EKC-MS or MEKC-MS or attached to the capillary wall in CEC-MS. In addition, CE-MS consumes much less sample volume especially when sample size for biological analysis is very limited.

Liu's *et al.* developed a chiral PFT EKC-MS/MS method for enantiomeric quantification of 3,4-dihydroxyphenylalanine (DOPA), phenylalanine and tyrosine using sulfated  $\beta$ -CD as chiral selector in less than 12 min [53]. This assay was successfully applied to study the metabolism of DOPA in PC-12 nerve cells. Prior to the metabolic study in chiral CE-MS, PC-12 cells were cultured in complete RPMI medium under 10% heat-inactivated horse serum and 5% fetal bovine serum for 4-5 days. The racemic or enantiomerically pure form of DOPA was then added at a concentration of 500  $\mu$ M and was incubated with 5-mL of PC-12 cell suspension ( $2 \times 10^6$  cells/mL) for 2 hrs at 37 °C. After incubation, cells were removed by centrifugation and the proteins were removed by precipitation with trichloroacetic acid.

Fig. 1.10 (A-C) shows the metabolic profiles of D- and L-DOPA. In Fig.10A, the two enantiomers of DOPA standard solution were separated before 11 min. Fig. 10B and C show the enantioseparation of DOPA incubated with the culture medium and with PC-12 cells, respectively. Interestingly, the peak areas of L-DOPA from incubation with PC-12 cells decreased greatly suggesting that L-DOPA was metabolized effectively, whereas D-DOPA was not metabolized. Thus, EKC-MS/MS analysis demonstrated the enantioselective metabolism of DOPA in vitro neuron model for the first time.

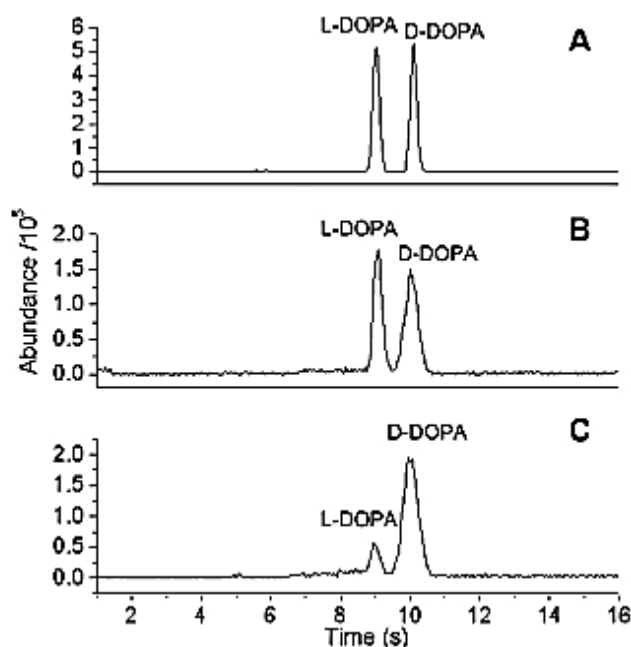


Fig.1.10 Electropherograms obtained from studying DOPA metabolism: (A) racemic DOPA standard solution (50  $\mu\text{M}$  for each enantiomer); (B) 500  $\mu\text{M}$  racemic DOPA incubated with the culture medium for 2 h; (C) 500  $\mu\text{M}$  racemic DOPA incubated with PC-12 cells ( $2 \times 10^6$  cells/ml) for 2 h. Chiral CE-MS/MS condition were as follows: sheath liquid, 50% methanol in water containing 0.1% formic acid at 3  $\mu\text{l}/\text{min}$ ; ESI spray voltage, +4 kV; capillary temperature, 220  $^{\circ}\text{C}$ ; sheath gas, 20 au; auxiliary gas, 0 au. Taken from ref [53] with permission.

When chiral CE-MS is applied in body fluid such as plasma or serum, sample preparation is required prior to the analysis. For example, solid phase extraction (SPE) and liquid-liquid extraction (LLE) are the most commonly used sample preparation techniques. More recently, polymeric dipeptide  $M_oM$ , *N*-undecenoyl-*L,L*-leucylvalinate (poly-*L,L*-SULV) was successfully utilized as PSP in CMEKC-MS/MS for the simultaneous separation of warfarin and its five hydroxyl warfarin metabolites in one single run [38]. The simultaneous enantioseparation were

realized using 25 mM poly-*L,L*-SULV added to the BGE, 25 mM NH<sub>4</sub>OAc at pH 5.0. Next, the authors compared the separation in MEKC-MS with CEC-MS using vancomycin as a packing material and found that CMEKC-MS was superior to CCEC-MS. As shown in Fig. 1.11, the comparison clearly showed that the total analysis time of packed column CEC-MS is 100 min while MEKC-MS offered much shorter analysis time of less than 40 min, though chiral resolution of warfarin and its metabolites were achieved in both CE-MS modes. To increase the detection sensitivity for application in biological samples, CMEKC-MS/MS was investigated. Fig.12 shows the comparison of the detection of warfarin and its hydroxylated metabolites by MEKC-MS and MEKC-MS/MS and it was found that triple quadrupole MS provided much higher *S/N* than single quadrupole MS. Finally, the CMEKC-MS/MS method was applied to analyze the patients serum samples with LOD at 2 ng/mL and limits of quantitation (LOQ) at 5 ng/mL.

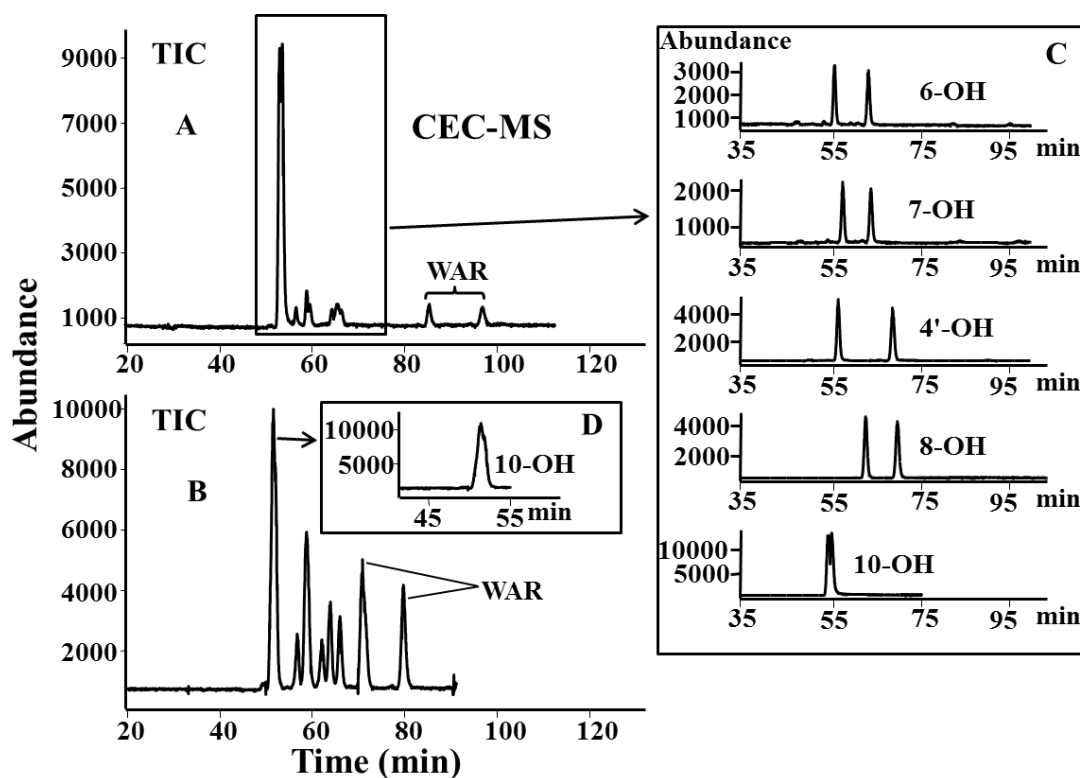


Fig.1.11 Optimized enantioseparation of WAR and its hydroxylated metabolites by CEC–ESI-MS (A–D). Conditions: 40 cm long vancomycin packed column (total long 65 cm, 375  $\mu\text{m}$  O.D. and 75  $\mu\text{m}$  I.D.). Running buffer, ACN/H<sub>2</sub>O (45/55, v/v), 10 mM NH<sub>4</sub>OAc at pH 4.0 (A) and ACN/MeOH/H<sub>2</sub>O (30/50/20, v/v/v), 10 mM NH<sub>4</sub>OAc at pH 4.0 (B). Applied voltage, +25 kV; injection, 5 kV, 3 s. Spray chamber and sheath liquid conditions nebulizer pressure: 4 psi, drying gas temp.: 200 °C, drying gas flow: 6 L/min, capillary voltage: –3000 V, fragmentor voltage, 91 V, SIM mode; sheath liquid: MeOH/H<sub>2</sub>O (80/20, v/v), 5 mM NH<sub>4</sub>OAc, pH 6.8 with flow rate of 0.5  $\mu\text{L}/\text{min}$ ; and sample concentration: 10  $\mu\text{g}/\text{mL}$  in ACN/H<sub>2</sub>O (40/60, v/v). Taken from ref [38] with permission.

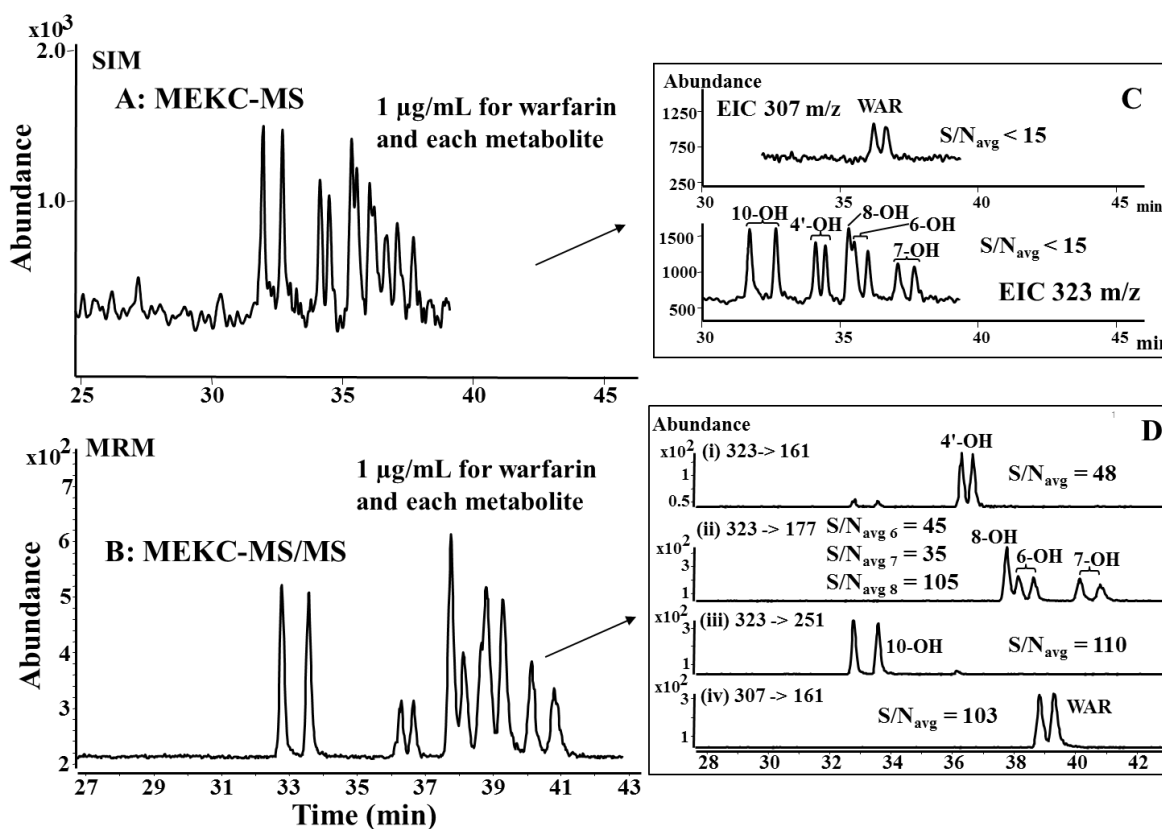


Fig.1.12 Comparison of the detection of WAR and its hydroxylated metabolites by MEKC–MS (A and C) and MEKC–MS/MS (B and D). For MEKC–MS, all the conditions are the same as in Fig. 1.11. MEKC–MS/MS conditions: 120 cm long (375  $\mu\text{m}$  O.D. and 50  $\mu\text{m}$  I.D.) fused silica capillary. Buffer: 25 mM NH<sub>4</sub>OAc pH 5.0, 25 mM poly-1,1-SULV with 15% (v/v) MeOH; injection: 5 mbar for 2 s; voltage: 30 kV; spray chamber parameters: drying gas temperature: 200 °C, drying gas flow rate: 8 L/min, nebulizer pressure: 4 psi, capillary voltage: –3000 V, collision energy: 20 eV for all except 5 eV for I.S., fragmentor voltage: 125 V for all except 75 V for I.S.

Sheath liquid: MeOH/H<sub>2</sub>O (80/20, v/v) with 5 mM NH<sub>4</sub>OAc, sheath liquid flow rate: 5  $\mu$ L/min. Taken from ref [38] with permission.

Besides the work we discussed in section 1.3.2 [38], there is one latest publication on CMEKC-MS/MS application for the simultaneous analysis of anti-depressant drug, venlafaxine (VX) and its structurally-similar major metabolite, *O*-desmethylvenlafaxine (*O*-DVX) in human plasma samples [54]. The MoM, poly-sodium *N*-undecenoyl-*L,L*-leucylalaninate (poly-*L,L*-SULA) was employed as the chiral selector after screening several dipeptide surfactants. Baseline enantio-separation of both *O*-DVX and VX enantiomers was achieved in ~15 min after optimizing the pH, poly-*L,L*-SULA concentration, nebulizer pressure and voltage. Calibration curves in spiked plasma (recoveries higher than 80%) were linear. The LODs were found to be as low as 30 ng/mL and 21 ng/mL for *O*-DVX and VX, respectively.

The CMEKC-MS method was implemented in a case study involving the plasma concentrations of human subjects receiving VX or *O*-DVX orally when co-administered without and with indinavir (used in HIV therapy). A series of electrochromatograms are compared in Fig. 1.13. When one particular human subject is treated without indinavir therapy, the *S/R* ratio of peak height of *O*-DVX slightly increases from 0.83 to 0.98 after drug is administered at 1 hr and 4 hrs, respectively (left column). In contrast, note that significant decrease in peak height ratio of *S/R* enantiomers of *O*-DVX is observed in the subject with indinavir therapy at 4 hrs compared to 1 hr. Further data in this studies suggested that MEKC-ESI-MS/MS is an effective alternative approach for the pharmacokinetic and pharmacodynamic studies of both *O*-DVX and VX enantiomers. Thus, potential drug-drug interactions involving VX and *O*-DVX enantiomers with indinavir could be identified.

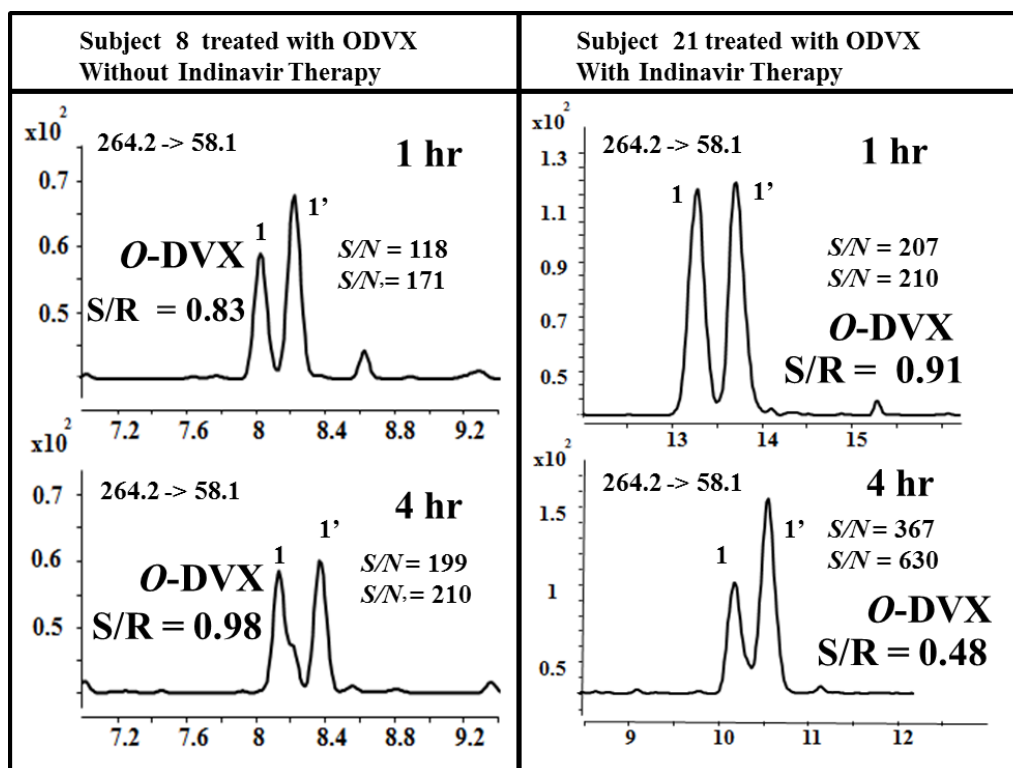


Fig.1.13 Total ion electrochromatograms of subject treated with O-DVX without and with indinavir therapy at 1 h and 4 h, respectively. The MEKC–MS/MS conditions: 60 cm long (375  $\mu\text{m}$  O.D., 50  $\mu\text{m}$  I.D.) fused silica capillary. Buffer: 20 mM  $\text{NH}_4\text{OAc}$  + 25 mM TEA, pH 8.5, 15 mM polydipeptide surfactant. Applied voltage, +25 kV, injection, 5 mbar, 100 s. Spray chamber parameters: nebulizer pressure: 3 psi, drying gas temp.: 200°C, drying gas flow: 8 L/min; capillary voltage: +3000 V; fragmentor voltage, 113 V for O-DVX and 117 V for VX; collision energy: 17 eV; MRM transition: O-DVX: 264.2  $\rightarrow$  58.1; VX: 278.2  $\rightarrow$  58.1. Sheath liquid: MeOH/ $\text{H}_2\text{O}$  (80/20, v/v), 5 mM  $\text{NH}_4\text{OAc}$ , pH 6.8 with flow rate of 0.5 mL/min; The MRM precursor to product ion transition for R-atenolol is 267.2  $\rightarrow$  145.2. The enantiomer S-O-DVX eluted first followed by the R-O-DVX. (1,1' = O-DVX). Without indinavir therapy:  $S/N_1 = 118$ ,  $S/N_{1'} = 171$  at 1 h and  $S/N_1 = 199$ ,  $S/N_{1'} = 210$  at 4 h. With indinavir therapy:  $S/N_1 = 207$ ,  $S/N_{1'} = 210$  at 1 h and  $S/N_1 = 367$ ,  $S/N_{1'} = 630$  at 4 h for S- and R-enantiomer of O-DVX, respectively. Taken from ref [54] with permission.

### 1.5. Conclusions and future prospects

One of the major limitations of HPLC-MS is the careful selection of chiral stationary phase and/or MS compatible mobile phase combinations for the separation of chiral drugs and its

metabolites. In addition, HPLC-MS is expensive, time consuming and resource consuming compared to CE-MS. High selectivity, high efficiency and low operation expense allows chiral CE-MS to be a powerful analytical method. The contamination of the MS source by low molecular weight chiral selectors can be avoided by using; (a) charged CDs with PFT, (b) high molecular weight M<sub>o</sub>Ms and (c) variety of low cost MS compatible chiral CEC columns. Therefore, CCEKC-MS, CMEKC-MS and CCEC-MS will continue to be advantageous for sensitive detection of enantiomers.

Over the past five years, the demonstration of the applicability for chiral analysis studies has continued in various modes of CE-MS, as indicated by 22 publications of which the majority was directed in targeted analysis (Table 1.1). A growing trend in chiromics is to use a combination of highly efficient chiral separations with highly sensitive MS detection. In addition, analysis of parent chiral drugs and its chiral metabolites in biological samples in a single run using a single method will be of great value in the future. In this regard, chiral CE-MS has demonstrated to be a highly useful complementary tool to HPLC-MS. The chiral CE-MS based application studies discussed in the last section are mainly application driven, with the potential to develop into a robust clinical assay.

To this date, CEKC-MS using a combination of charged CDs with PFT has great potential to be used in drug development and drug quality control, pharmacokinetic as well as pharmacodynamics studies due to the availability of commercially available chiral selectors. Furthermore, in the past few years, the application of CMEKC-MS using chiral M<sub>o</sub>Ms is particularly shown to be advantageous for the analysis of biological samples. Because CMEKC-MS mainly depends on the development of MS compatible chiral selectors, the commercial availability of MoM will foreseeably be of great significance.

To the best of our knowledge until now, various modes of chiral CE (EKC, MEKC and CEC)-MS have been carried out with a sheath flow interface. Further studies in the development of new interfacing techniques, such as the sheathless porous tip [34], and the EOF driven sprayer using borosilicate glass combined with sheath flow [55] has great promise to increase the sensitivity of chiral metabolites. Both of these interfaces are now commercially available. In addition, the compatibility of chiral nanoparticles and surfactant bound polymeric monoliths is an area that remains essentially unexplored.



## References

- [1] Gassmann E., Kuo, J.E., and Zare, R.N. Electrokinetic separation of chiral compounds. *Science*. (1985), 230, 813-814.
- [2] Fanali, S. Separation of optical isomers by capillary zone electrophoresis based on host-guest complexation with cyclodextrins. *J. Chromatogr. A* (1989), 474, 441-446.
- [3] Cherkaoui, S., Rudaz, S., Varesio, E., and Veuthey, J.L. On-line capillary electrophoresis-electrospray mass spectrometry for the stereoselective analysis of drugs and metabolites. *Electrophoresis*. (2001), 22, 3308-3315.
- [4] Rudaz, S, Cherkaoui, S, Gauvrit, J.Y, Lanteri, P., and Veuthey J.L. Experimental designs to investigate capillary electrophoresis-electrospray ionization-mass spectrometry enantioseparation with the partial-filling technique. *Electrophoresis*. (2001), 22, 3316-3326.
- [5] Sanchez-Lopez, E., Montealegre, C., Marina, M.L., and Crego, A.L. Development of chiral methodologies by capillary electrophoresis with ultraviolet and mass spectrometry detection for duloxetine analysis in pharmaceutical formulations. *J. Chromatogr. A* (2014), 1363, 356-362.
- [6] Shamsi, S. A. Chiral capillary electrophoresis-mass spectrometry: modes and applications. *Electrophoresis*. (2002), 23, 4036-4051.
- [7] Desiderio C., Rossetti, D.V., Perri, F., Giardina, B., Messina, IC., and Castagnola, M. Enantiomeric separation of baclofen by capillary electrophoresis tandem mass spectrometry with sulfobutylether-beta-cyclodextrin as chiral selector in partial filling mode. *J Chromatogr B Analyt Technol Biomed Life Sci*. (2008), 875, 280-287.

- [8] Shamsi, S. A. Micellar electrokinetic chromatography–mass spectrometry using a polymerized chiral surfactant *Anal. Chem.* (2001), 73, 5103–5108.
- [9] He, J., and Shamsi, S. A. Application of polymeric surfactants in chiral micellar electrokinetic chromatography (CMEKC) and CMEKC coupled to mass spectrometry. 2nd edition, In *Chiral Separations Methods and Proctocols*, Humana Press, Springer Science+ Business Media LLC, Clifton, NJ. Chapter 21, (2013), pp.319-48. DOI:10.1007/978-1-62703-263-6-21.
- [10] Zheng, J., Norton, D., and Shamsi, S. A. Fabrication of internally tapered capillaries for capillary electrochromatography electrospray ionization mass spectrometry. *Anal. Chem* (2006), 78, 1323-1330.
- [11] Sheppard, R. L., Tong, X., Cai, J., and Henion, J. D. Chiral separation and detection of terbutaline and ephedrine by capillary electrophoresis coupled with ion spray mass spectrometry. *Anal. Chem* (1995), 67, 2054–2058.
- [12] March, R. E. An introduction to quadrupole ion trap mass spectrometry. *J. Mass Spectrom.* (1997), 32, 351–369.
- [13] Chernushevich, I. V., Loboda, A. V., and Thomson, B. A. An introduction to quadrupole–time-of-flight mass spectrometry. *J. Mass Spectrom.* (2001), 36, 849–865.
- [14] Verhaert, P., Uttenweiler-Joseph, S., de Vries, M., Loboda, A., Ens, W., and Standing, K. Matrix-assisted laser desorption/ionization quadrupole time-of-flight mass spectrometry: An elegant tool for peptidomics. *Proteomics.* (2001), 1, 118–131.
- [15] Hirabayashi, Y., Hirabayashi, A., and Koizumi, H. A sonic spray interface for capillary electrophoresis/mass spectrometry. *Rapid Commun.Mass Spectrom.* 1999, 13, 712–715.

- [16] Schulte, G., Heitmeier, S., Chankvetadze, B., and Blaschke, G. Chiral capillary electrophoresis–electrospray mass spectrometry coupling with charged cyclodextrin derivatives as chiral selectors. *J.Chromatogr. A* (1998), 800, 77–82.
- [17] Palmer, C. P., and Terabe, S. Micelle polymers as pseudostationary phases in MEKC: chromatographic performance and chemical selectivity. *Anal. Chem.* (1997), 69, 1852-1860
- [18] Ahuja, E. S., and Foley, J. P. Influence of dodecyl sulfate counterion on efficiency, selectivity, retention, elution range, and resolution in micellar electrokinetic chromatography. *Anal. Chem.* (1995), 67, 2315-2324.
- [19] Terabe, S., Otsuka, K., and Ando, T. Electrokinetic chromatography with micellar solution and open-tubular capillary. *Anal. Chem.* (1985), 57, 834-841.
- [20] Shamsi, S. A., Akbay, C., and Warner, I. M. Polymeric anionic surfactant for electrokinetic chromatography: separation of 16 priority polycyclic aromatic hydrocarbon pollutants. *Anal. Chem.* (1998), 70, 3078–3083.
- [21] Hou, J., Zheng, J., Rizvi, S.A.A., and Shamsi, S. A. Simultaneous chiral separation and determination of ephedrine alkaloids by MEKC-ESI-MS using polymeric surfactant I: Method development. *Electrophoresis* (2007), 28, 1352-1363.
- [22] Zheng, J., Norton, D., and Shamsi, S. A. Fabrication of internally tapered capillaries for capillary electrochromatography electrospray ionization mass spectrometry. *Anal. Chem.* (2006), 78, 1323–1330.
- [23] Bragg, W., and Shamsi, S. A. high throughput analysis of chiral compounds using capillary electrochromatography (CEC) and CEC-mass spectrometry with cellulose based stationary phases. *J. Sep. Sci. Tech.* (2013), 48, 2589-2599.

- [24] Bragg, W., and Shamsi, S. A. Development of a fritless packed column for capillary electrochromatography–mass spectrometry. *J. Chromatogr. A*. (2011), 1218, 8691-8700.
- [25] Walz, S., Weis, S., Franz, M., Rominger, F., and Trapp, O. Investigation of the enantiomerization barriers of the phthalimidone derivatives EM12 and lenalidomide by dynamic electrokinetic chromatography. *Electrophoresis* (2015), 36, 796-804.
- [26] Sabela, M.I., Singh, P., Gumede, N. J., Bisetty, K., and Sagrado, S. Evaluation of enantioresolution of (• )-catechin using electrokinetic chromatography and molecular docking. *J. Sci. Res. in Pharm.* (2012), 1, 1-4.
- [27] Lipka, E., Landagaray, E., Ettaoussi, M., Yous, S., and Vaccher, C. Enhanced detection for determination of enantiomeric purity of novel agomelatine analogs by EKC using single and dual cyclodextrin systems. *Electrophoresis* (2014), 35, 2785-2792.
- [28] Asensi-Bernardi, L., Escuder-Gilabert, L., Martin-Biosca, Y., Medina-Hernandez, M. J., and Sagrado, S., Modeling the chiral resolution ability of highly sulfated  $\beta$ -cyclodextrin for basic compounds in electrokinetic chromatography. *J. Chromatogr. A* (2013), 1308, 152-160.
- [29] Asensi-Bernardi, L., Martin-Biosca, Y., Medina-Hernandez, M. J., and Sagrado, S. On the zopiclone enantioselective binding to human albumin and plasma proteins:an electrokinetic chromatography approach. *J. Chromatogr. A*. (2011), 1218, 3111-3117.
- [30] Lamoree, M. H., Sprang, A. F. H., Tjaden, U. R., van der Greef, J. *J. Chromatogr. A* (1996), 742, 235–242.
- [31] Lu, W., Cole, R. B. Use of heptakis (2, 6-di-O-methyl)- $\beta$ -cyclodextrin in on-line capillary zone electrophoresis-mass spectrometry for the chiral separation of ropivacaine. *J. Chromatogr. B* (1998), 714, 69–75.

- [32] Wu, H., Yuan, B., and Liu, Y. Chiral capillary electrophoresis–mass spectrometry of tetrahydroisoquinoline-derived neurotoxins: Observation of complex stereoisomerism. *J. Chromatogr. A* (2011), 1218, 3118-3123.
- [33] Merola, G., Fu, H., Tagliaro, F., Macchia, T., and McCord, R.B. Chiral separation of 12 cathinone analogs by cyclodextrin-assisted capillary electrophoresis with UV and mass spectrometry detection. *Electrophoresis* (2014), 35, 3231–3241.
- [34] Moini, M., and Rollman, C.M. Compatibility of highly sulfated cyclodextrin with electrospray ionization at low nanoliter/minute flow rates and its application to capillary electrophoresis/electrospray ionization mass spectrometric analysis of cathinone derivatives and their optical isomers. *Rapid Commun Mass Spectrom* (2015), 29, 304-310.
- [35] Toshiyasu, M., Yuko T. I., Hajime, M., Kenji, K., Kenji, T., Tatsuyuki, K, and Hiroyuki, I. The use of a sulfonated capillary on chiral capillary electrophoresis/mass spectrometry of amphetamine-type stimulants for methamphetamine impurity profiling. *Forensic Sci. Int.* (2015), 249, 59–65.
- [36] Hou, J., Zheng, J., and Shamsi, S. A. Separation and determination of warfarin enantiomers in human plasma using a novel polymeric surfactant for micellar electrokinetic chromatography–mass spectrometry. *J. Chromatogr. A* (2007), 1159, 208-216.
- [37] Rizvi, S. A. A., Zheng, J., Apkarian, R. P., Dublin, S. N., and Shamsi, S. A. Polymeric sulfated amino acid surfactants: a class of versatile chiral selectors for micellar electrokinetic chromatography (MEKC) and MEKC-MS. *Anal. Chem.* (2007), 79, 879-898.
- [38] Wang, X., Hou, J., Jann, M., Hon, Y.Y., and Shamsi, S.A. Development of a chiral micellar electrokinetic chromatography–tandem mass spectrometry assay for simultaneous analysis of

warfarin and hydroxywarfarin metabolites: Application to the analysis of patients serum samples.

*J. Chromatogr. A* (2013), 1271, 207-216.

[39] Hou, J., Zheng, J., and Shamsi, S.A. Simultaneous chiral separation of ephedrine alkaloids by MEKC-ESI-MS using polymeric surfactant II: Application in dietary supplements. *Electrophoresis*. (2007), 28, 1426-1434.

[40] Wang, B., He, J., and Shamsi, S. A. A High-throughput multivariate Optimization for the simultaneous enantioseparation and detection of barbiturates in micellar electrokinetic chromatography—mass spectrometry. *J. Chromatogr. Sci.* (2010), 48, 572-583.

[41] Rizvi, S.A. A., Zheng, J., Apkarian, R. P., Dublin, S. N., and Shamsi, S. A. Polymeric sulfated amino acid surfactants: a class of versatile chiral selectors for micellar electrokinetic chromatography (MEKC) and MEKC-MS. *Anal. Chem.* (2007), 79, 879-898.

[42] Rizvi, S. A.A., Simons, D. N., and Shamsi, S. A. Polymeric alkenoxy amino acid surfactants: III. Chiral separations of binaphthyl derivatives. *Electrophoresis*. (2004), 25, 712-722.

[43] Akbay, C., Rizvi, S. A. A., and Shamsi, S. A. Simultaneous enantioseparation and tandem UV-MS detection of eight  $\beta$ -blockers in micellar electrokinetic chromatography using a chiral molecular micelle. *Anal. Chem.* (2005), 77, 1672-1683.

[44] He, J., and Shamsi, S. A. Chiral micellar electrokinetic chromatography-atmospheric pressure photoionization of benzoin derivatives using mixed molecular micelles. *Electrophoresis*. (2011), 32, 1164–1175.

[45] Liu, Y., and Shamsi, S. A. Synthesis, characterization and application of polymeric *n*-alkyl- $\alpha$ -D-glucopyranoside surfactants for enantioseparation in micellar electrokinetic chromatography-tandem mass spectrometry. *Electrophoresis*. (2016), 00, 1-11.

- [46] Zheng, J., Shamsi, S. A. Combination of Chiral Capillary Electrochromatography with Electrospray Ionization Mass Spectrometry: Method Development and Assay of Warfarin Enantiomers in Human Plasma. *Anal. Chem.* (2003), 75, 6295-6305.
- [47] Zheng, J., and Shamsi, S. A. Capillary Electrochromatography Coupled to Atmospheric Pressure Photoionization Mass Spectrometry for Methylated Benzo[*a*]pyrene Isomers. *Anal. Chem.* (2006), 78, 6921-6927.
- [48] Bragg, W., Norton, D., and Shamsi, S. A. Optimized separation of  $\beta$ -blockers with multiple chiral centers using capillary electrochromatography–mass spectrometry. *J. Chromatogr. B* (2008), 875, 304-316.
- [49] Zheng, J., Bragg, W., Hou, J., Lin, N., Chandrasekaran, S., and Shamsi, S. A., Sulfated and sulfonated polysaccharide as chiral stationary phases for capillary electrochromatography and capillary electrochromatography–mass spectrometry. *J. Chromatogr. A.* (2009), 1216, 857-872.
- [50] Gu, C., and Shamsi, S. A., Evaluation of a methacrylate-bonded cyclodextrins as a monolithic chiral stationary phase for capillary electrochromatography (CEC)-UV and CEC coupled to mass spectrometry. *Electrophoresis.* (2011), 32, 2727-2737.
- [51] Bragg, W., and Shamsi, S. A. A novel positively charged achiral comonomer for beta cyclodextrin monolithic stationary phase: Improved chiral separation of acidic compounds using capillary electrochromatography coupled to mass spectrometry. *J. Chromatogr. A.* (2012), 1267, 144-145.
- [52] He, J., Wang, Morrell, M., Wang, X., and Shamsi, S. A. Amino acid bound surfactants: a new synthetic family of polymeric monoliths opening up possibilities for chiral separations in capillary electrochromatography. *Anal. Chem.* (2012), 84, 5236–5242.

- [53] Yuan, B., Wu, H., Sanders, T., McCullum, C., Zheng, Y., Tchounwou, P.B., and Liu, Y. Chiral capillary electrophoresis–mass spectrometry of 3, 4-dihydroxyphenylalanine: Evidence for its enantioselective metabolism in PC-12 nerve cells. *Anal. Biochem.* (2011), 416, 191–195.
- [54] Liu, Y., Jann, M., Vandenberg, C., and Shamsi, S. A. Development of an enantioselective assay for simultaneous separation of venlafaxine and *O*-desmethylvenlafaxine by micellar electrokinetic chromatography–tandem mass spectrometry: Application to the analysis of drug–drug interaction. *J. Chromatogr. A.* (2015), 1420, 119–128.
- [55] Sun, X., Lin, L., Liu, X., Zhang, F., Chi, L., Xia, Q., Linhardt, R. J. “Capillary Electrophoresis–Mass Spectrometry for the Analysis of Heparin Oligosaccharides and Low Molecular Weight Heparin.” *Anal. Chem.* 20, 2015 DOI:10.1021/acs.anal.chm.5b04405



## Chapter 2

**Synthesis, characterization and application of polymeric *n*-alkyl  $\alpha$ -D-glucopyranoside surfactants for enantioseparation in micellar electrokinetic chromatography-tandem mass spectrometry**

**(Chapter 2 has been published by the author and was taken from the author with permission)**

Sugar based ionic surfactants forming micelles are known to suppress electrospray ionization of various compounds due to decrease in surface tension upon micelle formation [1]. For the first time, polymeric  $\alpha$ -D-glucopyranoside-based surfactants with different chain length and head groups have been successfully synthesized, characterized and applied as compatible chiral selector in micellar electrokinetic chromatography-electrospray ionization-tandem mass spectrometry (MEKC-ESI-MS/MS). First, the effect of polymerization concentration of the monomer, *n*-undecenyl  $\alpha$ -D-glucopyranoside 4,6-hydrogen phosphate, sodium salt ( $\alpha$ -SUGP), was evaluated by enantioseparation of one anionic compound [1,1'-binaphthyl-2,2'-diyl-hydrogen phosphate (BNP)] and one zwitterionic compound (dansylated phenylalanine) in MEKC-UV to find the optimum molar concentration for polymerization. Next, MEKC-UV and MEKC-MS was compared for the enantioseparation of BNP. The influence of polymeric glucopyranoside-based surfactant head groups and carbon chain lengths on chiral *R<sub>s</sub>* was evaluated for two classes of cationic drugs (ephedrine alkaloids and  $\beta$ -blockers). Finally, enantioselective MEKC-MS of ephedrine alkaloids and  $\beta$ -blockers were profiled at their optimum pH 5.0 and 7.0, respectively using ammonium acetate buffer and optimum polymeric *n*- $\alpha$ -D-glucopyranoside surfactant. The LOD for most of the enantiomers ranges from 10 ng/mL-100 ng/ml with *S/N* of at least  $\geq 3.0$ .

## 2.1. Introduction

Increasing concerns on the resolution, sensitivity and structural identification of pharmaceutical drugs boosted the recent development of different types of chiral stationary phases for HPLC-MS [2-4]. However, over the years, CE-MS has emerged as a good alternative [5-7] because this microscale hyphenation technique provide efficient and low-cost assays,

which is particularly attractive in clinical settings where reduced requirement of biological samples and solvent consumptions is a contributing factor in future analysis of biological activity, *in vivo* studies and toxicity evaluation of pharmaceutical drugs.

The technique of CE-MS can be employed in two main approaches. The first approach is most common in which simply the chiral selector or chiral surfactant is added to the volatile buffer solution (aka. EKC-MS or MEKC-MS) [5-7]. The second approach involves the use of bonded or immobilized chiral selector on the capillary column (aka, CEC-MS), which presents high sensitivity and greater sample loading capacity [8-10]. There is potential in both EKC-MS or MEKC-MS as well as CEC-MS to improve with the development of new chiral selectors for the separation and sensitive detection of a large number of chiral compounds. Nevertheless, in all three aforementioned approaches of CE-MS, exotic chiral selector could be used to understand chiral separation and developed new chiral assays at much lower cost and high efficiency compared to HPLC-MS.

Among the different chiral selectors added to the volatile buffers in EKC-MS, cyclodextrins [11] and crown ethers [12] are useful at low micromolar concentrations, perhaps because they prevent ion suppression of the low molecular weight chiral selectors. Polymeric amino acid based surfactants (aka. molecular micelles, MoMs) are a promising class of chiral selector, which has significant advantages for MEKC-MS over conventional low molecular mass chiral selectors (e.g., cyclodextrins and crown ethers). First, they are covalently stabilized micellar aggregates with zero CMC, which can be used over a wide concentration range in MEKC-MS [13]. Second, due to high molecular weight they are not fragmented in the gas phase of ESI-MS [7,14,15]. Thus, the key to development of EKC-MS or MEKC-MS approaches is to

identify chiral selectors, which provide high separation selectivity and are MS compatible for sensitive detection of chiral compounds.

In this work, the synthesis, characterization and application of four new sugar-based polymeric chiral surfactants is described for MEKC-MS. Although unpolymerized dodecyl glucopyranoside-based surfactants was previously reported for chiral separations in MEKC-UV [16], to the best of our knowledge, poly (*n*-alkyl- $\alpha$ -D-glucopyranoside, sodium salt) based surfactants have never been studied as chiral selectors for MEKC-MS. To achieve high separation selectivity, we investigated the polymerization concentration of the surfactants monomers, two different head groups and two different chain lengths of the surfactant as well as buffer pH. The chiral separation of 1,1'-binaphthyl-2,2'-diyl-hydrogen phosphate (BNP) using the polymeric glucopyranoside-based surfactants in MEKC with UV and MS detection is compared. As illustrated, the use of optimum polymeric glucopyranoside based surfactant in MS gave higher enantioselectivity and efficiency with lower LOD for ten racemates.

## **2.2. Materials and methods**

### **2.2.1 Reagents and chemicals**

Racemic mixture and individual isomers of ephedrine alkaloids (norephedrine, pseudoephedrine, ephedrine, and methylephedrine),  $\beta$ -blockers (atenolol, metoprolol, carteolol, and talinolol) and 1,1'-binaphthyl-2,2'-diylhydrogen-phosphate (BNP), analytical-grade ammonium acetate (as 7.5 M NH<sub>4</sub>OAc solution) and HPLC grade methanol (MeOH) were all obtained from Sigma-Aldrich (St. Louis MO, USA). Racemic mixture of dansyl phenylalanine was purchased from Santa Cruz Biotechnology (Dallas, Texas, USA). Sodium phosphate dibasic heptahydrate and sodium phosphate monobasic monohydrate were purchased from Fisher Scientific (Fair Lawn, NJ, USA). Ammonium hydroxide and acetic acid were supplied by Fisher

Scientific (Springfield, NJ, USA). All four vinyl surfactant monomers (i.e., octyl and undecylenyl phosphated and sulfated sugar surfactants) were polymerized under 20 Mrad of  $^{60}\text{Co}$   $\gamma$ -radiation by Phoenix Memorial Laboratory (University of Michigan, Ann Arbor, MI).

The chemicals and reagents used for synthesis,  $\beta$ -D-glucose pentaacetate (98%), sulfur trioxide pyridine complex (98%), 10-undecen-1-ol (98%), phenyl dichlorophosphate (95%), boron trifluoride etherate (46.5%  $\text{BF}_3$  basis), hexane, ethyl acetate (EtOAc), methanol anhydrous, tetrahydrofuran (THF) anhydrous, sodium sulfate ( $\text{Na}_2\text{SO}_4$ ) pyridine anhydrous, dichloromethane anhydrous, Amberlyst® 15 hydrogen form were all purchased from Sigma-Aldrich (St. Louis MO, USA). The reagent, 7-Octen-1-ol (96%) was obtained from TCI America (Tokyo, Japan). Sodium bicarbonate (99.7%) and sodium hydroxide (NaOH, 50% v/v) were purchased from Fisher Scientific (Fair Lawn, NJ, USA). Triply deionized (DI) water used in this experiment was obtained from Barnstead Nanopure II water system (Barnstead International, Dubuque, IA, USA).

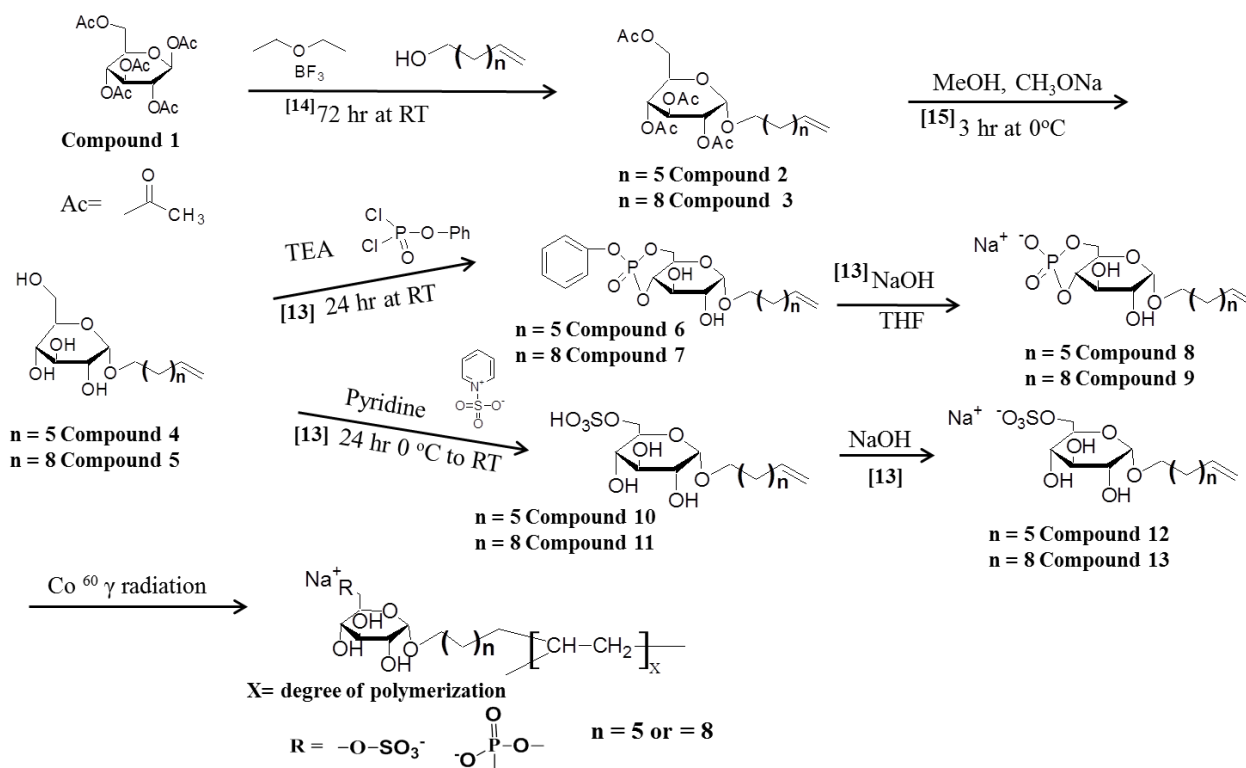
### **2.2.2 Synthesis of *n*-undecenyl and *n*-octenyl- $\alpha$ -D-glucopyranoside 4,6-hydrogen phosphate sodium salt, *n*-undecenyl and *n*-octenyl- $\alpha$ -D-glucopyranoside 6-hydrogen sulfate, monosodium salt.**

Both phosphated and sulfated sugar surfactants with eight and eleven chain lengths were synthesized with some modifications of the literature protocols [16,17,18] as detailed below.

#### **2.2.1 Synthesis of compounds 2 and 3**

The compounds **2** and **3** were synthesized according to step 1 of Scheme 2.1. A solution of 10-undecen-1-ol (3.9 mL, 0.0195 mol) or 7-octene-1-ol (2.9 mL, 0.0195 mol), and 8.0 mL (0.065 mol) boron trifluoride etherate were added to a stirring solution of 5g (0.013 mol)  $\beta$ -D-glucose pentaacetate in 50 mL dry dichloromethane under nitrogen. The resulting solution was then stirred

for 72 hrs under a blanket of nitrogen at room temperature. The mixture was neutralized by 250 mL saturated sodium bicarbonate solution (30 g, 0.36 mol) and then washed with 200 mL H<sub>2</sub>O. The lower organic layer was then dried with 10g Na<sub>2</sub>SO<sub>4</sub> and concentrated in vacuo. The residue was purified by column chromatography [SiO<sub>2</sub>, hexane-EtoAc, 1:3] to yield pure compound 2, *n*-undecenyl  $\alpha$ -D-glucopyranoside pentaacetate (1.9g, 29%) and compound 3, *n*-octenyl- $\alpha$ -D-glucopyranoside pentaacetate (1.5 g, 25 %).



**Scheme 2.1.** Synthesis of poly *n*-alkyl  $\alpha$ -D-glucopyranoside 4,6-hydrogen phosphate, sodium salt ( $\alpha$ -SUGP) and poly *n*-alkyl  $\alpha$ -D-glucopyranoside 6-hydrogen sulfate, monosodium salt ( $\alpha$ -SUGS).

### 2.2.2 Synthesis of compounds 4 and 5

The intermediate **2** and **3** were deacetylated in the presence of 20 mL anhydrous methanol and 1mL sodium methoxide solution (25%) under nitrogen for 3 hrs in ice bath. The resulting

reaction was then neutralized by 2g Amberlyst®15 hydrogen resin, filtered and concentrated in vacuo. The residue was purified by column chromatography [SiO<sub>2</sub>, EtoAc-MeOH, 10:0.5] to yield the pure intermediate **4**, undecenyl  $\alpha$ -D-glucopyranoside (1.1 g, 87%) and **5**, *n*-octenyl  $\alpha$ -D-glucopyranoside (0.82 g, 87 %).

### 2.2.3 Synthesis of product 6 and 7

To synthesize product **6** and **7**, phenyl dichlorophosphate (0.55 mL, 0.0037 mol) and dry triethylamine (0.69 mL, 0.0050 mL) was added to the solution containing intermediate **4** (1.1g, 0.0033 mol) or intermediate **5** (0.82 g, 0.0028 mol) in 20 mL of dichloromethane. The resulting solution was then stirred for 22 hrs under nitrogen to yield intermediate **6**, *n*-undecenyl  $\alpha$ -D-glucopyranoside 4,6-phenyl phosphate and **7**, *n*-octenyl  $\alpha$ -D-glucopyranoside 4,6-phenyl phosphate. The resulting reaction was concentrated in vacuo and then purified by column chromatography [SiO<sub>2</sub>, hexane- EtoAc, 2:1] to yield the pure intermediate **6** (1.0 g, 64%) and **7** (0.73 g, 61 %).

### 2.2.4 Synthesis of product 8 and 9

The product **8** *n*-undecenyl- $\alpha$ -D-glucopyranoside 4, 6-hydrogen phosphate, sodium salt and product **9**, *n*-octenyl- $\alpha$ -D-glucopyranoside 4, 6-hydrogen phosphate, sodium salt were formed by dissolving intermediates **6** (1.0 g, 0.0021 mol) and **7** (0.73 g, 0.0017 mol) in 20 mL THF and by stirring for 24 hrs in the presence of 5 mL NaOH (10%) solution. Finally, THF was removed by vacuo and the resulting solution of each product was neutralized by 1 M HCl and extracted with ethyl acetate for 3 times. Next, the bottom aqueous solution of  $\alpha$ -phosphate sugar surfactants were stirred for 1 day to remove trace ethyl acetate and lyophilized at  $-50$  °C collector temperature and 0.05 mbar pressure for 2 days to yield pure final product **8** (0.8g, 90%) and **9** (0.56 g, 88%)

### 2.2.5 Synthesis of product 10 and 11

To synthesize product **10** and **11**, sulfur trioxide pyridine complex (0.63 g, 0.0040 mol) was added to the stirring solution containing 20 mL pyridine anhydrous and intermediate **4** (1.1 g, 0.0033 mol) or intermediate **5** (0.82 g, 0.0028 mol). The resulting reaction was stirred for overnight under nitrogen to yield intermediate **10**, *n*-undecenyl  $\alpha$ -D-glucopyranoside 6-hydrogen sulfate and **11**, *n*-octenyl  $\alpha$ -D-glucopyranoside 6-hydrogen sulfate. The resulting reaction was concentrated in vacuo and then purified by column chromatography [SiO<sub>2</sub>, EtoAc-MeOH-H<sub>2</sub>O, 10:2:1] to yield the pure intermediate intermediate **10** (0.9 g, 66%) and **11** (0.59 g, 64%). .

### 2.2.6 Synthesis of product 12 and 13

The product **12** *n*-undecenyl- $\alpha$ -D-glucopyranoside 6-hydrogen sulfate, monosodium salt and product **13**, *n*-octenyl 6-hydrogen sulfate, monosodium salt was formed by the addition of 1 mL NaOH (10%) solution and was lyophilized at  $-50$  °C collector temperature and 0.05 mbar pressure for 2 days to yield pure final product **12** (0.9g, 95%) and **13** (0.59 g, 95%).

### 2.2.3 Characterization of $\alpha$ -D-Sugar Surfactants

The synthesized  $\alpha$ -D-sugar surfactants with different chain lengths and head groups were characterized by use of nuclear magnetic resonance (<sup>1</sup>H-NMR) spectroscopy and ESI-MS. The details of the characterization of intermediates and products of the four synthesized sugar surfactants could be found in the Supporting Information Figs. A1–13.

### 2.2.4 CE-MS instrumentation

#### 2.4.1 MEKC-UV and MEKC-MS conditions

The direct infusion ESI-MS experiments to obtain the deprotonated molecular ions [M-H]<sup>-</sup> of synthesized anionic sugar phosphated and sulfated surfactants could be found in Supporting Information Fig. A13a–d. The results discussed in Section 2.3.3 were carried out on an Agilent G1600 CE system (Agilent Technologies, Palo Alto, CA, USA) equipped with a



single quadrupole mass spectrometer. A typical procedure involves flushing 1 mg/mL of each synthesized surfactant (dissolved in triply deionized water) through a 60 cm long, 50  $\mu$ m id, fused-silica capillary at 50 mbar to the ESI sprayer interface and monitoring the ESI-MS spectrum of the synthesized surfactant. The details of MEKC-UV and MEKC-MS/MS instrumentation could be found in Supporting Information.

#### **2.4.2 Preparation of running MEKC-MS buffer and analyte solutions.**

For chiral separations of dansylated phenylalanine (DNS-PA) and BNP in MEKC, the stock solutions were prepared in pure MeOH at 2.0 mg/mL and then were diluted to 1.0 mg/mL in MeOH/H<sub>2</sub>O (50/50, v/v) and pressure injected at 5 mbar for 10 s. The separations were carried out under the normal polarity mode with an applied voltage of +20 kV. The background electrolytes (BGEs) for enantiomeric separation of DNS-PA consisted of 12.5 mM each of NaH<sub>2</sub>PO<sub>4</sub>/Na<sub>2</sub>HPO<sub>4</sub> buffer at pH 7.0. The final running MEKC buffer solution was prepared by addition of 45 mM poly- $\alpha$ -D-UGP at various polymerization concentrations (20 mM, 50 mM, 75 mM and 100 mM) to the BGE solution. The BGE for comparison of enantiomeric separation and sensitivity of BNP by MEKC-UV and MEKC-MS/MS was prepared in 20 mM NH<sub>4</sub>OAc solution by diluting 7.5 M NH<sub>4</sub>OAc stock solution in triply DI water and then adjusting to pH 10.8 by 13.4 M ammonium hydroxide. The final running MEKC buffer solution was prepared by adding 15 mM poly (*n*-undecyl  $\alpha$ -D-glucopyranoside 4,6-hydrogen phosphate, sodium salt) (poly- $\alpha$ -SUGP) to the BGE solution.

All MEKC-UV and MEKC-MS/MS experiments were performed under the normal polarity mode with an applied voltage of +20 kV. The ephedrine alkaloids,  $\beta$ -blockers and BNP were injected by applying a pressure of 5 mbar for 10 s. The final running MEKC-MS buffer for enantiomeric separation of BNP is the same as that in MEKC experiment. The BGEs for

enantiomeric separation of ephedrine alkaloids and  $\beta$ -blockers were 25 mM  $\text{NH}_4\text{OAc}$  prepared by diluting the 7.5 M  $\text{NH}_4\text{OAc}$  stock solution in triply DI water and then adjusted to pH 5.0 by acetic acid or to pH 7.0 by ammonium hydroxide, respectively. The final running MEKC-ESI-MS/MS buffer solutions for screening of enantioseparation were prepared by addition of 30 mM polymeric UGP, OGP, UGS or OGS to the BGE solutions. The composition and the flow rate of the sheath liquid were MeOH/ $\text{H}_2\text{O}$  (80/20, %v/v) containing 5 mM  $\text{NH}_4\text{OAc}$  at pH 6.8 and 5  $\mu\text{L}/\text{min}$ , respectively. Spray chamber parameters for BNP: nebulizer pressure: 3 psi, drying gas temp.: 250  $^\circ\text{C}$ , drying gas flow: 6 L/min; capillary voltage: -3000 V. For ephedrine alkaloids and  $\beta$ -blockers: nebulizer pressure: 3 psi, drying gas temp.: 200  $^\circ\text{C}$ , drying gas flow: 8 L/min; capillary voltage: +3000 V. The fragmentor voltage, collision energy and product ion formations for these analytes were optimized by optimizer software using Agilent LC-MS in flow injection mode. The details are tabulated in Table 2.1. The ESI-MS/MS detection was performed in the multiple reaction monitoring (MRM) negative ion mode. The sheath liquids were prepared by mixing 5 mM  $\text{NH}_4\text{OAc}$  aqueous solution with MeOH/ $\text{H}_2\text{O}$  (80/20, %v/v) for optimization study for BNP, ephedrines and  $\beta$ -blockers.

Table 2.1. Fragmentor voltage, collision energy and product ion formations for the analytes from optimization experiments using flow injection ESI-MS<sup>a)</sup>

Analyte	fragmentor voltage (V)	collision energy (eV)	MRM transition (m/z)
BNP	200	41	347.1 $\rightarrow$ 79.1
pseudoephedrine	88	25	166.1 $\rightarrow$ 115.1
ephedrine	88	25	166.1 $\rightarrow$ 115.1
norephedrine	64	17	152.2 $\rightarrow$ 117
methylephedrine	98	21	180.2 $\rightarrow$ 147.2
atenolol	137	25	267.2 $\rightarrow$ 145.2
metoprolol	107	17	268.2 $\rightarrow$ 116.2
carteolol	83	17	293.2 $\rightarrow$ 237.2
talinolol	98	13	364.3 $\rightarrow$ 308.3

## 2.3. Results and Discussion

### 2.3.1 Physicochemical Properties

Surface tension measurements were performed to evaluate the surface activity of all four  $\alpha$ -D-glucopyranoside-based surfactant in water at various molar concentrations. The surface tension of surfactants gradually decreases with increase in surfactant concentration and then reaches a plateau region, signaling micelle formation and the concentration of the break point represents the critical micelle concentration (CMC). As shown in Table 2.2, the values of CMC decreases in the following order:  $\alpha$ -SOGS >  $\alpha$ -SUGS >  $\alpha$ -SOGP >  $\alpha$ -SUGP, (where  $\alpha$ -SOGS is *n*-octenyl  $\alpha$ -D-glucopyranoside 6-hydrogen sulfate, monosodium salt;  $\alpha$ -SOGP is *n*-octenyl  $\alpha$ -glucopyranoside 4,6-hydrogen phosphate, sodium salt; and  $\alpha$ -SUGS is *n*-undecenyl  $\alpha$ -glucopyranoside 6-hydrogen sulfate, monosodium salt), suggesting that sulfate head group sugar surfactants have higher CMC than phosphate head group surfactants at equivalent surfactant chain length. This is perhaps due to increase in hydrogen bonding interactions, which decreases the repulsion between phosphate head groups within a micelle. The trend for chain length is in accordance with increased hydrophobicity owing to the extension of hydrocarbon chain from C<sub>8</sub> to C<sub>11</sub>. The CMC is lower for longer chain (i.e.,  $\alpha$ -SUGS and  $\alpha$ -SUGP), because it facilitates micelles formation at lower concentration and hence lower CMC. Aggregation number and polarity of both unpolymerized micelle and polymerized form of the four surfactants were calculated as reported earlier for amino acid surfactants [19]. With increase in chain of  $\alpha$ -D-glucopyranoside surfactants for each head group, aggregation increases and polarity decreases.

Table 2.2. Physicochemical properties of *n*-alkenyl  $\alpha$ -D-glucopyranoside monomers and polymers

	monomer			polymer		
	CMC (mM) <sup>a)</sup>	Aggregation # <sup>b)</sup>	Polarity( $I_1/I_3$ ) <sup>c)</sup>	CMC (mM) <sup>a)</sup>	Aggregation # <sup>b)</sup>	Polarity( $I_1/I_3$ ) <sup>c)</sup>
<b>C8 phosphated sugar</b>	20±2	86±10	1.019	0	50±10	1.023
<b>C11 phosphated sugar</b>	3.8±0.1	137±10	0.999	0	62±10	1.000
<b>C8 sulfated sugar</b>	58±4	71±10	1.007	0	34±10	1.039
<b>C11 sulfated sugar</b>	11±1	124±10	0.978	0	47±10	0.988

a) Critical micelle concentration is determined by the surface tension measurements

b) Aggregation number is determined by the fluorescence quenching experiment using pyrene as a probe and cetyl pyridinium chloride as a quencher.

c) Polarities of the surfactants are determined using ratio of the fluorescence intensity ( $I_1/I_3$ ) of pyrene.

### 2.3.2 Effect of Polymerization concentrations on chiral resolution and run time

It is well known that ionic MoMs facilitate the polymerization to produce high molecular weight polymers. The chiral recognition ability of MoM was characterized using two model test solutes (DNS-PA and BNP) using optimum pH and optimum buffer type by varying the analytical concentration of  $\alpha$ -SUGP monomers. The polymerization experiment was performed by varying the analytical concentrations at 20 mM, 50 mM, 75 mM and 100 mM  $\alpha$ -SUGP at a fixed dose of 20 Mrad of  $^{60}\text{Co}$ - $\gamma$ -radiation. Several interesting trends are noted in Fig. 2.1 when comparing the resolution and retention of two enantiomeric pairs. First, note that due to high reactivity of  $\alpha$ -SUGP monomers, even when polymerized at 20 mM (i.e., 5x CMC) provide significant retention of both chiral analyte was observed. Second, micelles formed using higher analytical concentration of  $\alpha$ -SUGP always resulted in longer run times irrespective of the type of chiral solute. This trend is primarily due to increase in aggregation number and hence hydrophobicity of the micelle. Note, that this effect of increasing migration time is less pronounced for BNP, (Fig. 2.1A right panel) compared to DNS-PA (Fig. 2.1B left panel).

Our hypothesis regarding the data shown in Fig. 2.1 is that when poly- $\alpha$ -SUGP micelles are used for chiral separation, the achiral hydrophobic tail, which is linked to a chiral linker (i.e., sugar moiety) does not participate in chiral separation, but it does contribute to experimentally observed retention of both enantiomers. The relatively higher increase in retention of DNS-PA compared to BNP suggests that the former enantiomeric pair is mainly retained by extensive contribution from nonenantioselective hydrophobic site of the MoMs. Consequently, the increase in enantiomeric resolution is smaller for DNS-PA than for BNP. Third, the enantioselectivity of BNP was observed at all surfactant concentration used for polymerization. On the other hand, the DNS-PA requires the use of micelles, which are formed using at least 12.5 times the CMC of  $\alpha$ -SUGP to show any hint of chiral resolution ( $R_s = 0.8$ ). To test the hypothesis on the data acquired above, a quantitative assessment of enantioselective versus non-enantioselective interaction in MEKC will be performed in our future communication using linear free energy relationship.

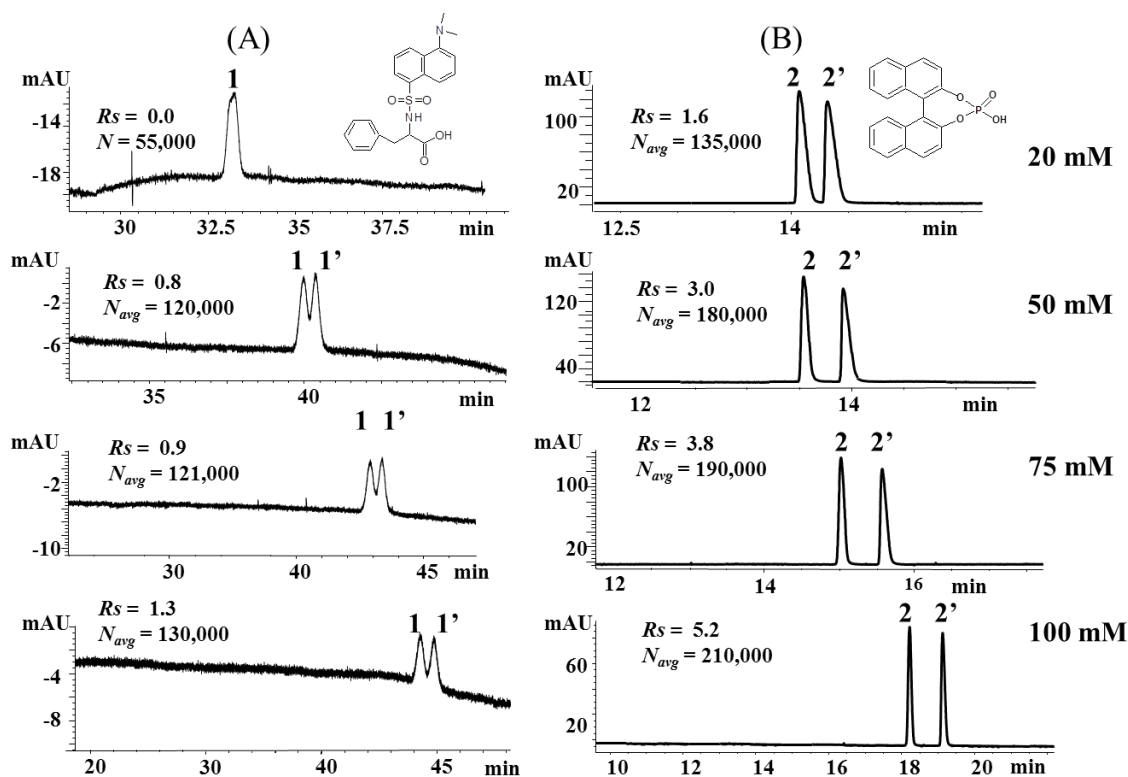


**Fig.2.1.** Effect of polymerization concentrations of SUGP surfactant monomers on chiral  $R_s$  of zwitterionic compound (dansyl phenylalanine) and anionic compound (BNP) in MEKC. Conditions: Panel (A): 56 cm effective length (375  $\mu$ m O.D., 50  $\mu$ m I.D.) fused silica capillary; sample concentration: 1.0 mg/mL in MeOH/H<sub>2</sub>O (50/50). Buffer: 12.5 mM NaH<sub>2</sub>PO<sub>4</sub> +12.5 mM Na<sub>2</sub>HPO<sub>4</sub>, pH 7.0, 45 mM poly- $\alpha$ -SUGP. Applied voltage: +20 kV, injection: 5 mbar, 10 s. Panel (B) sample concentration: 1.0 mg/mL in MeOH/H<sub>2</sub>O (50/50). Buffer: 20 mM NH<sub>4</sub>OAc, pH 10.8, 15 mM poly- $\alpha$ -SUGP. Conditions for applied voltage, injection and capillary dimensions are the same as panel A. Peak identification:  $I$  =  $R$ - DNS-PA,  $I'$  =  $S$ -DNA-PA,  $2$  =  $R$ -BNP,  $2'$  =  $S'$ -BNP.

### 2.3.3 Direct infusion ESI-MS of model test analyte

Our surface tension data suggest that sugar-based surfactants forming polymeric micelles are less surface active (surface tension  $\sim$  54 mN/m) and its surface tension is fairly constant in the studied range from 1-50 mM, compared to the corresponding unpolymerized micelles (surface tension  $\sim$  30 mN/m at the CMC) (data not shown). Thus, the lower surface activity of polymerized sugar micelles should reduce interferences in electrospray process. Therefore, these findings may have significant implications for sensitive CE-MS analysis of chiral compounds.

Fig. 2.2 compares the positive ion ESI-MS spectra (arbitrary y-units) of model test analyte, protonated DNS-PA ( $m/z = 397$ ) in the absence (2A) and presence of monomeric (unpolymerized  $\alpha$ -SUGP micelle, 2B) and polymeric (poly- $\alpha$ -SUGP, 2C).

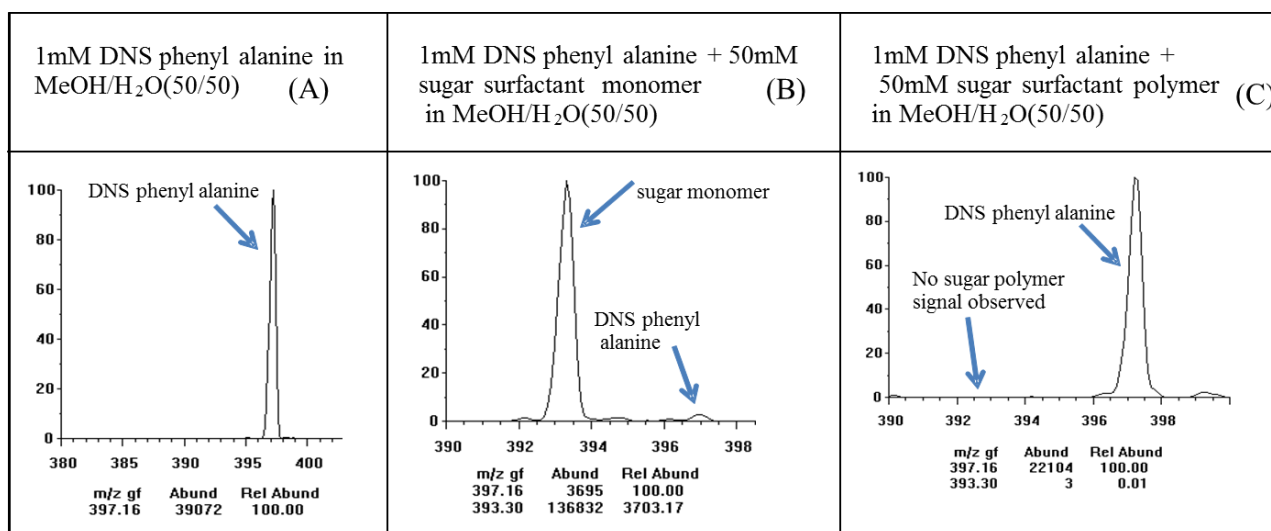


**Fig. 2.2.** Comparison of ESI-MS signal of DNS-PA obtained by direct infusion positive-ion ESI-MS in the presence of (A) no surfactant, (B) 50 mM unpolymerized  $\alpha$ -SUGP, and (C) 50 mM poly- $\alpha$ -SUGP.

Consistent with the surface tension data, significant ESI-MS suppression of protonated form of model test analyte, dansylated phenyl alanine (DNS-PA) was observed and the signal abundance of DNS-PA reduces from 39872 to only 3695, which is  $\sim 10\%$  in the presence of 50 mM of unpolymerized ( $\alpha$ -SUGP, Fig.2.2B). However, as evident from the right panel, the use of 50 mM poly- $\alpha$ -SUGP in the positive ion ESI-MS also suppresses the signal intensity of DNS-PA, but still 57% of the signal intensity (abundance = 22184) was observed (Fig.2.2C). This suggest that unlike commonly used low molecular weight selectors (e.g., sulfated  $\beta$ -CD, vancomycin, crown ether), direct infusion of the poly- $\alpha$ -SUGP into the ESI-MS does not

contaminate the ion source. Furthermore, no frequent MS cleaning is required. The absence of any monomer peak when infused with 50 mM poly- $\alpha$ -SUGP and no polymer peak observed at any upper  $m/z$  of the ESI-MS (Fig.2.1C) confirmed that the covalent bond formed between sugar surfactant monomers indeed generate a high molecular weight micelle, which is difficult to ionize during electrospray process. While 50 mM of chiral selector is only used for weakly binding analyte, we can state that for strongly binding analyte we could achieve excellent  $S/N$ , allowing trace level chiral drug detection as demonstrated in Section 2.3.4. Even with off-line MALDI-TOF we were unable to see any dimer or trimer peak of poly- $\alpha$ -SUGP. Direct infusion of poly- $\alpha$ -SUGP in the electrospray at much lower concentration (e.g., 25 mM), the signal intensity of DNS-PA was restored to 80% of its original value (data not shown).

#### **2.3.4 Comparison of MEKC-UV with MEKC-MS for chiral separations**

The UV absorbance is the most commonly used detection method for majority of chiral separations in MEKC. Although chiral MEKC-UV is inherently less sensitive than MEKC-MS, but the use of low molecular weight chiral selectors in MEKC-ESI-MS is detrimental and has several limitations [20]. For example, the low molecular weight selector produces abundant gas-phase molecular ions, which participate in charge competition as well as ion pair formation in the sprayer suppressing the analyte signal. It should be noted that the high molecular weight chiral polymeric surfactant (aka. MoMs) is nonvolatile but they are not fragmented in the ESI source. The benefit of using high molecular weight (e.g., >10 kDa) MoMs as chiral selector for MS is that the formation of covalent bond between vinyl terminated monomers in MoMs prevent fragmentation in the electrospray. Furthermore, MoMs are difficult to ionize and they migrate in a direction, which is opposite to EOF. Thus, the use of higher molecular weight chiral selector despite of being nonionizable and nonvolatile could provide very useful information about the



mass and structure associated with enantioseparation of unknown chiral compounds. On the other hand, UV cannot solve such identification problems. In fact, when samples containing contaminants are analyzed in MEKC-UV, several unknown peaks appear or coelutes in the electropherogram.

The binaphthyl derivative such as BNP is extensively used as asymmetric ligands in the synthesis of chiral catalysts and also employed as chiral probe solute in MEKC to evaluate the enantioselectivity of chiral stationary phase [21]. As is shown clearly in Fig. 2.3A and B, baseline chiral *Rs* has been achieved for BNP using poly- $\alpha$ -SUGP with ammonium acetate buffer in MEKC-UV and MEKC-MS/MS, respectively. However, MEKC-MS/MS using high molecular weight poly- $\alpha$ -SUGP provide higher efficiency and signal to noise ratio (*S/N*) even when injected at concentration ten folds lower than MEKC-UV. The levels of repeatability, which are expressed as the precision obtained under same operating condition was briefly investigated. Using BNP as a model test analyte for ten consecutive runs, the %RSD of migration time, peak area and resolution were 2.3, 20.5, and 2.2, respectively, without any normalization (Supporting Information Fig. A14).

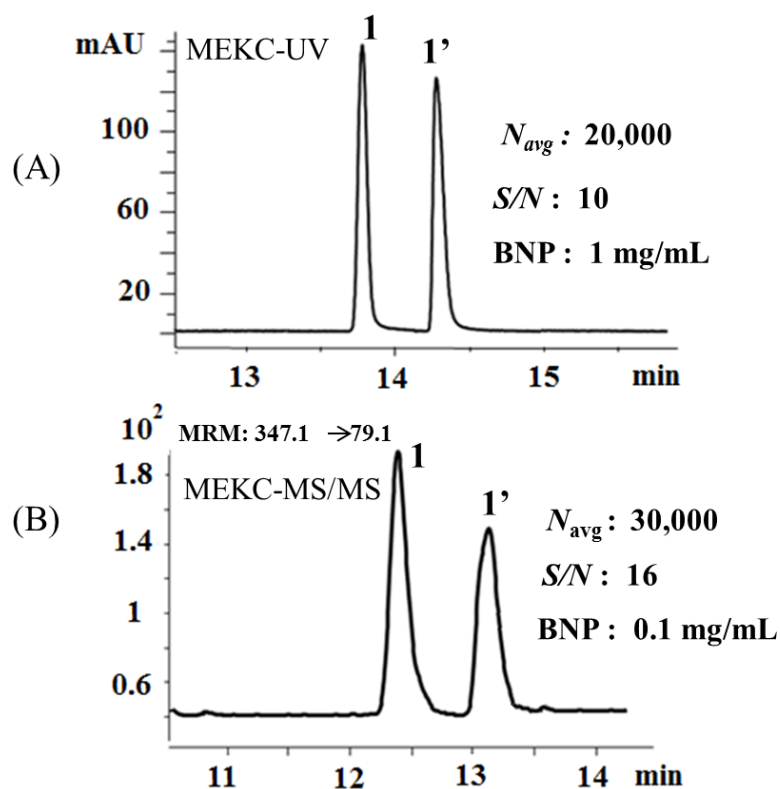


**Fig. 2.3** Comparison of MEKC-UV (A), and MEKC-MS/MS (B) for chiral separation of BNP. Conditions: (A) 56 cm effective length (375  $\mu\text{m}$  O.D., 50  $\mu\text{m}$  I.D.) fused silica capillary. BNP concentration: 1.0 mg/mL in MeOH/H<sub>2</sub>O (50/50). Buffer: 20 mM NH<sub>4</sub>OAc, pH 10.8, 15 mM poly- $\alpha$ -D-UGP. Applied voltage: +20 kV, injection: 5 mbar, 10 s. The capillary dimension in (B) are the same as (A) except for 60 cm effective length fused silica capillary. BNP concentration: 0.1 mg/mL in MeOH/H<sub>2</sub>O (50/50, v/v). Spray chamber parameters: nebulizer pressure: 3 psi; drying gas temp: 250  $^{\circ}\text{C}$ , drying gas flow rate: 6 L/min; capillary voltage: -3000 V; fragmentor voltage: 200 V, collision energy: 41 eV, MRM transition: 347.1  $\rightarrow$  79.1. Sheath liquid: MeOH/H<sub>2</sub>O (80/20, v/v), 5 mM NH<sub>4</sub>OAc, pH 6.8 with a flow rate of 0.5 mL/min. Peak identification: 1 = R-BNP, 1' = S'-BNP.

### 2.3.5 Effect of chain length and head groups of sugar surfactants on chiral separations

Four polymeric sugar surfactants with two different head groups (phosphate and sulfate) and two chain lengths (C<sub>8</sub> and C<sub>11</sub>) were selected to separate ephedrine alkaloids under the same

CE conditions to find out the optimum head group and chain length. The bar plots in Fig. 2.4 A and 2.4B compare the chiral  $R_s$  of four ephedrine alkaloids and four  $\beta$ -blockers, respectively, when the four polymeric sugar surfactants were used as chiral selector in MEKC-MS/MS. From Fig. 2.4A, polymeric  $\alpha$ -SUGP has the highest chiral  $R_s$  values among all of the four surfactants for all ephedrine alkaloids. Note, poly  $\alpha$ -SUGS gave baseline chiral  $R_s$  for norephedrine only, whereas partial  $R_s$  was obtained for methylephedrine and norephedrine using  $\alpha$ -SUGS and  $\alpha$ -SOGS, respectively. However, no chiral  $R_s$  was observed when using polymeric  $\alpha$ -SOGP.

Similarly, in Fig. 2.4B, the highest chiral  $R_s$  value was again achieved by poly  $\alpha$ -SUGP for the four  $\beta$ -blockers. Using the other three polymeric surfactant, only atenolol provided partial chiral  $R_s$  irrespective of the chain length and head group. Therefore, it could be concluded that poly  $\alpha$ -SUGP is the optimum chiral selector among the four surfactants for the enantioseparations of ephedrine alkaloids and  $\beta$ -blockers. Furthermore, it is noted that poly  $\alpha$ -SUGP with phosphate head group and C<sub>11</sub> chain length are better resolved than poly  $\alpha$ -SUGS using sulfate head group with equivalent chain length with regard to enantioseparations of BNP (data not shown). This could be explained by the fact that phosphate head group has a more rigid bicyclic structure than sulfate group [16], which contributes to higher enantioseparation and better interaction between poly  $\alpha$ -SUGP and the analytes.

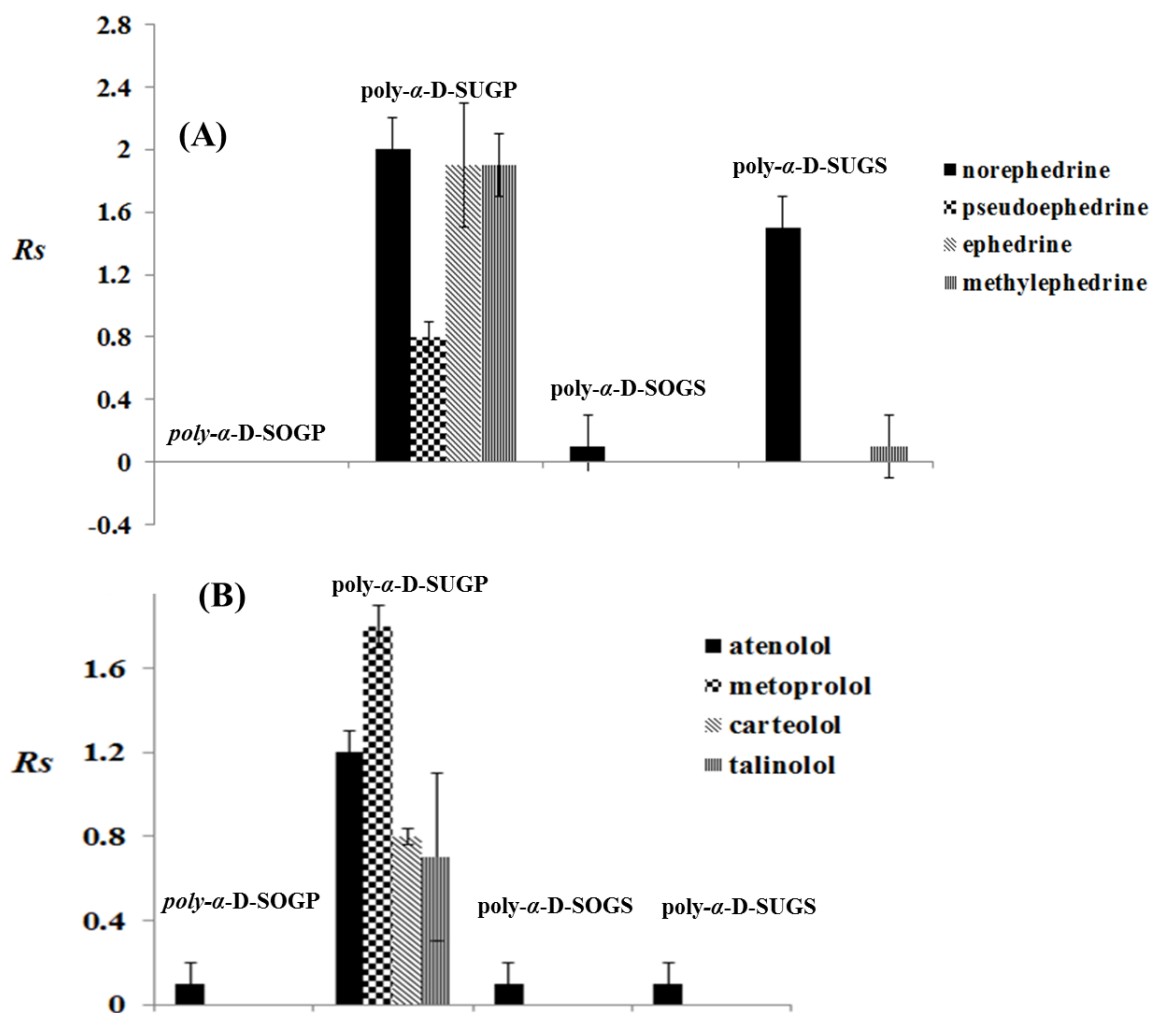


**Fig. 2.4** Bar plots illustrating the effect of chain length and head groups of sugar surfactants on chiral  $R_s$  of ephedrine alkaloids in MEKC-MS/MS. Conditions: 75 cm long (375  $\mu$ m O.D., 50  $\mu$ m I.D.) fused silica capillary. Buffer: 25 mM  $\text{NH}_4\text{OAc}$ , pH 5.0, 30 mM polymeric SUGP, SUGS, SOGP and SOGS. Applied voltage, +20 kV, injection, 5 mbar, 10 s. Spray chamber and sheath liquid conditions are the same as Fig. 3. Sample concentration: 10  $\mu$ g/mL in MeOH/ $\text{H}_2\text{O}$  (10/90, v/v). (B) Bar plots illustrating the effect of chain length and head groups of sugar surfactants on chiral  $R_s$  of  $\beta$ -blockers in MEKC-MS/MS. Conditions and spray chamber parameters are the same as Fig. 2 except 25 mM  $\text{NH}_4\text{OAc}$  adjusted to pH 7.0 by  $\text{NH}_4\text{OH}$ . Fragmentor voltage, collision energy and product ion formations of ephedrine and  $\beta$ -blockers are listed in Table 2.2.

### 2.3.6 Effect of buffer pH

The effect charge on the chiral analyte and chiral polymeric surfactant as well as the magnitude of the electroosmotic flow (EOF) are greatly affected by the pH of the volatile BGE.

According to previous study in our group using amino acid based polymeric surfactants [19, 22-23], the enantioseparation of ephedrine alkaloids and  $\beta$ -blockers were achieved at pH 6.0 and 8.8, respectively using ammonium acetate buffer. Thus, pH ranges were investigated from 5.0 to 6.0 for ephedrine alkaloids and 6.0 to 9.5 for  $\beta$ -blockers using poly  $\alpha$ -SUGP.

Fig. 2.5A shows the chiral  $R_s$  of ephedrine alkaloids vs. buffer pH. The  $R_s$  value of four ephedrine alkaloids decreased with the increase of pH from 5.0-6.0. This is because increasing pH increases the EOF resulting in faster electroosmotic mobility and weaker interactions with poly  $\alpha$ -SUGP. The chiral  $R_s$  of  $\beta$ -blockers vs. buffer pH is shown in Fig. 2.5B. As stated earlier, the increase in EOF of ammonium from 5.0 to 6.0 caused decreasing enantioseparation of ephedrine alkaloids. However, the  $\beta$ -blockers seem to encounter the most favorable (fastest) EOF at pH 7.0 compared to pH 6.0. Further increase in pH from 7.0 to 9.5 (by titration with  $\text{NH}_4\text{OH}$ ) caused an increase in ionic strength because at higher pH values the buffer solution also contains excess of ammonium ions and hydroxide ions resulting in much slower electroosmotic mobility. Consequently increasing migration time and decreasing the chiral  $R_s$ . Thus, the majority of  $\beta$ -blockers provided highest  $R_s$  value at pH 7.0.

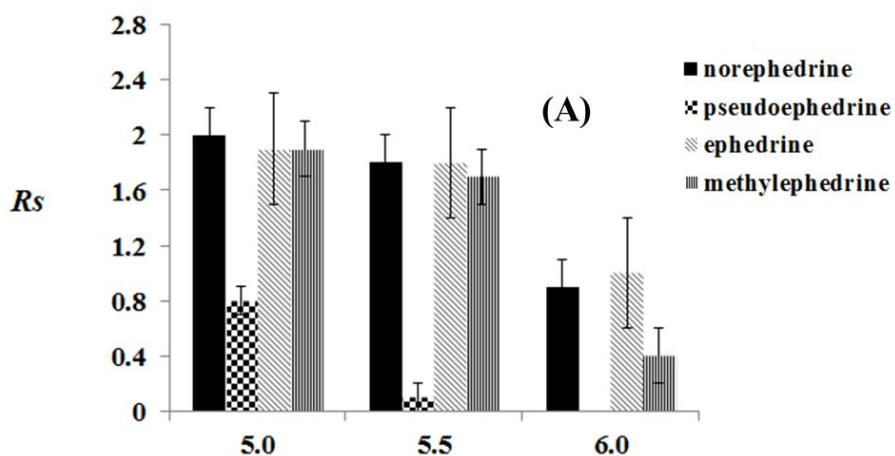


**Fig. 2.5** (A) Bar plots illustrating the effect of pH on chiral *Rs* of ephedrine alkaloids in MEKC-MS/MS. Buffer conditions and spray chamber parameters are the same as in Fig. 2.3 (A) except 30 mM poly- $\alpha$ -D-UGP was used at pH 5.0, 5.5 and 6.0. (B) Bar plots illustrating the effect of pH on chiral *Rs* of  $\beta$ -blockers in MEKC-MS/MS. Conditions and spray chamber parameters are the same as in Fig. 2.4 (B) except 30 mM poly- $\alpha$ -D-UGP was used in the pH range of 6.0 to 9.5.

### 2.3.6.1 Optimum chiral MEKC-MS/MS of ephedrine alkaloids and beta blockers

Using 25 mM poly  $\alpha$ -SUGP at optimum pH 5.0 in MEKC-MS/MS the enantioresolutions and enantioselectivity of four ephedrine alkaloids follows the decreasing order: (methylephedrine > epdedrine ~ norephedrine > pseudoephedrine) in MEKC-MS/MS (Fig.2.6). The enantiomer pair of ephedrine and pseudoephedrine has the same precursor and the daughter ions. Thus, neither mass (accurate mass) nor MS/MS could distinguish the two pairs of enantiomers. The simultaneous baseline separation based on MEKC retention of pseudoephedrine from ephedrine prevents any cross talk of daughter ions. This would allow the

two isomers to be quickly identified and quantitated in biological samples. The pseudoephedrine enantiomers has partial  $R_s$  of 0.9 but still it was well resolved from ephedrine enantiomers. The other three enantiomers were baseline separated with methylephedrine being the longest retained and norephedrine is the shortest retained among all four chiral analytes.

Fig. 2.7 shows the electropherograms of the enantioseparations of four  $\beta$ -blockers: atenolol, metoprolol, carteolol and talinolol using the optimum 25 mM poly  $\alpha$ -SUGP at optimum pH 5.0. Interestingly, polymeric SUGP is capable of separating these  $\beta$ -blockers based on their hydrophobicity ( $\log P$ ). Note that the migration time increases in the order of increasing retention: atenolol < carteolol < metoprolol < talinolol, which is consistent with the  $\log P$  (atenolol: 0.34 < carteolol: 1.34 < metoprolol < 1.63 < talinolol: 2.98). However,  $R_s$  and  $\alpha$  trends do not seem to follow the  $\log P$  order. The chromatograms shown in Supporting Information Table 2.1 indicate that LOD is analyte dependent and ranges from 10 – 100 ng/mL, which could be further improved using preconcentration techniques.

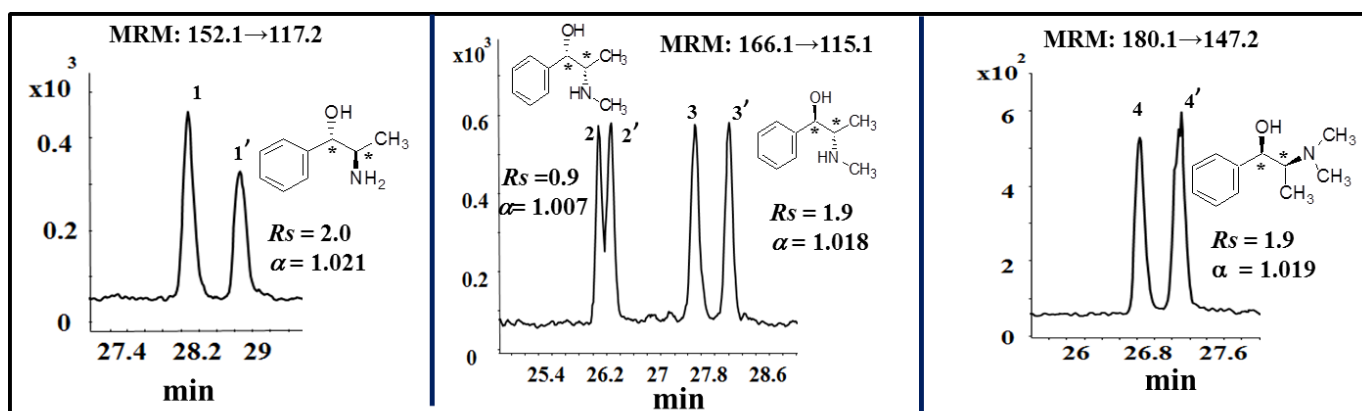


**Fig. 2.6** Electropherograms for enantioseparation of ephedrine alkaloids using sugar surfactant with optimum head group and chain length at optimum pH 5.0 in MEKC-MS/MS. Conditions and spray chamber parameters are the same as Fig.2.5 (A) except 30 mM poly- $\alpha$ -D-UGP was employed. Peak identifications: 1 = (*1R,2S*)-(-)norephedrine, 1' = (*1S,2R*)-(+)-norephedrine, 2 = (*1R,2R*) (-)pseudoephedrine, 2' = (*1S,2S*)(+) pseudoephedrine; 3 = (*1R,2S*)-(-)ephedrine, 3' = (*1S,2R*)-(+)-ephedrine; 4 = (*1R,2S*)-(-)*N*-methylephedrine, 4' = (*1S,2R*)-(+)*N*-methylephedrine.

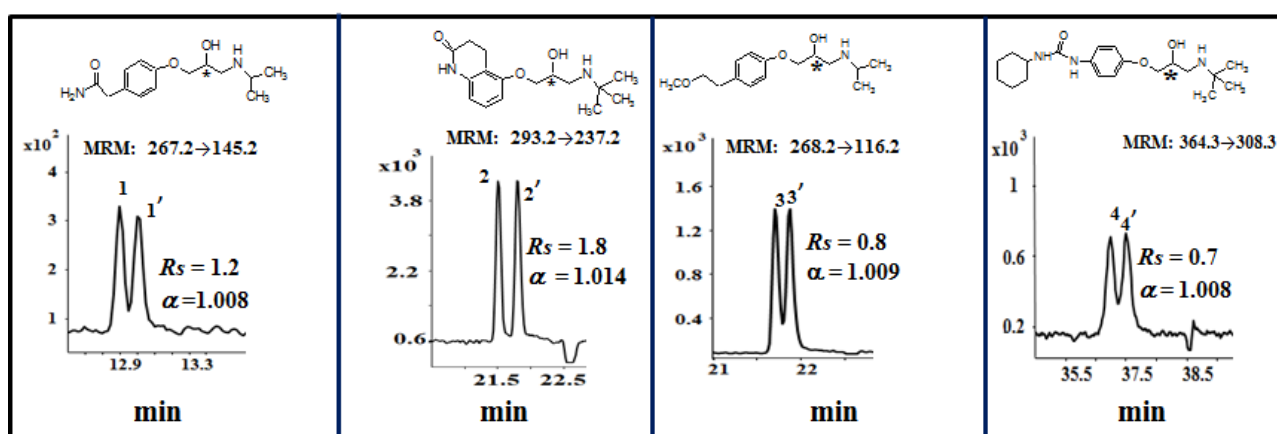


**Fig. 2.7** Electropherograms for enantioseparation of  $\beta$ -blockers using sugar surfactant with optimum head group and chain length at optimum pH 7.0 in MEKC-MS/MS. Conditions and spray chamber parameters are the same as Fig.5 (B) except 30 mM poly- $\alpha$ -D-UGP was employed. Peak identifications: 1,1' = atenolol, 2,2' = carteolol, 3,3' = metoprolol, 4,4' = talinolol. For each  $\beta$ -blocker the *R*-enantiomer always eluted first than *S*-enantiomer.

## 2.4 Concluding remarks

Four polymers of  $\alpha$ -D-glucopyranoside based surfactants were synthesized, characterized and screened for chiral analysis in MEKC-MS. The use of polymers instead of the monomers of the same surfactants shows significantly enhanced signal intensity in ESI-MS. The addition of poly- $\alpha$ -SUGP at pH 5.0 and pH 7.0 to the MEKC-MS buffer provided the optimum separation of



two classes of analytes such as ephedrine alkaloids and  $\beta$ -blockers, respectively. While only ten runs were performed to test the repeatability of chiral analysis, the results could be improved further using absolute migration time and standardization of peak areas. Furthermore, the use of a chemically modified capillary with buffer containing sugar surfactant polymers as pseudophase is in progress in our laboratory.

## References

- [1] Ishihama, Y., Katayama, H., Asakawa, N. *Anal. Biochem.* 2000, 287, 45-54.
- [2] Zhang, X., Luo, F., Luo, Z., Lu, M., Chen, Z., *J. Chromatogr. A* 2014, 1359, 212-223.

- [3] Li, Y., Dong, F., Liu, X., Xu, J., Li, J., Kong, Z., Chen, X., Liang, X., Zheng, Y. *J. Chromatogr. A* 2012, 1224, 51-60.
- [4] Yu, J., Han, K. S., Lee, G., Paik, M. J., Kim, K. R., *J. Chromatogr. B* 2010, 878, 3249-3254.
- [5] Wuethrich, A., Haddad, P. R., Quirino, J. P., *Electrophoresis* 2014, 35, 2-11.
- [6] Wang, X., Hou, J., Jann, M., Hon, Y., Shamsi, S. A., *J. Chromatogr. A* 2013, 1217, 207-216.
- [7] He, J., Shamsi, S. A., *J. Sep. Sci.* 2009, 32, 1916-1926.
- [8] Zhang, Y., Huang, L., Chen, Q., Chen, Z., *Chromatographia* 2012, 75, 289-296.
- [9] Gu, C. Y., Shamsi, S. A., *Electrophoresis* 2011, 32, 2727-2737.
- [10] Zheng, J., Bragg, W., Hou, J. G., Lin, N., Chandrasekaran, S., Shamsi, S. A., *J. Chromatogr. A* 2009, 1216, 857-872.
- [11] Giuffrida, A., Leon, C., Garcia-Canas, V., Cucinotta, V., Cifuentes, A., *Electrophoresis* 2009, 30, 1734-1742.
- [12] Xia, S., Zhang, L., Lu, M., Qiu, B., Chi, Y., Chen, G., *Electrophoresis* 2009, 30, 2837-2844.
- [13] He, J., Shamsi, S. A. *J. Chromatogr. A* 2009, 1216, 845-856.
- [14] Hou, J., Zheng, J., Shamsi, S. A., *J. Chromatogr. A* 2007, 1159, 208-216.
- [15] Rizvi, S. A. A., Zheng, J., Apkarian, R. P., Dublin, S. N., Shamsi, S. A., *Anal. Chem.* 2007, 79, 879-898.
- [16] Tickle, D.C.; Okafo, N.G.; Camilleri, P.; Jones, R.F.D.; Kirby A.J., *Anal. Chem.* 1994, 66, 4121-4126.

- [17] Li, X., Turanek, J., Knotigova, P., Kudlackova, H., Masek, J., Pennington, D.B., Rankin, S.E., Knutson, B.L., Lehmler, H.J., *New J. Chem*, 2008, 32, 2169-2179.
- [18] Didier, D., Florence, D., *J. Phytochemistry* 1994, 36, 289-298.
- [19] Rizvi, S.A.A., Shamsi, S.A., *Electrophoresis* 2003, 24, 2514-2526.
- [20] Shamsi, S. A., *Anal. Chem.* **2001**, 73 , 5103–5108.
- [21] Billiot, E., Thibodeaux, S., Warner, I.M., *Anal.Chem.* 1999, 71, 4044-4049.
- [22] Rizvi, S. A.A., Shamsi, S. A., *Electrophoresis* 2005, 26, 4172-4186.
- [23] Hou, J. Zheng, J., Rizvi, S.A.A., Shamsi, S. A., *Electrophoresis* 2007, 28, 1352-1363.

## Chapter 3

# **Chiral Capillary Electrophoresis-Mass Spectrometry: Turning an Analytical Technique into High Throughput Screening of Chiral Compounds Using Novel Polymerized $\beta$ -D-Glucopyranoside Surfactants**

Polymeric glucopyranoside based surfactants have been successfully employed as chiral selector in micellar electrokinetic chromatography-mass spectrometry (MEKC-MS/MS). The  $\beta$ -D-alkyl-glucopyranoside based surfactants, containing charged head groups such as sodium-*n*-alkyl  $\beta$ -D-glucopyranoside 4,6-hydrogen phosphate, sodium salt and *n*-alkyl  $\beta$ -D-glucopyranoside 6-hydrogen sulfate, monosodium salt were able to enantioseparate 21 cationic drugs and 8 binaphthyl atropisomers (BAIs) in MEKC-MS/MS, which promises to open up the possibility of turning an analytical technique into high throughput screening of chiral compounds. Physicochemical properties and enantioseparation capability of  $\beta$ -D-glucopyranoside based surfactants with different head groups and chain lengths were compared. Moreover, the comparison of  $\alpha$ - and  $\beta$ -D-glucopyranoside 4,6-hydrogen phosphate, sodium salt were further explored with regard to enantioseparations of ephedrine alkaloids and b-blockers. The concept of multiplex chiral MEKC-MS for high throughput quantitation is demonstrated for the first time in scientific literature.

### 3.1 Introduction

Chirality on analytical scale is a major concern in pharmaceutical industry due to different pharmacological activities of enantiomers such as pharmacokinetic and pharmacodynamics studies [1]. Nearly 56% of the pharmaceuticals currently used are chiral compounds. There has been eminent push in developing racemic chiral switches, still nearly 50% of these synthetic drugs used therapeutically are racemates [2-3]. Furthermore, the US Food and Drug administration as well the International Conference of Harmonization recommends that a given methodology for quality control of a new chiral drug must be able to detect at least 0.1 % of enantiomeric impurity in an active enantioselective pharmaceutical [4].

The UV detection is the mostly used for chiral CE mainly due to its simplicity and low cost. However, lack of sensitivity due to short path length (i.e., 25-100  $\mu\text{m}$ ), matrix effects in biological fluids, lack of structural information have limited the use of this detector for analysis of chiral compounds. Therefore, there is an urgent need to develop new approaches not only for chiral separation but also achieving high detection sensitivity of chiral compounds used in therapeutics and diagnostics.

Mass spectrometry (MS) is a useful approach for achieving low detection sensitivity of enantiomers. Furthermore, extract ion electropherogram in single ion monitoring mode provides matrix free detection of enantiomers in biological fluids and identify the enantiomers by its mass to charge ratio ( $m/z$ ) ratio as long as they are well separated and structural information by MS/MS fragmentation pattern. While chiral reagents (cyclodextrins, macrocyclic antibiotics and crown ethers) are very popular and effective chiral selectors but none of these aforementioned low molecular weight CE-UV reagents are fully compatible with MS and the loss of sensitivity due to ion suppression is still a problem. To avoid this problem, several approaches are employed: (a) counter migration techniques in which chiral selector migrate away from the detector [5], (b) partial filling technique in which only a part of the capillary is filled with a plug of chiral selector [6], (c) low flow sheathless interface [7]; (d) high molecular weight polymeric surfactants [8].

The ability of molecular micelles  $M_oM_s$  as reagents for chiral separations (CE or MEKC) is explored for just over two decades. Wang and Warner [9], Shamsi and Warner [10], Billiot and Warner [11-12], are among the first few scientists to discuss the enantioselectivity of chiral amino acid (AA) and dipeptide (DP) polymeric surfactants for chiral separations in MEKC. Later, a new generation of amino acid (AA) based  $M_oM_s$  with carbamate linker was introduced

by Akbay and Shamsi [13], which improve enantioresolution and decrease tailing of a variety of basic drugs (e.g, ephedrine alkaloids and  $\beta$ -blockers) [13, 14]. The development of amino acids  $M_oM_s$  containing amide or carbamate linkers with different head group charge and chain length has enabled the synthesis of many new AA based  $M_oM_s$  for fundamental studies and their separation performance is well demonstrated in MEKC with UV detection [15].

The use of AA-based  $M_oM_s$  as pseudostationary phase was proposed for chiral MEKC-MS by our research group as early as 2001 [8]. In spite of higher degree of MS compatibility of using AA and dipeptide based  $M_oM_s$  for MEKC-MS, there is a need to develop new chiral selectors to extend the window for separations of structurally diverse chiral analytes. In this work, we introduce a new generation of MS compatible vinyl terminated  $\beta$ -D glucose based surfactants (*n*-alkenyl-glucoopyranoside) as chiral  $M_oM_s$  for chiral MEKC-MS. Several key advantages of this new generation of glucoopyrnaoside based  $M_oM_s$  are noted: (a) multiple stereogenic centers favors enantioseparation of diverse group of analytes; (b) environmental friendly and low surface tension, thus high surface activity compared to their corresponding monomers; (c) due to zero critical micelle concentration (CMC) the chiral  $M_oM_s$  can be used at significantly lower concentration resulting in lower operating current for CE-MS; (d) separation of multichiral center compounds using only a single chiral selector is possible. In particular, the advantages (b) and (c) noted above enables this class of  $M_oM_s$  to be fully compatible with electrospray ionization (ESI)-MS. Several enantioseparation parameters such as head group charge, chain length and anomeric configurations of *n*-alkyl  $\beta$ -D- glucoopyranoside is varied to understand the effect of these parameters on chiral recognition for a diverse group of cationic compounds (primary amines, secondary, amino alcohols and quaternary amines) as well as various structural analogs of anionic and neutral biaryl atropisomers (BAIs). New strategy based

on multiplex injection allowing highthroughput quantitation of enantiomers in MEKC-MS is demonstrated for the first time.

## 3.2. Materials and methods

### 3.2.1 Reagents and chemicals

Racemic mixture of 1,1'-binaphthyl-2,2'-diyl hydrogen phosphate (BNP), 1,1'-bi-2-naphthol (BOH), 1,1'-binaphthalene-2,2'-diamine (BNA) and all 23 cationic drugs, analytical-grade ammonium acetate (as 7.5 M NH<sub>4</sub>OAc solution), HPLC grade methanol (MeOH) and acetic acid (99.7%) were supplied by Sigma-Aldrich (St. Louis MO, USA). Five racemic mixture of biaryl atropisomers (BAI) [(1-(2-amino-3-chloro-6-methylphenyl) naphthalen-2-ol, 1-(2-amino-3-chloro-5-methylphenyl) naphthalen-2-ol, 1-(2-amino-3-bromo-4-methylphenyl) naphthalen-2-ol, 1-(2-amino-3,4,5-trichloro-phenyl) naphthalen-2-ol, and 1-(2-amino-3-bromophenyl)-6-methoxy naphthalen-2-ol)] were kindly provided by Prof. Daniel W. Armstrong's laboratory (University of Texas at Arlington, Arlington, TX). Ammonium hydroxide (25%) was obtained from Acros organics (NJ, USA).

The chemicals and reagents used for synthesis,  $\beta$ -D-glucose pentaacetate (98%), sulfur trioxide pyridine complex (98%), 10-undecen-1-ol (98%), phenyl dichlorophosphate (95%), boron trifluoride etherate (46.5% BF<sub>3</sub> basis), hexane, ethyl acetate (EtOAc), methanol anhydrous, 1,4-dioxane anhydrous, sodium sulfate (Na<sub>2</sub>SO<sub>4</sub>), pyridine anhydrous, dichloromethane anhydrous, Amberlyst® 15 hydrogen form were purchased from Sigma-Aldrich (St. Louis MO, USA). The reagent, 7-octen-1-ol (96%) was purchased from TCI America (Tokyo, Japan). Sodium bicarbonate (99.7%) and sodium hydroxide (NaOH, 50% v/v) were obtained from Fisher Scientific (Fair Lawn, NJ, USA). Triply deionized (DI) water used in



the experiments was obtained from Barnstead Nanopure II water system (Barnstead International, Dubuque, IA, USA).

### 3.2.2 Synthesis of $\alpha$ - and $\beta$ -D sugar surfactants

Both eight and eleven carbon  $\beta$ -D-phosphated and sulfated sugar surfactants were synthesized according to the modified protocols of synthesizing  $\alpha$ -D-glucopyranoside-based surfactants [16-19].

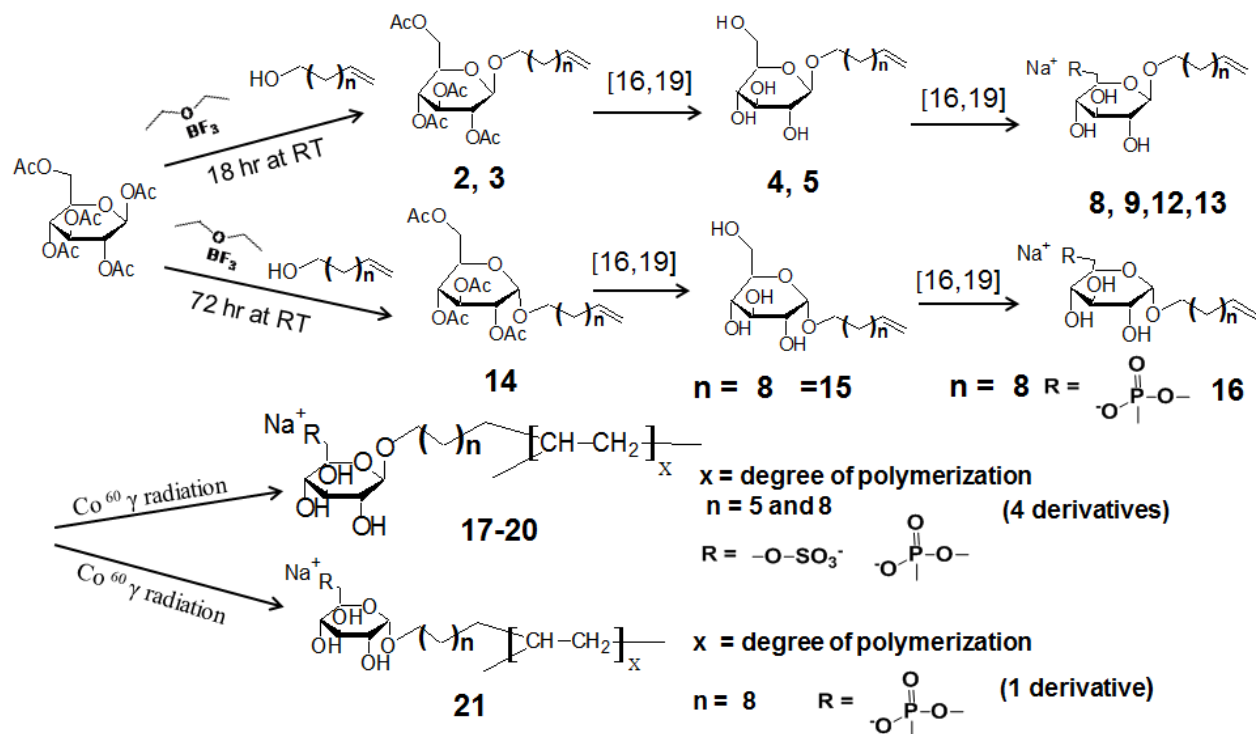
Product 2 and 3. To synthesize  $\beta$  configuration of sugar surfactants, a solution of 10-undecen-1-ol (3.9 mL, 0.0195 mol) or 7-octene-1-ol (2.9 mL, 0.0195 mol), and 2.1 mL (0.0169 mol) boron trifluoride etherate were added to a stirring solution of 5g (0.013 mol)  $\beta$ -D-glucose pentaacetate in 50 mL dry dichloromethane. The resulting solution was then stirred for 18 hrs under a blanket of nitrogen at room temperature. Next, the mixture was neutralized by adding 250 mL saturated sodium bicarbonate solution (30 g, 0.36 mol) and then washed with 200 mL H<sub>2</sub>O. The lower organic layer was then dried with Na<sub>2</sub>SO<sub>4</sub> and concentrated in vacuo.

Product 4 and 5. Next, the crude undecenyl or octenyl- $\beta$ -D-glucopyranoside acetate was deacetylated in the presence of 20 mL anhydrous methanol and 1mL sodium methoxide solution (25%) under nitrogen for 3 hrs in ice bath. The resulting reaction product was then neutralized by 2g Amberlyst<sup>®</sup>15 hydrogen resin, filtered and concentrated in vacuo. To yield pure  $\beta$ -D undecenyl- or  $\beta$ -D-octenyl-glucopyranoside, the residue containing a mixture of both  $\alpha$ - and  $\beta$ -D-glucopyranoside was purified by flash column chromatography [SiO<sub>2</sub>, EtOAc-MeOH, 10:0.5]. The eluent volume collection started at a point when the spot appeared on the TLC plate. To determine the pure  $\beta$ -product in the eluent, first a series of <sup>1</sup>H-NMR optimization was conducted by collecting first ten tubes (i.e., 110 mL) of eluent each time (data not shown). It was found that the first two sets of collection, i.e., first twenty tubes (~ 220 mL) contains predominately  $\beta$ -D

glucopyranoside and very little  $\alpha$  product (less than 5%) as verified  $^1\text{H-NMR}$  spectrum (Fig. S3). Next, the phosphorylation and sulfation steps to obtain products (6,7,10,11) were performed as reported previously [16-19].

Product 15. To synthesize  $\alpha$ -configuration of sugar surfactants, only the first two steps [Scheme 3.1] were modified as discussed below. Five grams (0.013 mol) of  $\beta$ -D-glucose pentaacetate was stirred in 50 mL anhydrous dichloromethane. Aliquots of 3.9 mL 10-undecen-1-ol (0.0195 mol) and 8.0 mL (0.065 mol) boron trifluoride etherate were added to the stirring solution. The resulting reaction was then allowed to proceed at room temperature for 72 hrs under a blanket of nitrogen. Next, 250 mL saturated sodium bicarbonate solution (30 g, 0.36 mol) was used to neutralize the reaction before the reaction mixture was washed with 200 mL  $\text{H}_2\text{O}$ . The lower organic layer was then dried with 10 g  $\text{Na}_2\text{SO}_4$  and concentrated in vacuo. The deacetylation reaction to obtain  $\alpha$ -D-undecenyl glucopyranoside is the same as synthesizing  $\beta$ -D-undecenyl glucopyranoside except when performing flash column chromatography [ $\text{SiO}_2$ , EtoAc-MeOH, 10:0.5] all of the eluent was collected after the appearance of spot on the TLC plate. The next two steps to obtain  $\alpha$ -D-undecenyl glucopyranoside 4,6-hydrogen phosphate, sodium salt (product 16) are the same as reported previously [16-19].

Four vinyl surfactant monomers (ie., *n*-undecenyl  $\beta$ -D-glucopyranoside) with sulfated and phosphated head groups (products 8,9,12,13, Scheme 1) and one vinyl surfactant monomer,  $\alpha$ -D-undecenyl glucopyranoside (product 16, Scheme 1) with phosphated head group were polymerized to obtain products (17-21) using a total dose of 20 M rad of  $^{60}\text{Co}$   $\gamma$ -radiation by Breazale nuclear reactor laboratory (Pennsylvania State University, University Park, PA ).



**Scheme 3.1** Synthesis scheme for poly(*n*-undecyl  $\alpha$ -D-glucopyranoside 4,6-hydrogen phosphate, sodium salt **21**) (poly- $\alpha$ -SUGP), poly(*n*-undecyl  $\beta$ -D-glucopyranoside 4,6-hydrogen sodium phosphate, sodium salt **17**) (poly- $\beta$ -SUGP), poly(*n*-undecyl  $\beta$ -D-glucopyranoside 6-hydrogen sulfate, monosodium salt **18**) (poly- $\beta$ -SUGS), poly(*n*-octyl  $\beta$ -D-glucopyranoside 4,6-hydrogen phosphate, sodium salt **19**), (poly- $\beta$ -SOGP), poly(*n*-octyl  $\beta$ -D-glucopyranoside 6-hydrogen sulfate, monosodium salt **20**) (poly- $\beta$ -SOGS).

### 3.2.3 CE-MS instrumentation

#### 3.2.3.1 MEKC-MS conditions

All MEKC-ESI-MS/MS experiments were carried on an Agilent 7100 CE system (Agilent Technologies, Palo Alto, CA, USA) coupled to an Agilent 6410 series triple quadrupole mass spectrometer (Agilent Technologies, 207 Palo Alto, CA). The CE instrument consisted of an on line diode array detector and 0-30 kV high voltage power supply. Mass spectrometer was equipped with Agilent CE-MS adapter kit (G1603A), an Agilent CE-ESI-MS sprayer kit

(G1607) and Agilent 1100 series isocratic HPLC pump to deliver the sheath liquid with a 1:100 splitter. Nitrogen was used as nebulizing gas and drying gas. The Agilent ChemStation software and Agilent Mass-Hunter Workstation (version B.02.01) were used for instrumental control and data acquisition as well as for qualitative and quantitative data analysis. The fused silica capillary with 60 cm effective length (375  $\mu\text{m}$  O.D., with 50  $\mu\text{m}$  I.D) used for MEKC-MS/MS experiments was purchased from Polymicro Technologies (Phoenix, AZ, USA). The applied voltage was +20 kV with injection of 5 mbar, 10 s. All samples were prepared in 100  $\mu\text{g}/\text{mL}$  in MeOH/H<sub>2</sub>O (10/90, v/v). The composition and the flow rate of the sheath liquid were MeOH/H<sub>2</sub>O (80/20, %v/v) containing 5 mM NH<sub>4</sub>OAc and 5  $\mu\text{L}/\text{min}$ , respectively. Spray chamber parameters: nebulizer pressure: 3 psi, drying gas temp.: 200 °C, drying gas flow: 8 L/min; capillary voltage: +3000 V. The fragmentor voltage, collision energy and product ion formations for all the analytes were optimized using optimizer software using Agilent LC-MS in flow injection mode.

#### **3.2.3.1.1 Multisegment injection configuration**

All series of hydrodynamic injection were performed at 5 mbar using alternating segments of sample/internal standard (BNP and *R*-BOH) and M<sub>o</sub>M<sub>s</sub> spacer (BGE containing 15 mM poly- $\beta$ -SUGS) was programmed in the injection table of Agilent ChemStation software. A 4-sample segment format used for the quantitation of BNP was set up in the following injection sequence: (1) 10 s sample (100  $\mu\text{g}/\text{mL}$  BNP and 250  $\mu\text{g}/\text{mL}$  of *R*-BOH), 120 s spacer; (2) 10 s sample (200  $\mu\text{g}/\text{mL}$  BNP and 250  $\mu\text{g}/\text{mL}$  of *R*-BOH), 120 s spacer; (3) 10 s sample (300  $\mu\text{g}/\text{mL}$  BNP and 250  $\mu\text{g}/\text{mL}$  of *R*-BOH), 120 s spacer; (4) 10 s sample (500  $\mu\text{g}/\text{mL}$  BNP and 250  $\mu\text{g}/\text{mL}$  of *R*-BOH), 120 s spacer. The total time injection time was about 9 min.

### 3.2.3.2 CE-MS conditions and preparation of buffers and analyte solutions

For chiral separations of all cationic drugs and binaphthyl derivatives, the stock solutions were prepared in pure methanol at 5.0 mg/mL and then were diluted to 100  $\mu$ g/mL in MeOH/H<sub>2</sub>O (10/90, v/v) and pressure injected at 5 mbar for 10 s.

All MEKC-MS/MS experiments were performed under the normal polarity mode with an applied voltage of +20 kV. The ESI-MS/MS detection was performed in the multiple reaction monitoring (MRM) positive ion mode for cationic drugs and negative ion mode for binaphthyl derivatives. The MRM transitions were optimized using Optimizer software using flow injection HPLC (Table S1). The BGEs for enantiomeric separation of cationic drugs and binaphthyl derivatives were 25 mM NH<sub>4</sub>OAc prepared by diluting the 7.5 M NH<sub>4</sub>OAc stock solution in triply DI water and then adjusted from pH 5.0 to 10.8 by acetic acid or ammonium hydroxide, respectively. The final running MEKC-ESI-MS/MS buffer solutions were prepared by addition of 15 mM or 30 mM polymeric sugar surfactants with different chain length and head group to the BGE solutions.

### 3.2.4 Characterization of $\beta$ -D-Sugar Surfactants

The mobility of both monomeric and polymeric sugar surfactants was determined by CE-MS and CE-UV experiments, respectively using a fused silica capillary with  $L_d = 60$  cm and  $L_t = 120$  cm. A mixture of four monomeric sugar surfactants with chain length and head group was prepared at a concentration of 5 mM in triply deionized water. This monomer mixture was profiled, apparent as well as effective electrophoretic mobility was calculated from migration time of CE-MS electropherograms using 25 mM NH<sub>4</sub>OAc as background electrolyte (BGE) at pH 7.0. Next, the mobility of polymeric sugar surfactants with different chain lengths and head

groups was determined by MEKC-UV. The BGE composition was 25 mM NH<sub>4</sub>OAc buffer with the addition of 15 mM polymeric sugar surfactants in BGE. The mobility of polymeric sugar surfactant was traced using 5 mg/mL of Sudan III prepared in 90/10 methanol/water.

The synthesized monomeric  $\beta$ -D-sugar surfactants with different chain lengths and head groups were characterized by using proton nuclear magnetic resonance (<sup>1</sup>H-NMR) (data shown in the supplementary information). Solutions of a series of concentration from 0.5 mM to 50 mM of monomers and polymers were prepared in triply deionized water and their surface tension and CMC values were measured by sigma 7<sup>03</sup> digital tensiometer (KVS Instruments, Monroe, CT, USA). Fluorescence Measurements was conducted on a Perkin Elmer LS 55 Fluorescence spectrometer (PerkinElmer Instruments, Norwalk, CA, USA) to determine the aggregation number and polarities using pyrene as a probe and cetylpyridinium chloride as a quencher as described elsewhere [20].

### **3.3. Results and Discussion**

#### **3.3.1 Physicochemical properties**

The key to synthesizing  $\alpha$  or  $\beta$  sugar surfactant anomers with different chain length and head group depends on the reaction specified in the first step i.e., the glycosylation step (Scheme 1) because this reaction takes place at the anomeric carbon site. Table 3.2 summarizes the optimized molar ratio of the boron trifluoride diethyl etherate used and reaction time in synthesizing  $\alpha$ - and  $\beta$ -D-undecenyl glucopyranoside surfactants. Unlike the glycosylation step of  $\beta$ -D-glucopyranoside in which 95% of  $\beta$ -D-undecenyl glucopyranoside is obtained (Fig.B3 and Table 3.2), the glycosylation reaction of  $\beta$ -D-glucose-6-pentacetate yields 99%  $\alpha$ -D-undecenyl glucopyranoside but only after 72 hrs of reaction time (Fig.B4-B5). Because the  $\alpha$ - and  $\beta$ -SUGP surfactants are diastereomeric they have distinguishable NMR spectra. For example, the anomeric

protons of  $\alpha$ -SUGP resonates further downfield (4.788-4.779 ppm) from the anomeric beta proton (4.271-4.252 ppm) of  $\beta$ -SUGP. Thus, the J-J-coupling constant between the two anomeric protons of  $\alpha$ -SUGP and  $\beta$ -SUGP were about 3.6 and 7.6 Hz, respectively (Figure B3 and B5).

**Table 3.2.** Optimized molar ratio and reaction time for glycosylation reactions of  $\alpha$ - and  $\beta$ -SUGP

	molar ratio of $\beta$ -D-glucose Pentaacetate	molar ratio of Undecylenyl alcohol	molar ratio of boron trifluoride diethyl etherate	Reaction Time (hr)	J,J- coupling constant of anomeric proton (Hz)
$\alpha$ -sugar surfactant	1	1.5	5	72	3.6 (99%)
$\beta$ -sugar surfactant	1	1.5	1.3	18	7.6 (95%)

$\tau = J = (\Delta\delta)(\nu_{\text{Larmor}}) \text{ (MHz)}/10^6$ , the calculations of J,J- coupling constant of  $\alpha$  and  $\beta$  anomeric proton were shown in supporting information (Fig. S3 and S5)

Physicochemical properties of both  $\beta$ -D-glucopyranoside-based surfactant monomers and polymers are summarized in Table 3.1. The CMC was determined from surface tension measurements, which was used to evaluate the surface activity of all four surfactants with increasing molar concentration in water. As shown in Table 1, the CMC decreases in the following order:  $\beta$ -SOGS >  $\beta$ -SOGP >  $\beta$ -SUGS >  $\beta$ -SUGP. In general a lower CMC is more favorable as there will less free monomers, reducing operating currents if unpolymerized micelles are used as pseudophase for chiral separations. The higher CMC of sulfate head groups compared to phosphate head groups at equivalent chain length could be possibly explained by the fact that

strong intramolecular hydrogen bonding interactions decreases the repulsion between phosphate head groups facilitating micelle formation. In addition,  $\beta$ -SOGS and  $\beta$ -SOGP have higher CMC than  $\beta$ -SUGS and  $\beta$ -SUGP, respectively. The trend for decreasing CMC with increasing chain length is not too surprising as hydrophobicity increases owing to the extension of hydrocarbon chain from C<sub>8</sub> to C<sub>11</sub>. Aggregation number and polarity of both sugar surfactant monomers and polymers were measured and determined according to the early work in our group [21]. Aggregation number increases and polarity decreases with increasing chain length of sugar surfactants for both sulfate and phosphate charged on the head groups.

**Table 3.1:** Physicochemical properties of *n*-alkenyl  $\beta$ -D-glucopyranoside monomers and polymers

monomer				polymer		
	CMC (mM) <sup>a)</sup>	Aggregation # <sup>b)</sup>	Polarity ( <i>I</i> <sub>1</sub> / <i>I</i> <sub>3</sub> ) <sup>c)</sup>	CMC (mM) <sup>a)</sup>	Aggregation # <sup>b)</sup>	Polarity ( <i>I</i> <sub>1</sub> / <i>I</i> <sub>3</sub> ) <sup>c)</sup>
<b><math>\beta</math>-SOGP</b>	11	92	1.024	0	70	1.043
<b><math>\beta</math>-SUGP</b>	2.2	110	0.947	0	76	0.941
<b><math>\beta</math>-SOGS</b>	18	84	0.963	0	49	1.011
<b><math>\beta</math>-SUGS</b>	3.7	105	0.932	0	60	0.978

a) Critical micelle concentration (CMC) is determined by the surface tension measurements

b) Aggregation number is determined by the fluorescence quenching experiment using pyrene as a probe and cetyl pyridinium chloride as a quencher.

c) Polarities of the surfactants are determined using ratio of the fluorescence intensity (*I*<sub>1</sub>/*I*<sub>3</sub>) of pyrene.



The effective mobility ( $\mu_{\text{eff}}$ ) of both monomers and polymers of  $\beta$ -D-alkyl glucopyranoside are listed in Table 3. It is worth mentioning that  $\beta$ -SOGP and  $\beta$ -SOGS as well as  $\beta$ -SUGP and  $\beta$ -SUGS have very similar  $\mu_{\text{eff}}$  value. It seems that the sulfate and phosphate charge on the head group have little influence on the mobility. However, increasing the length of carbon chain provided some difference in  $\mu_{\text{eff}}$  with longer chain surfactants having less negative mobility. Furthermore, all four sugar polymeric surfactants have less negative  $\mu_{\text{eff}}$  suggesting that  $M_oM_s$  provides much larger elution window compared to their corresponding monomers and the longest chain  $M_oM_s$  will provide the maximum peak capacity when used as a pseudophase for simultaneous separation of parent drug and its metabolites. Interestingly, the effect of chain length of sugar surfactants on elution window seems to be opposite compared to the previous studies on amino acid type polymeric surfactants [22].

**Table 3.3.** Effective mobility of  $\beta$ -D sugar surfactant monomers and polymers of different head group and chain length

Type of Sugar Surfactant	<sup>1</sup> Effective mobility ( $\text{cm}^2/(\text{V}\cdot\text{s})$ )
$\beta$ -SOGP	$-0.000615 \pm 0.000018$
$\beta$ -SUGP	$-0.000604 \pm 0.000018$
$\beta$ -SOGS	$-0.000619 \pm 0.000017$
$\beta$ -SUGS	$-0.000606 \pm 0.000018$
Poly- $\beta$ -SOGP	$-0.000394 \pm 0.000011$
Poly- $\beta$ -SUGP	$-0.000319 \pm 0.000015$
Poly- $\beta$ -SOGS	$-0.000383 \pm 0.000023$
Poly- $\beta$ -SUGS	$-0.000351 \pm 0.000014$

<sup>1</sup> Effective mobility ( $\mu_{\text{eff}}$ ) =  $\mu_a - \mu_{\text{EOF}}$  of all sugar monomers was calculated from the migration time or apparent mobility ( $\mu_a$ ) of monomer peak observed in CZE-MS electropherogram and mobility of EOF ( $\mu_{\text{EOF}}$ ) observed using methanol as  $t_0$  marker via on line CZE-UV-MS on the same capillary; effective mobility of all sugar polymers was calculated using methanol as  $t_0$  marker and Sudan III as  $t_{\text{mc}}$  marker for all sugar polymers in MEKC-UV

Figure 3.1 (Panel A and B), shows the effect of mM concentration of eight and eleven carbon chain polymeric and monomeric sugar surfactants containing phosphated and sulfated charges on the head groups on surface tension. Two main trends are evident. First, polymeric surfactants (poly- $\beta$ -SUGS and poly- $\beta$ -SUGP) do not concentrate at the air/water interface and their CMC essentially remains zero. Polymeric surfactants with zero CMC are advantageous compared to their unpolymerized micelles in reducing CE-MS operating current. This is because when surfactants are dialyzed after polymerization, the process essentially removes any unreacted surfactant monomers. In addition, much lower concentrations could be used when polymeric surfactants are used as pseudostationary phase allowing the operator to easily work under 50  $\mu\text{A}$  limits. Thus, the polymeric sugar surfactants can be used at lower concentrations without compromising enantio-separation. Second, note that both sulfated and phosphated surfactant polymers bearing  $\text{C}_8$  and  $\text{C}_{11}$  chain lengths have low surface activity (high surface tension) compared to their corresponding monomers. This suggests that polymers should be more beneficial in providing sensitive detection of enantiomeric signal in ESI-MS compared to the corresponding low molecular weight monomers [23]. Perhaps, it could be hypothesized that poly- $\beta$ -SUGP should provide the best LOD as it the most surface active polymer. Considering the above mentioned effects and the data shown in Fig. 1 we evaluated the effect of charge on the head group, chain length and anomeric configuration of  $\beta$ -D-alkenyl glucopyranoside based surfactants for enantioselective MEKC-MS.

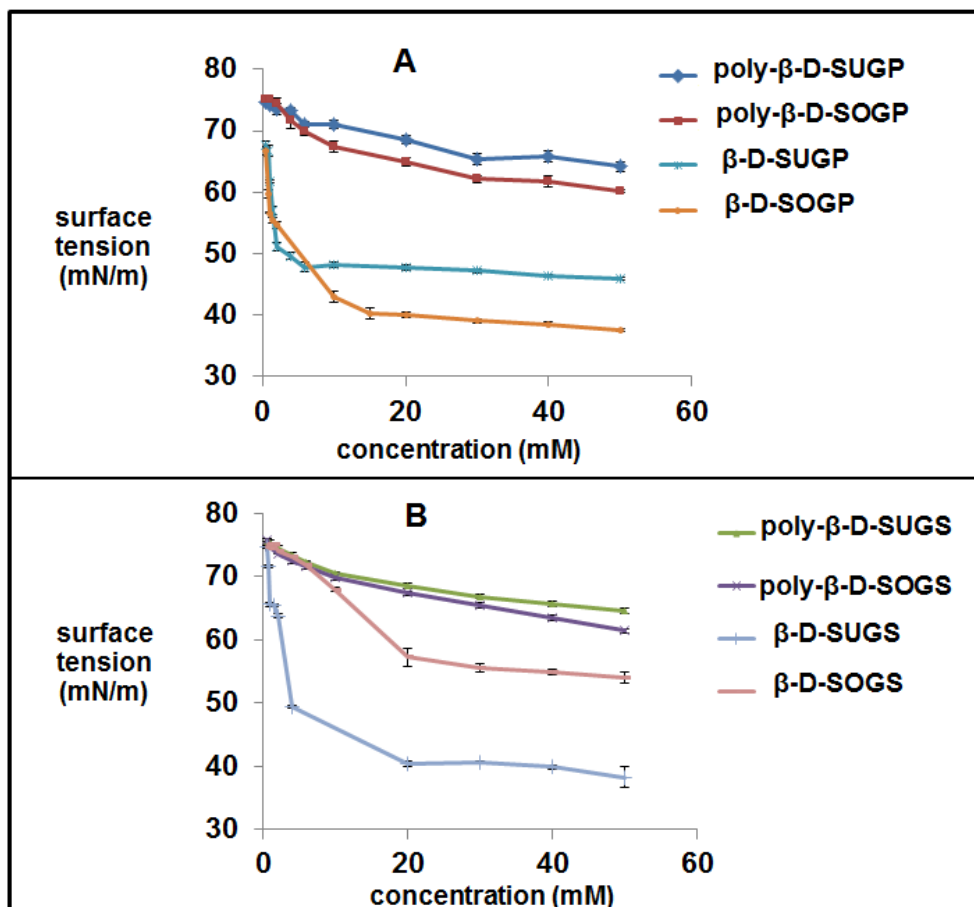


**Fig. 3.1** Plot comparing the surface tension versus concentration of monomers and polymers of (A) phosphated surfactants ( $\beta$ -SOGP and  $\beta$ -SUGP); and (B) sulfated surfactants ( $\beta$ -SOGS and  $\beta$ -SUGS).

### 3.3.2 Effect of charge on the head group of $\beta$ sugar surfactants

Enantioseparation of primary, secondary, tertiary and quaternary amines as well as amino alcohols ( $\beta$ -blockers) and BAI are compared using eleven carbon chain polymeric surfactant with sulfated and phosphated charge on the head groups (i.e., poly- $\beta$ -SUGS (18) and poly- $\beta$ -SUGP (17), Scheme 3.1]. The BGE consisted of 25 mM  $\text{NH}_4\text{OAC}$  at the optimized pH (A-E) for each analyte. Even though poly- $\beta$ -SUGS and poly- $\beta$ -SUGP have equal number of hydrocarbon chain, longer retention times were observed for most compounds on the more polar

poly- $\beta$ -SUGS pseudophase (Table 3.4). The retention differences between the two phases are related to the degree of strength of intermolecular interactions (hydrogen bonding and ion-pairing) with the type of chiral analyte. Interestingly, the longer retention time using poly- $\beta$ -SUGS does not always result in higher  $R_s$  and  $N_{avg}$  for most of the chiral compounds studied. For example, the more polar, poly- $\beta$ -SUGS phase did not enantioseparate as many positively charged compounds when compared to poly- $\beta$ -SUGP. Significantly higher enantioresolution was observed with the later surfactant for primary and secondary amines as well as amino alcohols (Table 3.4). These results suggest that the enhanced chiral selectivity on poly- $\beta$ -SUGP compared to poly- $\beta$ -SUGS for the aforementioned chiral analytes is perhaps due to structural rigidity of the phosphate charge substitution with respect to glucose ring, which in turn promotes stronger chiral interactions with oppositely charged analytes. On the other hand, the sulfate charge on the glucose ring has more flexible orientation in poly- $\beta$ -SUGS surfactant. However, in Table 3.4, there are several noted exceptions, and  $\sim$  one third (i.e., 8 out of 25) of chiral compounds are resolved better with poly- $\beta$ -SUGS. Further, the data in Table 3.4 reveals that majority of investigated BAI (i.e., 5 out of 6) are better separated with poly- $\beta$ -SUGS compared to poly- $\beta$ -SUGP.

**Table 3.4:** Effect of head group on resolution ( $R_s$ ), migration time ( $tr_2$ ), selectivity ( $\alpha$ ) and efficiency ( $N_{avg}$ ) of 25 enantiomeric compounds using poly  $\beta$ - $n$ -undecyl glucopyranoside surfactant pseudophases

Compound name	$tr_2$					
	PSP	$R_s$	(min)	$N_{avg}$	$\alpha$	$^1BGE$
norephedrine	$\beta$ -SUGP	1.8	33.0	47,000	1.02	A1
	$\beta$ -SUGS	1.6	32.2	36,000	1.02	A2
pseudoephedrine	$\beta$ -SUGP	1.5	29.8	56,000	1.02	A1
	$\beta$ -SUGS	2.4	37.9	87,000	1.04	A2
ephedrine	$\beta$ -SUGP	2.0	32.3	66,000	1.02	A1
	$\beta$ -SUGS	1.5	37.4	46,000	1.01	A2
methylephedrine	$\beta$ -SUGP	2.1	32.0	54,000	1.04	A1
	$\beta$ -SUGS	2.0	43.3	46,000	1.03	A2
pindolol	$\beta$ -SUGP	0.5	21.8	6,300	1.01	B1
	$\beta$ -SUGS	0.0	27.7	3,000	1.00	B2
alprenolol	$\beta$ -SUGP	0.5	44.9	6,000	1.01	B1
	$\beta$ -SUGS	0.0	27.7	4,800	1.00	B2
metoprolol	$\beta$ -SUGP	0.4	16.6	69,000	1.01	B1
	$\beta$ -SUGS	0.2	24.8	61,000	1.01	B2
nadolol		3.5		25,000	1.12	
	$\beta$ -SUGP	1.8	21.5	20,000	1.04	B1
		2.7		24,000	1.12	
	$\beta$ -SUGS	0.0	18.6	10,000	1.00	B2

<b>octopamine</b>	$\beta$ -SUGP	1.8	12.8	10,000	1.02	B3
	$\beta$ -SUGS	0.5	8.7	8,000	1.01	B4
<b>isoproterenol</b>	$\beta$ -SUGP	2.0	9.5	2,000	1.03	A3
	$\beta$ -SUGS	0.0	10.8	1,500	1.00	A4
<b>terbutaline</b>	$\beta$ -SUGP	2.1	9.4	13,000	1.04	D1
	$\beta$ -SUGS	1.5	14.7	11,000	1.03	B4
<b>bupivacaine</b>	$\beta$ -SUGP	1.4	17.8	16,000	1.03	A3
	$\beta$ -SUGS	0.0	15.2	10,000	1.00	D2
<b>3- pinanemethylamine</b>	$\beta$ -SUGP	0.3	22.4	39,000	1.01	B3
	$\beta$ -SUGS	0.0	23.4	35,000	1.00	D2
<b>normetanephrine</b>	$\beta$ -SUGP	1.8	7.2	4,000	1.06	B3
	$\beta$ -SUGS	0.0	6.6	1,100	1.00	D2
<b>Atropine</b>	$\beta$ -SUGP	0.0	16.3	1,000	1.00	A3
	$\beta$ -SUGS	1.5	46.5	7,200	1.03	A4
<b>Homatropine</b>	$\beta$ -SUGP	5.0	10.0	12,000	1.52	A3
	$\beta$ -SUGS	1.5	13.5	7,500	1.04	D2
<b>norphenylephrine</b>	$\beta$ -SUGP	2.0	13.8	10,000	1.03	B3
	$\beta$ -SUGS	0.1	10.7	7,000	1.01	A4
<b>synepherine</b>	$\beta$ -SUGP	1.4	16.5	7,300	1.05	A3
	$\beta$ -SUGS	0.0	9.4	5,000	1.00	A4
<b>Aminoglutethimide</b>	$\beta$ -SUGP	0.0	9.3	1,000	1.00	A3
	$\beta$ -SUGS	0.3	16.0	8,000	1.01	A4

<b>BNP</b>	$\beta$ -SUGP	4.5	25.3	23,000	1.10	D1
	$\beta$ -SUGS	5.0	29.7	24,000	1.20	C1
<b>1-(2-amino-3-chloro-6-methylphenyl)naphthalen-2-ol</b>		1.0		25,000	1.02	
	$\beta$ -SUGP	0.2	13.6	22,000	1.01	E1
		1.5		17,000	1.04	
	$\beta$ -SUGS	1.4	39.4	15,000	1.03	C1
<b>1-(2-amino-3-chloro-5-methylphenyl)naphthalen-2-ol</b>		1.0		25,000	1.02	
	$\beta$ -SUGP	0.2	13.6	22,000	1.01	E1
		1.5		17,000	1.04	
	$\beta$ -SUGS	1.4	39.4	15,000	1.03	C1
<b>1,1'-binaphthalene-2,2'-diamine</b>	$\beta$ -SUGP	0.2	21.0	5,300	1.00	B3
	$\beta$ -SUGS	0.0	22.5	4,800	1.00	E1
<b>BOH</b>	$\beta$ -SUGP	1.5	13.6	8,500	1.04	E1
	$\beta$ -SUGS	3.5	45.7	10,000	1.10	C1
<b>1-(2-amino-3-bromophenyl)-6-methoxynaphthalen-2-ol</b>	$\beta$ -SUGP	0.2	20.0	14000	1.01	E1
	$\beta$ -SUGS	1.5	42.1	33,000	1.03	C1

<sup>1</sup>All BGE contains 25 mM NH<sub>4</sub>OAc. A1: 30 mM poly  $\beta$ -SUGP, pH 5; A2: 30 mM poly  $\beta$ -SUGS, pH 5; A3: 15 mM poly  $\beta$ -SUGP, pH 5; A4: 15 mM poly  $\beta$ -SUGS, pH 5; B1: 30 mM poly  $\beta$ -SUGP, pH 7; B2: 30 mM poly  $\beta$ -SUGS, pH 7; B3: 15 mM poly  $\beta$ -SUGP, pH 7; B4: 15 mM poly  $\beta$ -SUGS, pH 7; C: 15 mM poly  $\beta$ -SUGS, pH 6; D1: 15 mM poly  $\beta$ -SUGP, pH 9; D2: 15 mM poly  $\beta$ -SUGS, pH 9; E: 15 mM poly  $\beta$ -SUGP, pH 10.8

Fig. 3.2 shows a complementary chiral effect for sulfate and phosphate charge on the head group of the polymeric surfactant for two structurally similar quaternary amines (atropine and homatropine). Both atropine and homatropine are used as eye dilator before eye examinations, before and after eye operation, and for treatment of eye conditions (e.g., uveitis or posterior synechiae) [24]. Note that atropine has a chiral center one carbon atom away from the hydroxyl group whereas in case of homatropine chiral center is located next to the hydroxyl group. Thus, poly- $\beta$ -SUGS gave baseline enantioseparation for atropine, while poly- $\beta$ -SUGP provided no enantioseparation for atropine. This could be possibly due to steric hindrance of extra methylene group) in atropine structure, which possibly made it harder to interact with the rigid phosphate charge on the sugar head group. On the other hand, the chiral Rs of homatropine is achieved by both chiral surfactants. However, with poly- $\beta$ -SUGP the Rs is 5.0, which is much higher than 1.7 realized by the sulfate charge on the head group of poly- $\beta$ -SUGP.



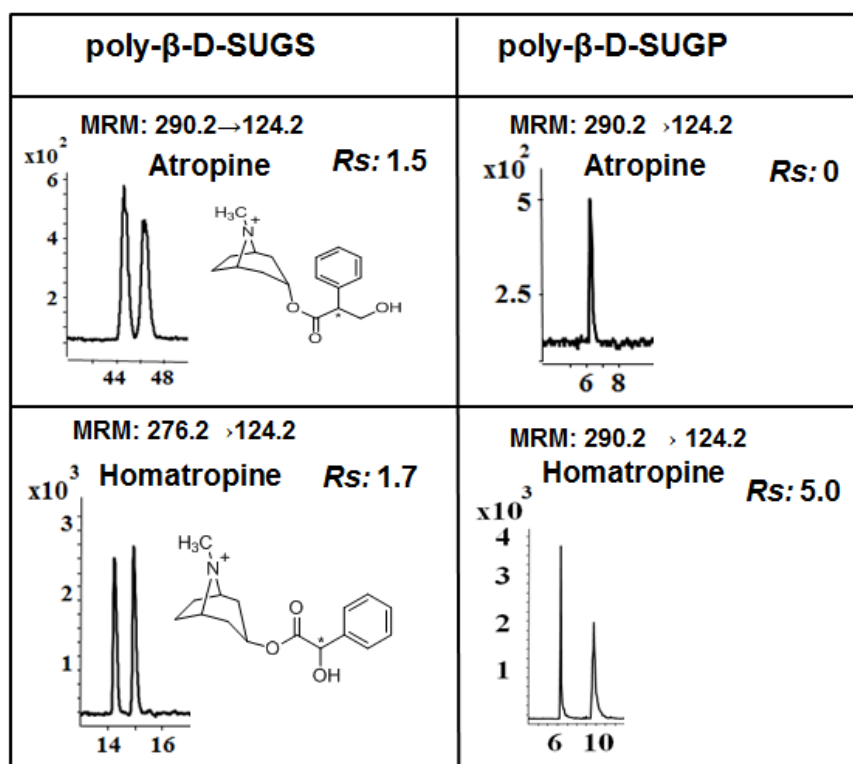


**Fig. 3.2** Electropherograms comparing the effect of head group of polymeric sugar surfactants on chiral separation of atropine and homatropine in MEKC-MS/MS. Conditions: 25 mM  $\text{NH}_4\text{OAc}$ , pH 5.0, using 15 mM poly- $\beta$ -SUGS (left) and poly- $\beta$ -SUGP (right). Sample concentration: 100  $\mu\text{g}/\text{mL}$  in  $\text{MeOH}/\text{H}_2\text{O}$  (10/90, v/v). Other conditions are the same as discussed in section 3.2.3.1.

### 3.3.3 Effect of chain length of $\beta$ -D sugar surfactants

Separation of multichiral center drug is a special challenge due to complex structure of these analytes. Fig. 3.3(A-D) shows the comparisons of the chiral *Rs* of nadolol, 5-{3-[1,1-dimethylethyl amino]-2-hydroxypropoxy}1,2,3,4-tetrahydro-cis-2,3-naphthalene diol. As Figure 3 inset shows nadolol is a non-selective  $\beta$ -blocker, which contains four stereoisomers. Although nadolol has three chiral centers, only four stereoisomers are possible because the two adjacent hydroxyl groups on the cyclohexane ring are conformationally locked. This chiral compound is useful for the treatment of hypertension and angina pectoris. Comparing Fig. 3.3A vs. Fig.3.3B, it can be seen that migration time as well resolution of stereoisomers of nadolol increases with

the increase in chain length of the sulfated surfactants with total analysis time increased from 9 to 19 min. No chiral Rs for nadolol was observed for poly- $\beta$ -SOGS while partial Rs was obtained by poly- $\beta$ -SUGS. In contrast, increase in run time from 7 to 22 min in Fig. 3.3C vs. Fig. 3.3D provided significant improvement resulting in baseline resolution of all four stereoisomers using C<sub>11</sub> phosphated (i.e., poly- $\beta$ -SUGP) compared to C<sub>8</sub> phosphated (i.e., poly- $\beta$ -SOGP) surfactant. Perhaps, nadolol, penetrates less inside the hydrophobic micellar core of poly- $\beta$ -SOGS and poly- $\beta$ -SOGP, resulting in faster migration time and poorer Rs.

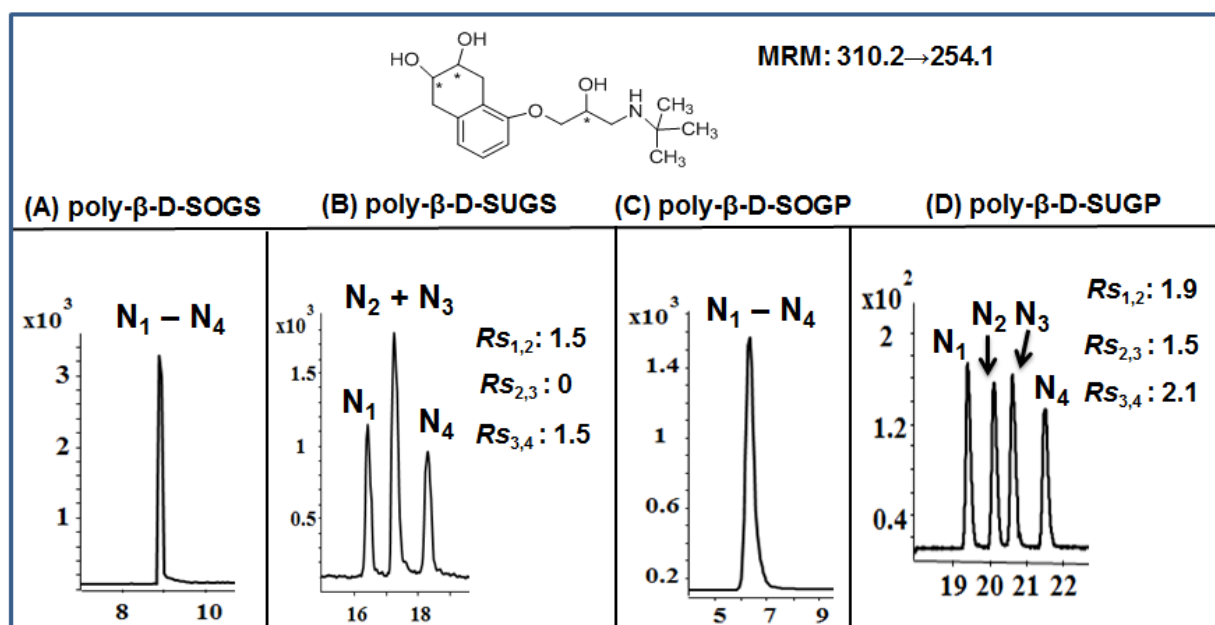


**Fig. 3.3** Electropherograms comparing the effect of chain length of polymeric sugar surfactants on chiral separation of nadolol in MEKC-MS/MS. Conditions: 25 mM NH<sub>4</sub>OAc, pH 5.0, using 30 mM (A) poly- $\beta$ -SOGS, (B) poly- $\beta$ -SUGS, (C) poly- $\beta$ -SOGP and (D) poly- $\beta$ -SUGP. Sample concentration: 100  $\mu$ g/mL in MeOH/H<sub>2</sub>O (10/90, v/v). Other conditions are the same as discussed in section 3.2.3.1.

In contrast to separation of multichiral center  $\beta$ -blocker (nadolol), enantioseparation of single chiral center  $\beta$ -blockers (metoprolol, alprenolol and pindolol) is not significantly enhanced

with the increase in chain length (Table 3.5). However, enhanced separation of primary and secondary amines was mostly observed with longer chain length surfactants. Interestingly, benzodiazepines only showed some indication for enantioresolution but with only one polymeric surfactant, i.e., short chain, poly- $\beta$ -SOGP. The BAI were best enantioseparated using shorter chain phosphated surfactants compared to longer ones with the same head group. For example, poly- $\beta$ -SOGP separates 6 out of 8 BAI (last 8 rows, Table 3.5) better than the remaining three polymeric surfactants. This shows that less hydrophobic interactions of shorter chain surfactant is sometimes more favorable and cannot be neglected as it can enhance hydrogen bond interactions of the analyte with the charge on the surfactant head group. Nevertheless, this trend shows that the chiral recognition mechanism in polymeric sugar surfactants cannot be simply reduced to one type of interaction, rather it involves several types. Thus, this new generation of polymeric surfactants are particularly effective and versatile.

**Table 3.5:** Effect of chain length on resolution ( $R_s$ ), migration time ( $tr_2$ ), selectivity ( $\alpha$ ) and efficiency ( $N_{avg}$ ) of enantiomeric compounds using poly  $\beta$ - $n$ -undecyl glucopyranoside surfactant pseudophases

Compound name	PSP	$R_s$	$tr_2$ (min)	$N_{avg}$	$\alpha$	$^1BGE$
norphenylephrine	$\beta$ -SUGP	2.0	13.8	10,000	1.03	A3
	$\beta$ -SUGS	0.1	10.7	7,000	1.01	A4
	$\beta$ -SOGP	1.5	6.2	7,000	1.05	D3
	$\beta$ -SOGS	0.0	5.8	2,000	1.00	D4
octopamine	$\beta$ -SUGP	1.8	12.8	10,000	1.02	B5
	$\beta$ -SUGS	0.5	8.7	8,000	1.01	B6
	$\beta$ -SOGP	1.5	6.1	10,000	1.07	D3
	$\beta$ -SOGS	0.0	5.9	2,300	1.00	D4
pindolol	$\beta$ -SUGP	0.5	21.8	6,300	1.01	B1
	$\beta$ -SUGS	0.0	27.7	3,000	1.00	B2
	$\beta$ -SOGP	0.6	44.8	26,000	1.01	B3
	$\beta$ -SOGS	0.0	13.5	5,900	1.00	B4
alprenolol	$\beta$ -SUGP	0.5	44.9	6,000	1.01	B1
	$\beta$ -SUGS	0.0	27.7	4,800	1.00	B2
	$\beta$ -SOGP	0.6	44.9	24000	1.00	B3
	$\beta$ -SOGS	0.0	13.5	5,900	1.00	B4
metoprolol	$\beta$ -SUGP	0.4	16.6	69,000	1.01	B1
	$\beta$ -SUGS	0.2	24.8	61,000	1.01	B2
	$\beta$ -SOGP	0.5	31.0	46,000	1.01	B3
	$\beta$ -SOGS	0.0	11.7	13,000	1.00	B4
propranolol	$\beta$ -SUGP	0.0	41.6	7,000	1.00	B1
	$\beta$ -SUGS	0.0	28.9	11,000	1.00	B2
	$\beta$ -SOGP	0.1	39.2	110,000	1.01	B3
	$\beta$ -SOGS	0.1	22.8	150,000	1.00	B4
3-pinane-methylamine	$\beta$ -SUGP	0.3	22.4	39,000	1.01	B5
	$\beta$ -SUGS	0.0	23.4	35,000	1.00	D2
	$\beta$ -SOGP	0.1	10.2	12,000	1.01	A5
	$\beta$ -SOGS	0.0	15.0	3,000	1.00	D4
oxazepam	$\beta$ -SUGP	0.0	17.7	5,000	1.00	D1
	$\beta$ -SUGS	0.0	18.0	4,300	1.00	D2
	$\beta$ -SOGP	0.0	11.8	700	1.00	A1
	$\beta$ -SOGS	0.1	17.6	16,000	1.00	A2

<b>temazepam</b>	$\beta$ -SUGP	0.0	15.0	2,100	1.00	D1
	$\beta$ -SUGS	0.0	16.9	9,300	1.00	D2
	$\beta$ -SOGP	0.0	10.6	700	1.00	D3
	$\beta$ -SOGS	0.3	16.3	26,000	1.01	D4
<b>lorazepam</b>	$\beta$ -SUGP	0.0	18.7	3,900	1.00	D1
	$\beta$ -SUGS	0.0	19.1	5,800	1.00	D2
	$\beta$ -SOGP	0.0	13.2	600	1.00	A1
	$\beta$ -SOGS	0.7	20.1	9,000	1.04	A2
<b>BNP</b>	$\beta$ -SUGP	4.5	25.3	23,000	1.10	D1
	$\beta$ -SUGS	5.0	29.7	24,000	1.20	C1
	$\beta$ -SOGP	7.8	52.9	30,000	1.13	A1
	$\beta$ -SOGS	9.4	64.8	31,000	1.37	A2
<b>BOH</b>	$\beta$ -SUGP	1.5	13.6	8,500	1.04	E1
	$\beta$ -SUGS	3.5	45.7	10,000	1.10	C1
	$\beta$ -SOGP	2.5	20.9	18,000	1.07	E3
	$\beta$ -SOGS	1.5	16.4	13,000	1.04	E4
<b>1,1'-binaphthalene-2,2'-diamine</b>	$\beta$ -SUGP	0.2	21.0	5,300	1.00	B5
	$\beta$ -SUGS	0.0	22.5	4,800	1.00	E2
	$\beta$ -SOGP	0.2	20.7	18,000	1.01	E3
	$\beta$ -SOGS	0.0	17.1	7,300	1.00	E4
<b>1-(2-amino-3-chloro-6-methylphenyl)naphthalen-2-ol</b>	$\beta$ -SUGP	1.0		29,000	1.02	
	$\beta$ -SUGP	0.2	13.6	26,000	1.01	E1
	$\beta$ -SUGS	1.5		13,000	1.04	
	$\beta$ -SUGS	1.4	39.4	11,000	1.03	C1
	$\beta$ -SOGP	2.2		37,000	1.05	
	$\beta$ -SOGP	1.6	16.8	31,000	1.04	E3
$\beta$ -SOGS	0.9		26,000	1.01		
$\beta$ -SOGS	0.0	20.4	11,000	1.00	B7	

<b>1-(2-amino-3-chloro-5-methylphenyl)naphthalen-2-ol</b>	$\beta$ -SUGP	1.1		37,000	1.02	
	$\beta$ -SUGP	0.2	13.6	29,000	1.01	E1
	$\beta$ -SUGS	1.5		12,000	1.04	
	$\beta$ -SUGS	1.4	39.4	11,000	1.03	C1
	$\beta$ -SOGP	2.2		37,000	1.05	
<b>1-(2-amino-3-bromo-4-methylphenyl)naphthalen-2-ol</b>	$\beta$ -SOGP	1.7	19.1	36,000	1.04	E3
	$\beta$ -SUGS	0.7		19,000	1.01	
	$\beta$ -SUGS	0.0	23.9	11,000	1.00	B7
	$\beta$ -SUGP	0.0	15.2	22,000	1.00	E1
	$\beta$ -SUGS	0.0	20.7	8,500	1.00	E2
<b>1-(2-amino-3-bromophenyl)-6-methoxynaphthalen-2-ol</b>	$\beta$ -SOGP	1.7	20.9	27,000	1.03	E3
	$\beta$ -SUGS	0.0	16.5	8,900	1.00	E4
	$\beta$ -SUGP	0.2	20.0	14,000	1.01	E1
	$\beta$ -SUGS	1.5	42.1	33,000	1.03	C1
<b>1-(2-amino-3,4,5-trichlorophenyl)naphthalen-2-ol</b>	$\beta$ -SOGP	1.9	20.1	39,000	1.04	E3
	$\beta$ -SUGS	0.1	15.9	25,000	1.00	E4
	$\beta$ -SUGP	0.0	16.3	11,000	1.00	E1
	$\beta$ -SUGS	0.0	23.2	5,100	1.00	E2
<b>1-(2-amino-3,4,5-trichlorophenyl)naphthalen-2-ol</b>	$\beta$ -SOGP	0.2	25.6	46,000	1.01	E3
	$\beta$ -SUGS	0.1	23.9	11,000	1.01	E4
	$\beta$ -SUGP	0.0	16.3	11,000	1.00	E1
	$\beta$ -SUGS	0.0	23.2	5,100	1.00	E2

<sup>1</sup>All BGE contains 25 mM NH<sub>4</sub>OAc. A1: 15 mM poly  $\beta$ -SOGP, pH 5; A2: 15 mM poly  $\beta$ -SUGS, pH 5; A3: 15 mM poly  $\beta$ -SUGP, pH 5; A4: 15 mM poly  $\beta$ -SUGS, pH 5; A5: 15 mM poly  $\beta$ -SOGP, pH 5; B1: 30 mM poly  $\beta$ -SUGP, pH 7; B2: 30 mM poly  $\beta$ -SUGS, pH 7; B3: 30 mM poly  $\beta$ -SOGP, pH 7; B4: 30 mM poly  $\beta$ -SUGS, pH 7; B5: 15 mM poly  $\beta$ -SUGP, pH 7; B6: 15 mM poly  $\beta$ -SUGS, pH 7; B7: 15 mM poly  $\beta$ -SUGS, pH 7; C1: 15 mM poly  $\beta$ -SUGS, pH 6; D1: 15 mM poly  $\beta$ -SUGP, pH 9; D2: 15 mM poly  $\beta$ -SUGS, pH 9; D3: 15 mM poly  $\beta$ -SOGP, pH 9; D2: 15 mM poly  $\beta$ -SUGS, pH 9; E1: 15 mM poly  $\beta$ -SUGP, pH 10.8; E2: 15 mM poly  $\beta$ -SUGS, pH 10.8; E3: 15 mM poly  $\beta$ -SOGP, pH 10.8; E4: 15 mM poly  $\beta$ -SUGS, pH 10.8;

### 3.3.4 Optimized eantioseparations of cationic compounds and biaryl atropisomers

Fig. 3.4A shows the electropherograms of 21 cationic chiral compounds enantioresolved by  $\beta$ -D sugar surfactants using optimum head group and optimum chain length at their respective optimized pH. Almost half of the cationic compounds were best enantioresolved by poly- $\beta$ -SUGP. Besides the longer chain length of poly- $\beta$ -SUGP, which enables the analytes to participate more with the hydrophobic core of polymeric sugar micelles, we hypothesize that this is probably due to enhanced attractive interaction, (e.g., electrostatic and hydrogen bonding) between the amine moiety of the analytes and the rigid bicyclic structure of the phosphate head group.

The enantioresolutions of 8 BAIs using the optimized head group and optimized chain length of polymeric  $\beta$ -D-sugar surfactant at pH 10.8 are shown in Fig. 3.4B. Interestingly, majority of the BAIs were better separated by short chain polymeric surfactants. For example, 5 out of 8 atropisomers were better enantioresolved by C<sub>8</sub> chain, poly- $\beta$ -D-SOGP compared to C<sub>11</sub> chain poly- $\beta$ -SUGP (analyte 14-18, Table 3.5, Figure 3.4B). The only exception was (+/-) BNA which enantioresolved best with the longer chain polymeric surfactant but provided only partial resolution. Similarly, C<sub>8</sub> chain, poly- $\beta$ -SOGS provided the highest resolution value ( $R_s = 9.4$ ) for the enantiomeric separation of (+/-)-BNP, and this was the only polymeric surfactant, which provided a hint of chiral resolution for difficult to separate enantiomers of 1-(2-amino-3,4,5-trichlorophenyl) naphthalen-2-ol. Overall, it appears that the chiral recognition for BAI seems to be dominated by short chain polymeric surfactants, which are weakly hydrophobic.

Screening of a total of 43 chiral compounds including 35 cationic compounds and 8 BAI using four  $\beta$ -D polymeric sugar surfactants with different head groups and chain lengths (Fig. 3.5) reveals that poly- $\beta$ -SUGP offered the highest success rate for chiral  $R_s$  (53%), in which 35%

of the analytes had excellent chiral Rs ( $R_s > 1.5$ ). The eleven carbon chain, poly- $\beta$ -SUGS provided the second best success rate (44%) in which 28% of the analytes had chiral Rs higher than 1.5. Among all 43 compounds, 30 analytes were enantioresolved using these four polymeric sugar surfactants and the overall success rate of analytes resolved was 70%.



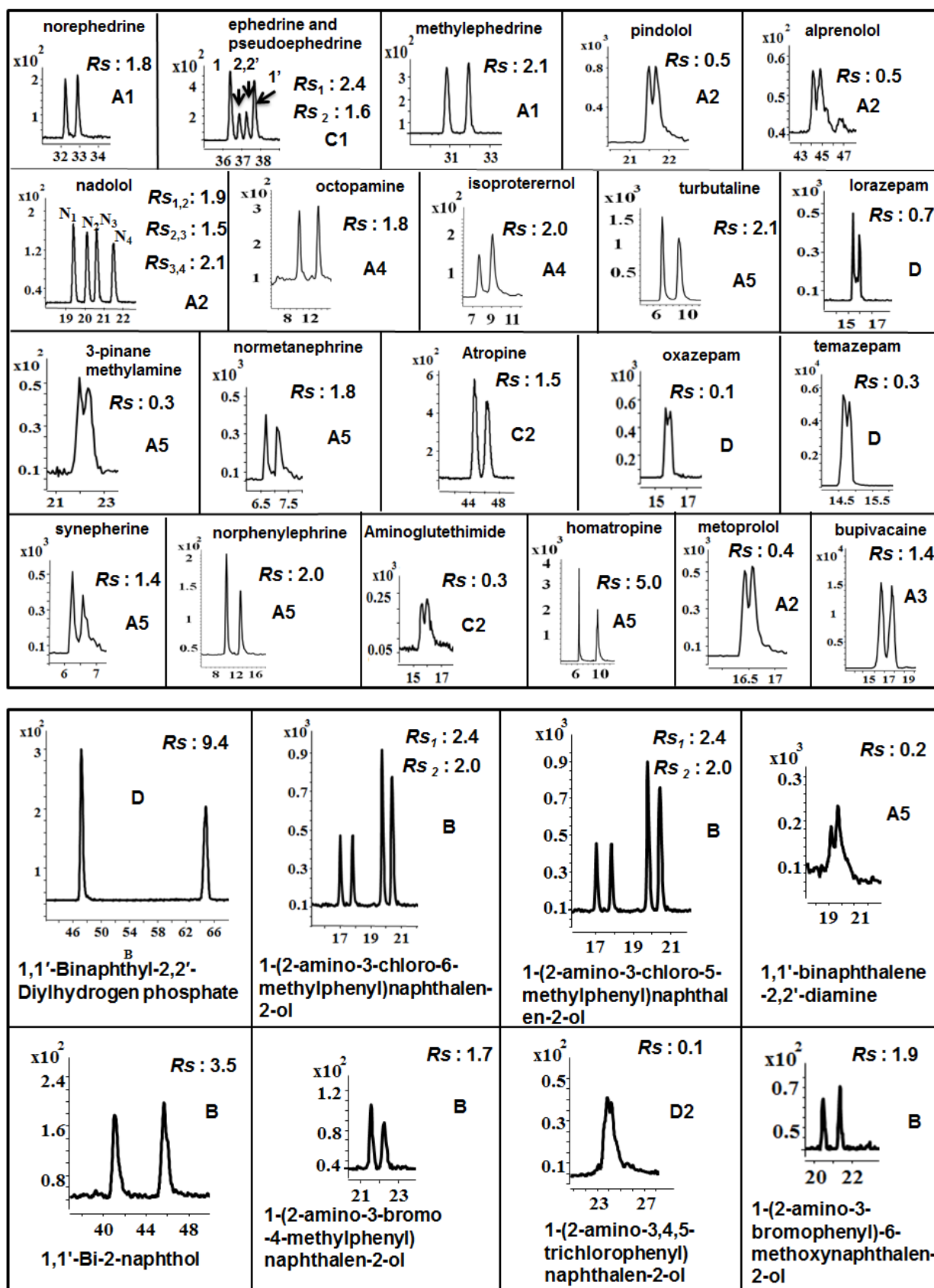


**Fig. 3.4** MEKC-MS of (A) 21 resolved cationic compounds and (B) 8 binaphthyl derivatives using four sugar surfactants using the optimum head group and optimum chain length of polymeric sugar surfactants. Buffer conditions: 25 mM NH<sub>4</sub>OAc was used as BGE in all separations, pH 5, 30 mM poly- $\beta$ -SUGP (A1); pH 7, 30 mM poly- $\beta$ -SUGP (A2); pH 5, 15 mM poly- $\beta$ -SUGP (A3) pH 6, 15 mM poly- $\beta$ -SUGP (A4) pH 7, 15 mM poly- $\beta$ -SUGP (A5); pH 5, 30 mM poly- $\beta$ -SUGS (C1); pH 5, 15 mM poly- $\beta$ -SUGS (C2); pH 5, 15 mM poly- $\beta$ -SOGS (D); pH 10.8 with 15 mM poly- $\beta$ -SOGP (B); pH 10.8, 15 mM poly- $\beta$ -SOGS (D2); Sample concentration: 100  $\mu$ g/mL in MeOH/H<sub>2</sub>O (10/90, v/v), Other conditions are the same as in Fig. 3.2.

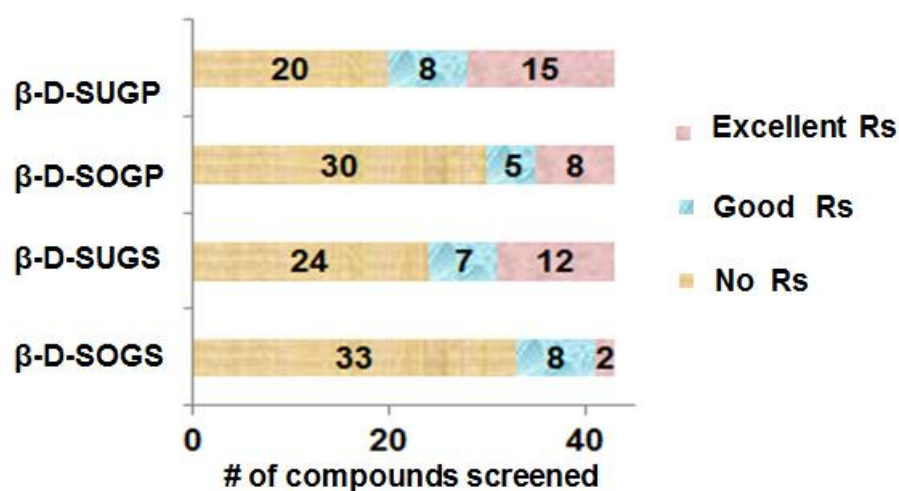


**Fig. 3.5** Bar plots showing the chiral resolution values from the chiral screening using sugar surfactant polymers with different head groups and chain lengths. The  $R_s$  values are classified as poor ( $R_s = 0$ ), fair-to-good ( $0 < R_s < 1.5$ ), and excellent ( $R_s > 1.5$ ).

### 3.3.5 Comparison of $\alpha$ - and $\beta$ - sugar surfactants

The only difference between  $\alpha$ - and  $\beta$ -glucopyranoside based surfactants is the anomeric orientation of the hydrocarbon chain with respect to the glucopyranoside ring. However,  $\alpha$ -D and  $\beta$ -D sugar surfactant exhibit distinct structural differences according to earlier study on the molecular modeling of C<sub>14</sub>- chain of D-glucopyranoside [25].

Fig. 3.6 (A-D) represents comparison of  $\alpha$ - and  $\beta$ -glucopyranoside based polymeric surfactants using the same BGE conditions for chiral separations of pseudoephedrine and metoprolol. Poly- $\beta$ -SUGP provided baseline enantioseparation of pseudoephedrine, while pseudoephedrine was partially enantioresolved using  $\alpha$ -form of the same polymer. Interestingly, complementary effect was observed when poly- $\alpha$ -SUGP provided higher chiral Rs for metoprolol compared to poly- $\beta$ -SUGP. This complementary effect could be possibly due to the different surface distribution of electrostatic potential for  $\alpha$ - and  $\beta$ -configuration. The  $\beta$ -micelles contain more negative potential on the phosphate head group surface, which enabled stronger attraction with the positively charged hydrophilic analyte such as pseudoephedrine ( $\log P = 1.05$ ) resulting in baseline Rs. However, since metoprolol ( $\log P = 1.88$ ) is more hydrophobic than pseudoephedrine, it penetrates deeper in the micellar core of poly- $\alpha$ -SUGP. Similar trend to metoprolol was observed for talinolol ( $\log P = 3.20$ ), the most hydrophobic among all three. Thus,  $\alpha$ -form of SUGP was superior to  $\beta$ -form as a chiral selector for this class of chiral compounds.

The bar plots shown in Fig. 3.6E provides a comparison of enantioseparation of ~30-40 chiral compounds between poly- $\alpha$ -SUGP and poly- $\beta$ -SUGP. While more chiral compounds were screened with poly- $\beta$ -SUGP and this polymer exhibited an overall higher success rate of 53% compared to 47% success rate observed with poly- $\alpha$ -SUGP. Clearly, there is a complementary trend. For example, most cationic chiral compounds which were separated better by poly- $\alpha$ -SUGP were relatively more hydrophobic suggesting that the chiral recognition is more likely related to hydrophobicity of the analyte with hydrophobic charged analyte separates better with poly- $\alpha$ -SUGP.

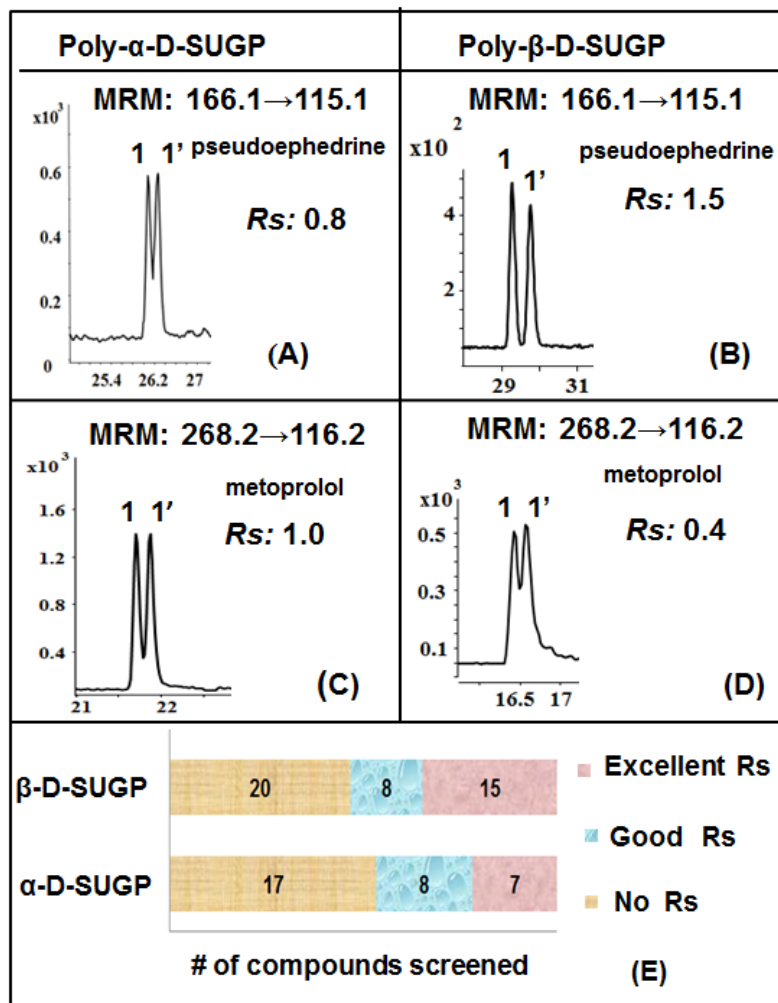


**Fig. 3.6** Electropherograms comparing the effect of anomeric configuration of 30 mM polymeric phosphated sugar on the enantioseparation of (A-B) pseudoephedrine and (C-D) metoprolol in MEKC-MS/MS. Buffer: 25 mM  $\text{NH}_4\text{OAc}$ , pH 5.0 and 7.0 for pseudoephedrine and metoprolol, respectively. Sample concentration: 100  $\mu\text{g}/\text{mL}$  in  $\text{MeOH}/\text{H}_2\text{O}$  (10/90, v/v). Other conditions are the same as Fig.3.2. The bar plots in (E) showing the chiral resolution values from the chiral screening using sugar surfactant polymers with different anomeric configurations. The  $R_s$  values are classified as poor ( $R_s = 0$ ), fair-to-good ( $0 < R_s < 1.5$ ), and excellent ( $R_s > 1.5$ ).

### 3.3.6 Multiplexed analysis

Multisegment injection in CE-MS is an emerging tool for high-throughput analysis of drugs and metabolites, in which serial hydrodynamic injection of multiple segments of sample

are performed within one single run without sacrificing chiral Rs [26]. Such a system has been proposed recently for metabolomics [6], but this is a first time chiral MEKC-MS has been used to support such a scenario. The advantage of using multisegment injection was utilized to acquire a four point calibration curve of BNP standard (100 to 500  $\mu\text{g/mL}$ ) and the R-BOH as I.S in MEKC-MS (Fig. 3.7). The spacer (i.e., BGE containing molecular micelle) segments were studied over a range of injection time from 80 sec to 240 sec to optimize the enantioseparations of BNP and I.S (i.e., BOH). The longer segment such as 200 sec was found to be beneficial for the separation of I.S but BNP exhibited partial peak overlap with this segment time. In contrast, shorter spacer segments of 80s provided better chiral Rs for BNP, whereas I.S cannot be separated (Fig. B20, Supporting Information). Therefore, 120 sec was found to be the best trade-off for the simultaneous enantioseparation of BNP from the separation of I.S. However, the use of EIC mode allows simultaneous determination of peak areas. Overall, good linearity of both R- and S-BNP was demonstrated ( $R^2 > 0.990$ ) using multisegment injection MEKC-MS, which opens up the possibility to quantitate the two isomers in biological matrix efficiently.

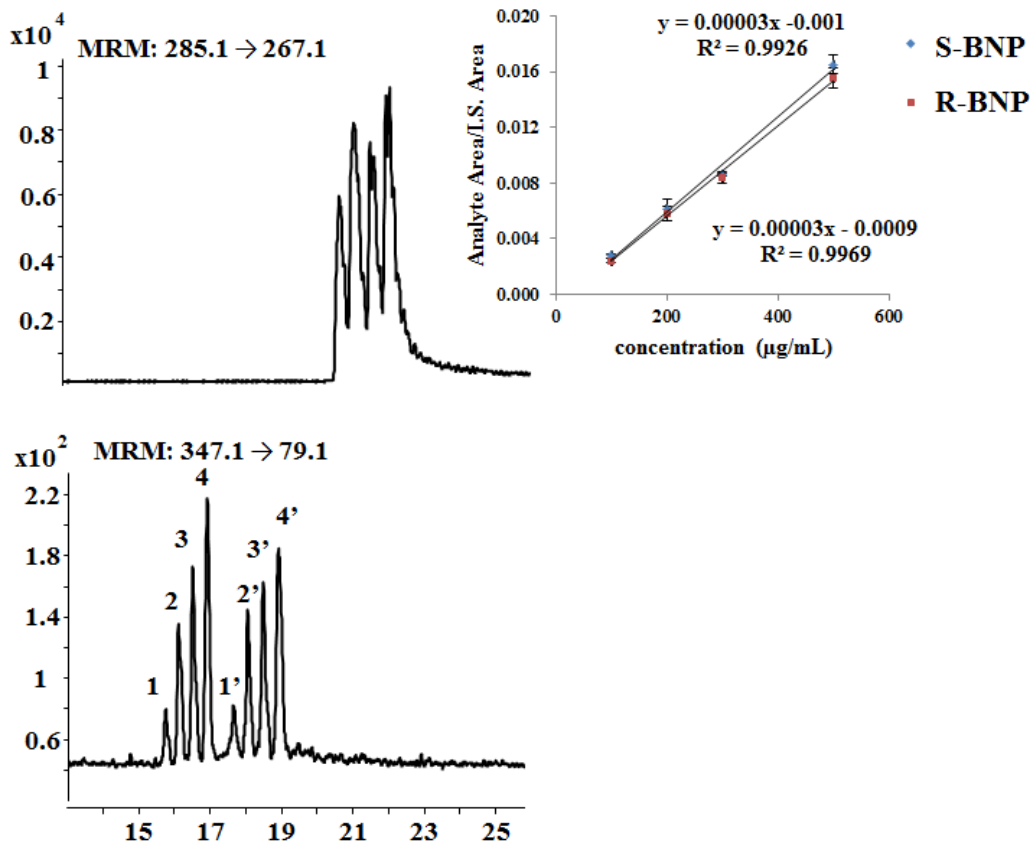


**Fig. 3.7** Multiplexed enantioseparation of 1, 1'-binaphthyl phosphate (BNP) using serial dilution of four discrete sample segments with concentrations of 1,1' = 100 µg/mL, 2,2' = 200 µg/mL, 3,3' = 300 µg/mL and 4,4' = 500 µg/mL (bottom electropherogram) at fixed concentration (250 µg/mL) of *R*-binaphthol as an internal standard (top electropherogram) in a single run using an optimum micelle spacer of 5mbar, 120s. Buffer: 25 mM NH<sub>4</sub>OAc, pH 5.0, 15 mM SUGS. The Fig 6 inset shows a calibration curve for a single step acquisition of four point calibration linear over the range of 100 µg/mL to 500 µg/mL. Other conditions are the same as discussed in section 3.2.3.1.

### 3.4. Conclusions

Four polymeric β-D-glucopyranoside based surfactants were successfully synthesized, characterized, polymerized and screened for enantioselective MEKC-MS. Sulfate and phosphate charge on the head group polymeric surfactants with C<sub>11</sub> carbon chain showed complementary chiral separations of cationic amines. On the other hand, shorter chain length

phosphated surfactants (e.g., poly- $\beta$ -D-SOGP) exclusively separate majority of the BAI. Nevertheless, either too strong or too weak hydrophobic interactions between sugar micelle polymer and the chiral analyte leads to poor Rs. Thus, it is important to have proper hydrophobic–hydrophilic balance between polymeric sugar surfactants and the analytes to achieve good Rs. Overall, enantiomeric separations of 30 out of 43 chiral compounds (70% successful rate) were realized by using  $\beta$ -D-glucopyranoside based surfactants with different chain lengths and head groups in MEKC-MS/MS.

The  $\alpha$ - and  $\beta$ -SUGP exhibits complementary behavior in enantioseparation of amines (e.g., secondary amines (pseudoephedrine) vs. amino alcohols (metoprolol). Further detailed exploration in the chiral recognition of  $\alpha$ -D and  $\beta$ -D configuration of glucopyranoside surfactant is warranted for better understanding of chiral recognition mechanism with this new generation of MS compatible polymeric surfactants. Finally, multiplexed quantitative analysis of R/S-BNP using multisegment injection MEKC-MS demonstrates the feasibility of high throughput quantitation of enantiomers, which could be applied conveniently for analysis of biological samples.

## References

- [1] Mitra,S., Chopra,P. *Indian J Anaesth.* 2011, 55,(6),555-562.
- [2] Mohan,J.S., Mohan,E.S., Reddy,S., Manda,S., Yamsani,M. R. “Chiral Interactions and Chiral Inversions-New Challenges to Chiral Scientists.” *Pharmacie, Globale.* 2011,3, 1-9.
- [3] Peepliwal,A.K., Bagade,S. B., Bonde,C.G. *J. Biomed Sci and Res.* 2010, 2(1), 29-45.
- [4] Q3B: Impurities in new drug products. International Conference on Harmonization. ICH Harmonized Tripartite Guidelines, 2006.
- [5] Chankvetadze, B., Endresz, G., Blaschke, G., *Electrophoresis.* 1994, 15, 804-807.
- [6] Simó C., García-Cañas,V., Cifuentes, A. *Electrophoresis.* 2010, 31, 1442-1456.
- [7] Moini, M., Rollman, C.M. *Rapid Commun. Mass Spectrom.* 2015, 29, 304-310.
- [8] Shamsi, S. A. *Anal. Chem.* 2001, 73, 5103-5108.
- [9] Wang, J., Warner, I.M., *Anal. Chem.* 1994, 66, 3773-3776.
- [10] Shamsi, S. A., Macossay, J, Warner, I.M., *Anal. Chem.*, 1997, 69, pp 2980–2987.
- [11] Billiot,F.H., McCarroll M.; Billiot , E.J., Rugutt, J., Morris, K Isiah M. Warner *Langmuir*, 2002, 18, 2993–2997.
- [12] Billiot, E.,Isiah M. Warner, *Anal. Chem.*, 2000, 72 . 1740–1748
- [13] Akbay C, Rizvi SA, Shamsi S.A. *Anal Chem.* 2005 , 77, 1672-1683.
- [14] Hou J, Zheng J, Shamsi SA. *Electrophoresis.* 2007, 28, 1426-1434.
- [15] Rizvi SA, Shamsi S.A. Chiral Analysis Using Polymeric Surfactants in MEKC in “Chiral Separation Techniques: A Practical Approach.” G. Subramanian (Ed) Wiley-VCH, Wiley and Sons, 3<sup>rd</sup> Revision, 2007, pp. 505-559
- [16] Tickle, D.C.; Okafo, N.G.; Camilleri, P.; Jones. R.F.D.; Kirby A.J., *Anal.Chem.* 1994, 66, 4121-4126.



- [17] Li, X., Turanek, J., Knotigova, P., Kudlackova, H., Masek, J., Pennington, D.B., Rankin, S.E., Knutson, B.L., Lehmler, H.J., *New J. Chem.*, 2008, 32, 2169-2179.
- [18] Didier, D., Florence, D., *J. Phytochemistry* 1994, 36, 289-298.
- [19] Liu, Y., Wu, B., Wang, P., Shamsi, S.A., *Electrophoresis*, 2016, 00,1-11
- [20] Liu, Y., Shamsi, S.A., *J.Chromatogr. A.* 2014, 1360, 296-304.
- [21] Rizvi, S.A.A., Shamsi, S.A., *Electrophoresis.* 2003, 24, 2514–2526.
- [22] Rizvi, S.A.A., Shamsi, S.A., *Electrophoresis.* 2005, 26, 4172–4186.
- [23] Rundlett, K. L., Armstrong. D. W., *Anal. Chem.* 1996, 68, 3493-3497.
- [24]<http://www.mayoclinic.org/drugs-supplements/atropine-homatropine-and-scopolamine-ophthalmic-route/description/drg-20069679>
- [25] Tickle, D.; George. A.; Jennings, K.; Camilleri, P.; Kirby, A.J.; *J. Chem. Soc., Perkin Trans.* 1998, 2, 467-474.
- [26] Kuehnbaum, N.L.; Kormendi, A.; Britz-McKibbin, P.; *Anal. Chem.* 2013, 85, 10664–10669.



**Appendix A**  
**Supporting Material for Chapter 2**

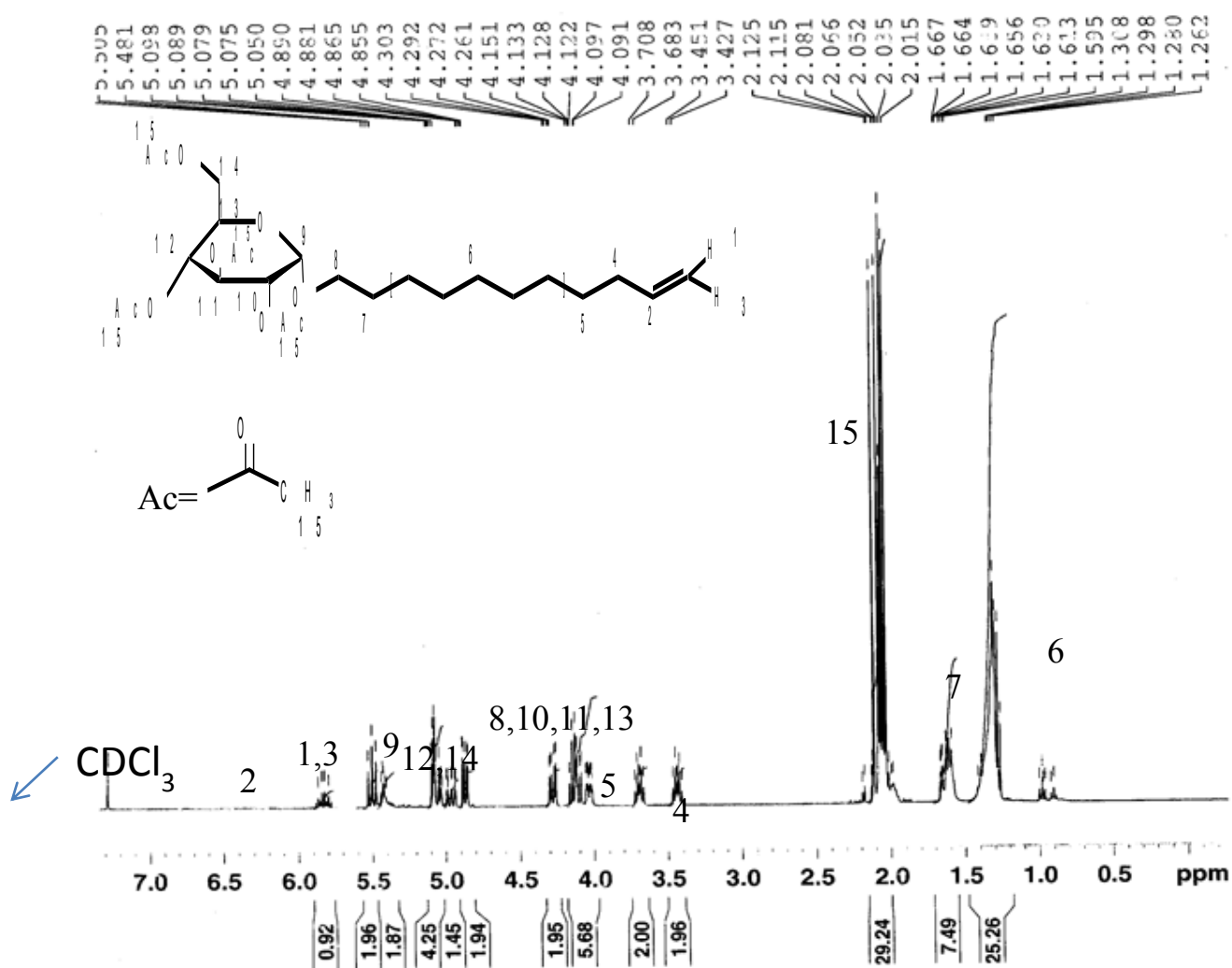


**Figure A1.**  $^1\text{H-NMR}$  spectrum of Product 2, *n*-undecenyl  $\alpha$ -D-glucopyranoside, pentaacetate in  $\text{CDCl}_3$

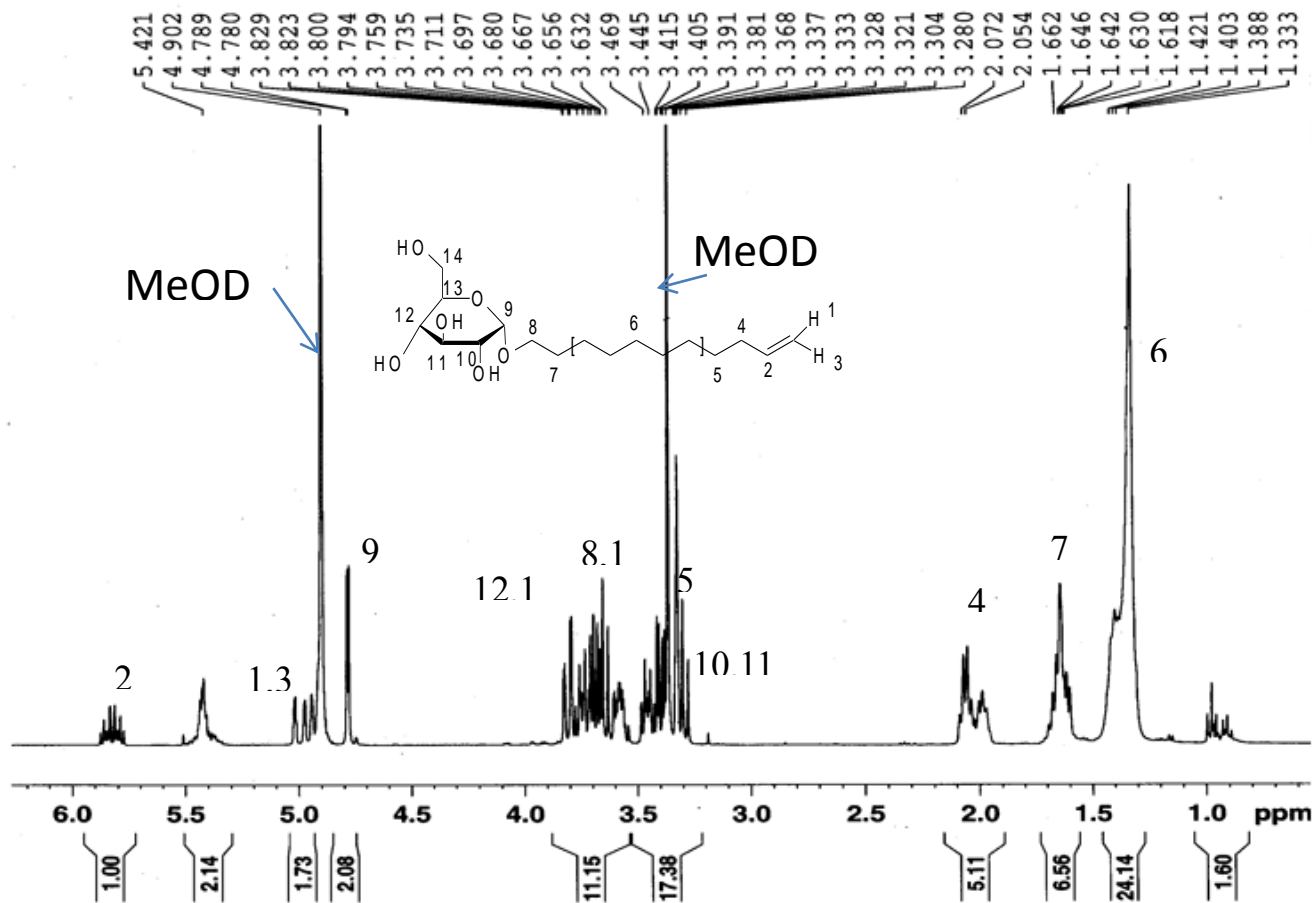


**Figure A2.**  $^1\text{H-NMR}$  spectrum of Product 3, *n*-undecenyl  $\alpha$ -D-glucopyranoside in MeOD

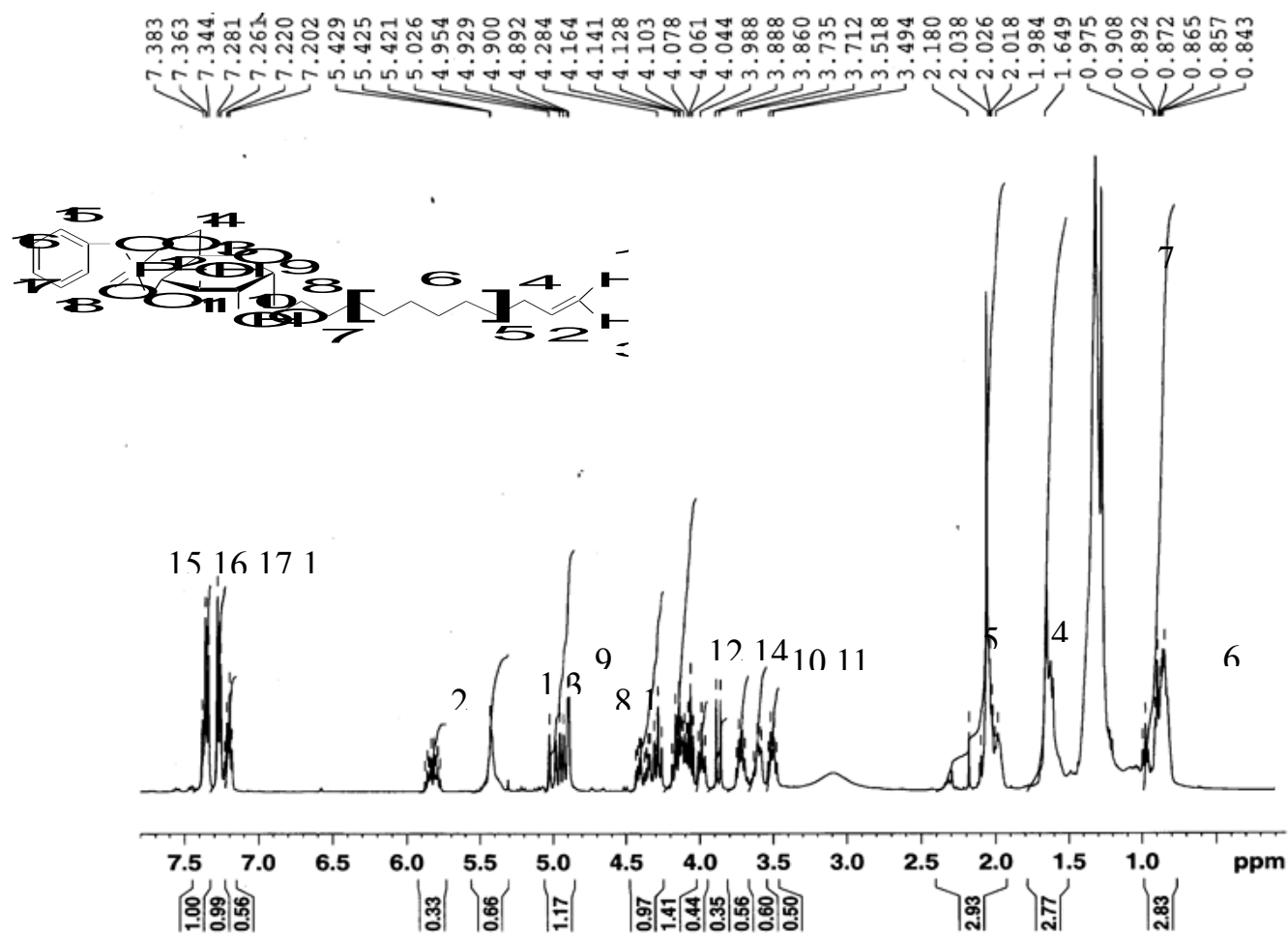


**Figure A3.** <sup>1</sup>H-NMR spectrum of Product 4, *n*-undecenyl α-D-glucopyranoside 4,6-phenyl phosphate in CDCl<sub>3</sub>

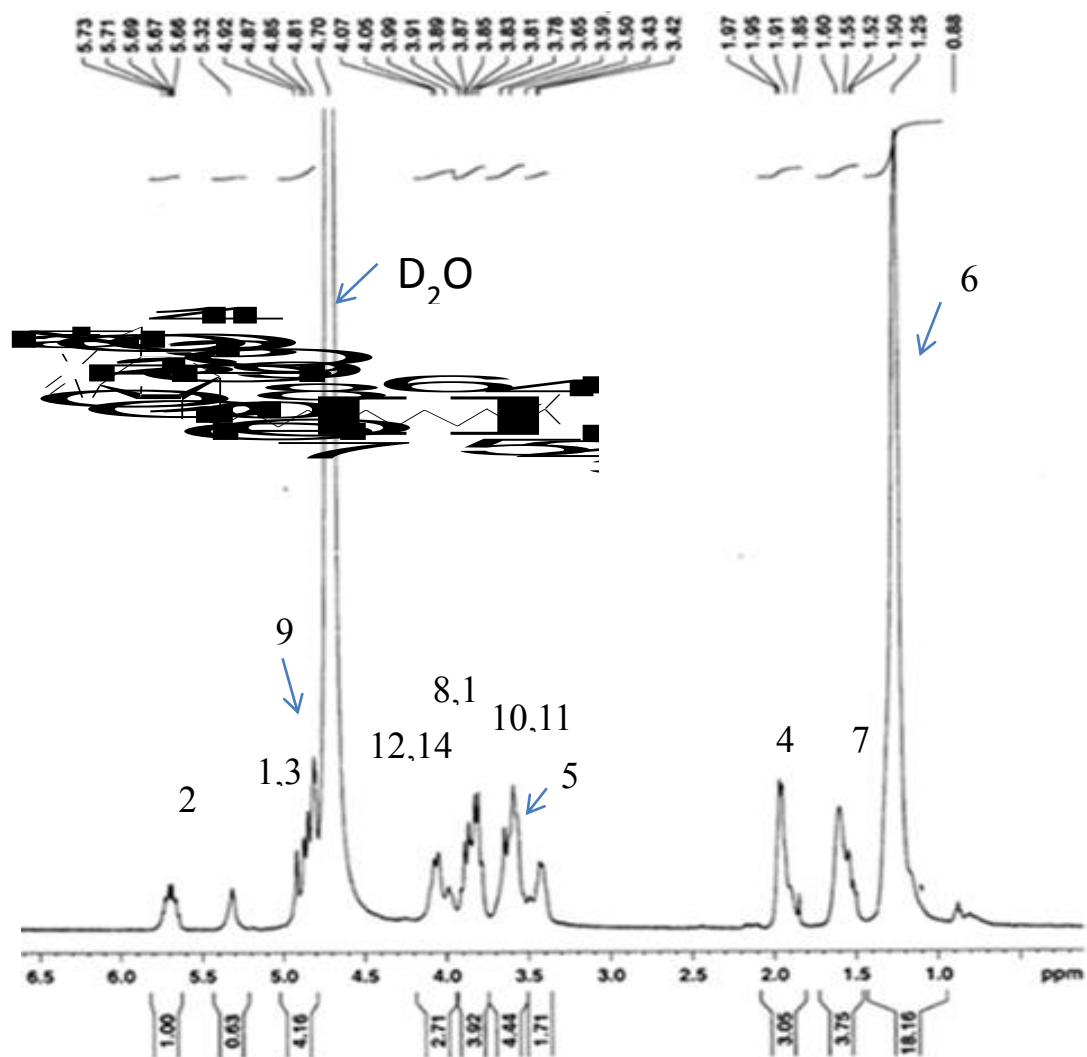


**Figure A4.**  $^1\text{H-NMR}$  spectrum of *n*-undecenyl  $\alpha$ -D-glucopyranoside 4,6-hydrogen phosphate, sodium salt in  $\text{D}_2\text{O}$

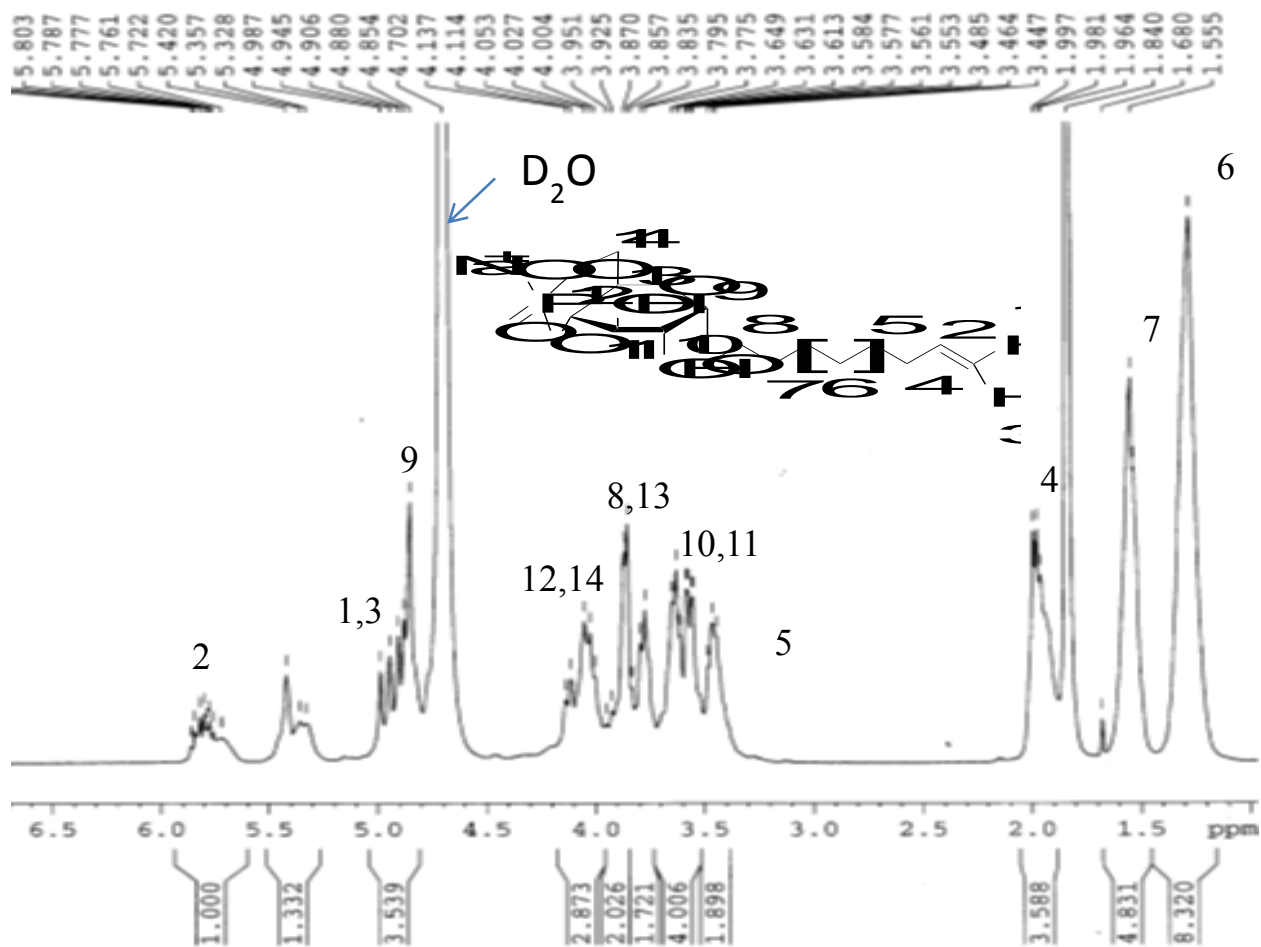


**Figure A5.**  $^1\text{H-NMR}$  spectrum of *n*-octenyl  $\alpha$ -D-glucopyranoside 4,6-hydrogen phosphate, sodium salt in  $\text{D}_2\text{O}$



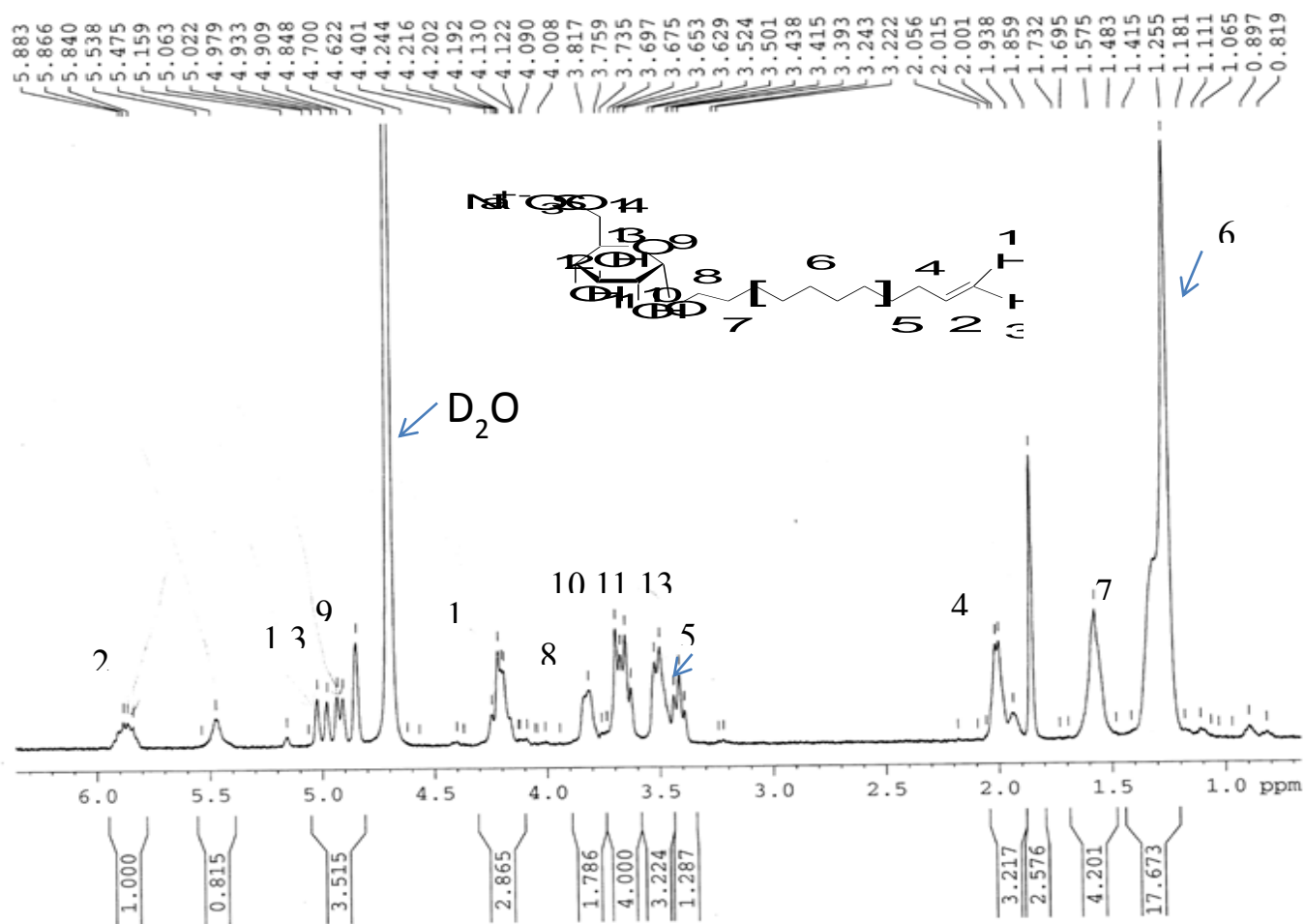


**Figure A6.**  $^1\text{H-NMR}$  spectrum of *n*-undecenyl  $\alpha$ -D-glucopyranoside 6-hydrogen sulfate, monosodium salt in  $\text{D}_2\text{O}$

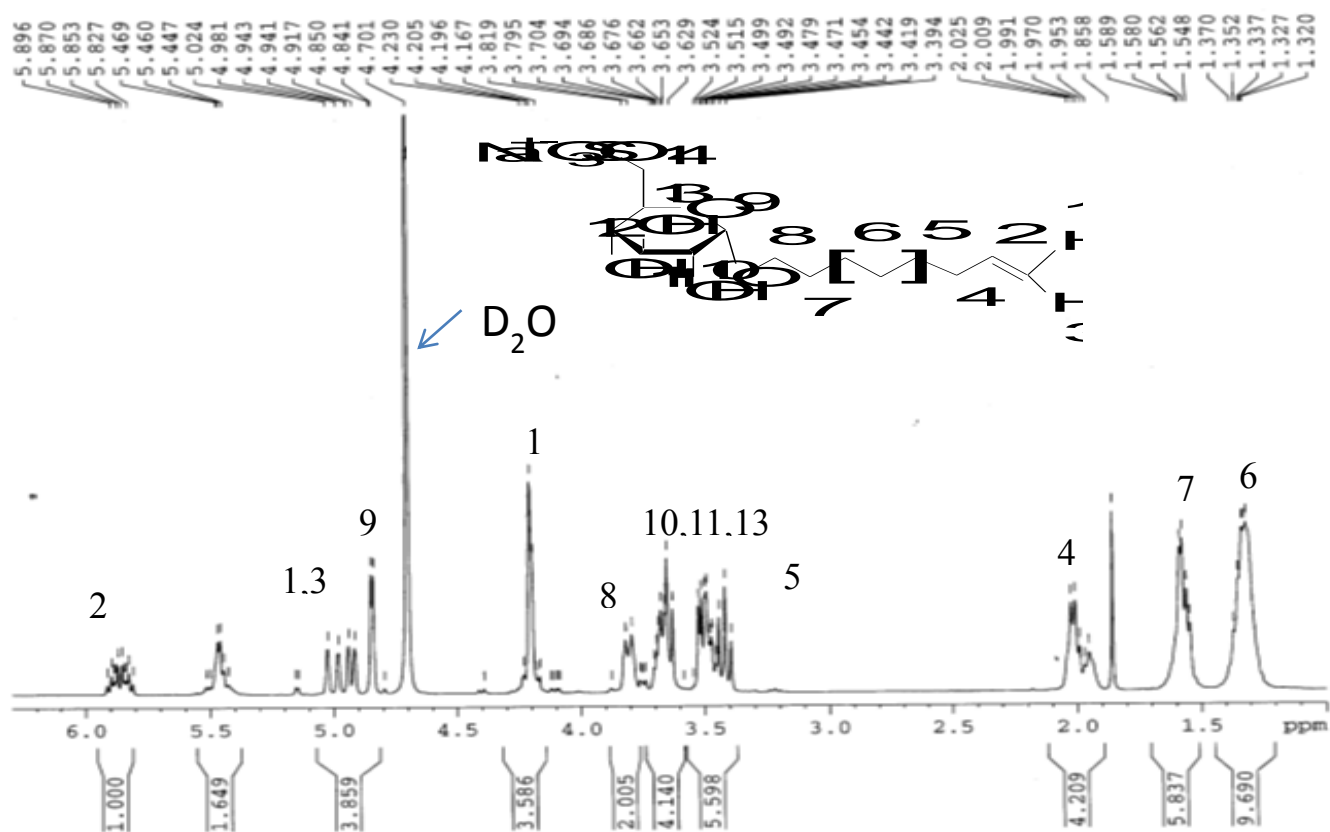
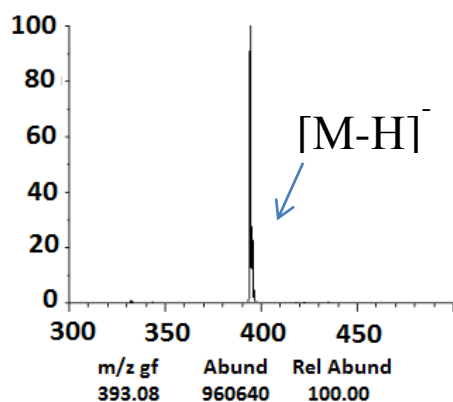
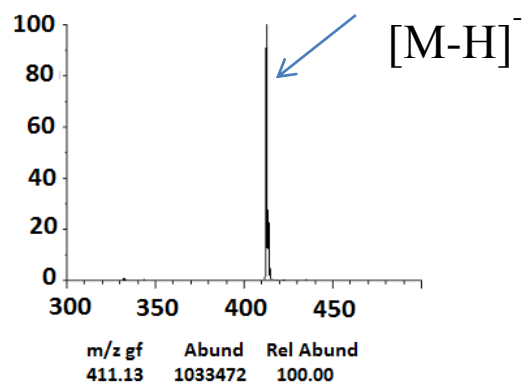


**Figure A7.**  $^1\text{H-NMR}$  spectrum of *n*-octenyl  $\alpha$ -D-glucopyranoside 6-hydrogen sulfate, monosodium salt in  $\text{D}_2\text{O}$

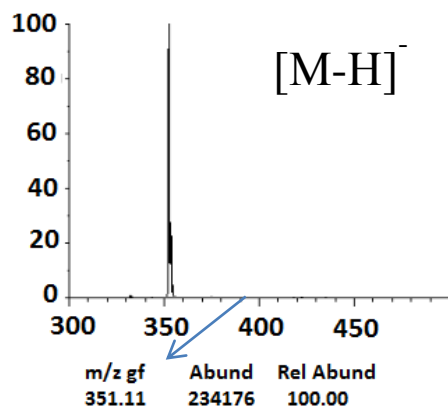
*n*-undecenyl  $\alpha$ -D-glucopyranoside  
4,6-hydrogen phosphate, sodium salt (A)



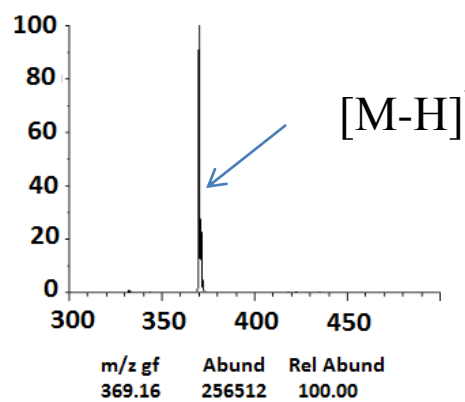
*n*-undecenyl  $\alpha$ -D-glucopyranoside  
6-hydrogen sulfate, monosodium salt (B)



*n*-octenyl  $\alpha$ -D-glucopyranoside  
4,6-hydrogen phosphate, sodium salt (C)

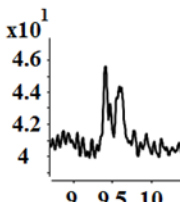
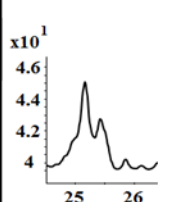
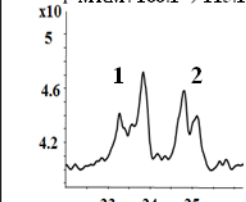
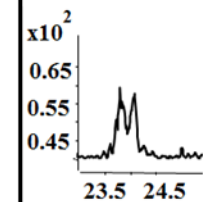
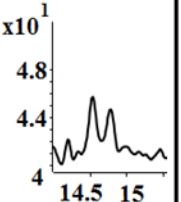
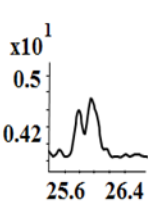


*n*-octenyl  $\alpha$ -D-glucopyranoside  
6-hydrogen sulfate, monosodium salt (D)



**Figure A8.** ESI-MS of sugar surfactants in negative mode

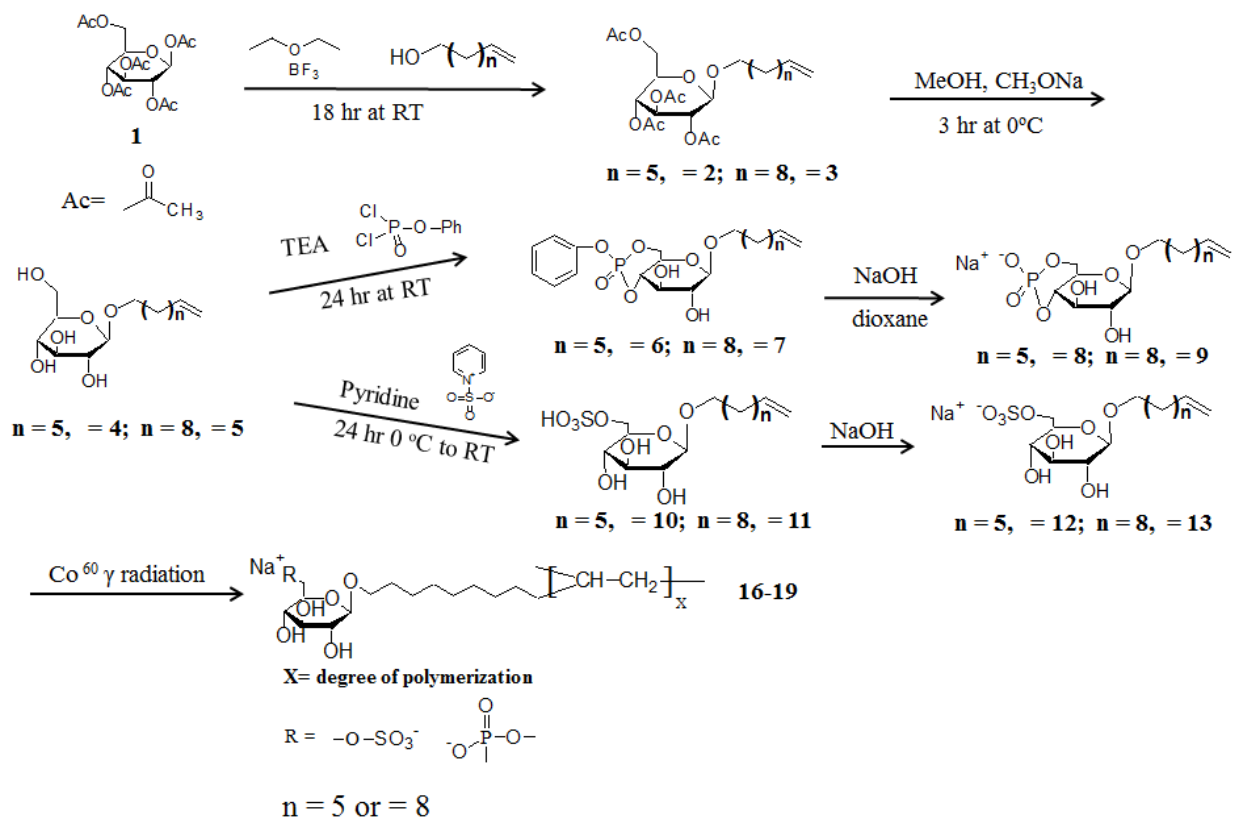
**Table A1.** Limit of detection (LOD) chromatogram of BNP, ephedrines and  $\beta$ -blockers in MEKC-MS/MS

100 ng/mL $S/N_{avg}$ : 6.0	10 ng/mL $S/N_{avg}$ : 8.6	10 ng/mL $S/N1_{avg}$ : 6.6, $S/N2_{avg}$ : 5.4	50 ng/mL $S/N_{avg}$ : 10	50 ng/mL $S/N_{avg}$ : 4.8	50 ng/mL $S/N_{avg}$ : 9.0
*BNP MRM: 347.1 $\rightarrow$ 79.1 	*Norephedrine MRM: 152.1 $\rightarrow$ 117.2 	* Ephedrine and Pseudoephedrine MRM: 166.1 $\rightarrow$ 115.1 	Methylephedrine MRM: 180.1 $\rightarrow$ 147.2 	*Atenolol MRM: 267.2 $\rightarrow$ 145.2 	*Metoprolol MRM: 293.2 $\rightarrow$ 237.2 

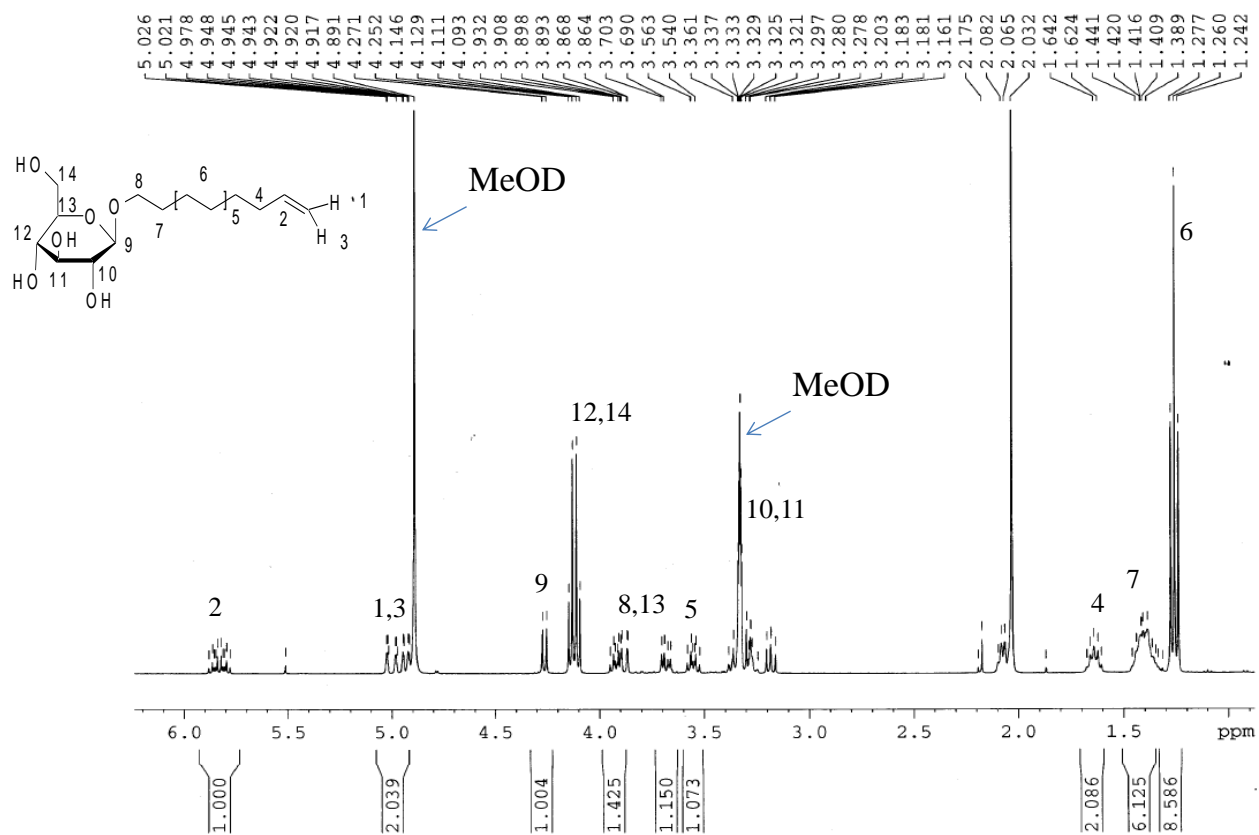
\*chromatograms were smoothed by Agilent Mass Hunter Workstation (version B.02.01)

**Appendix B**

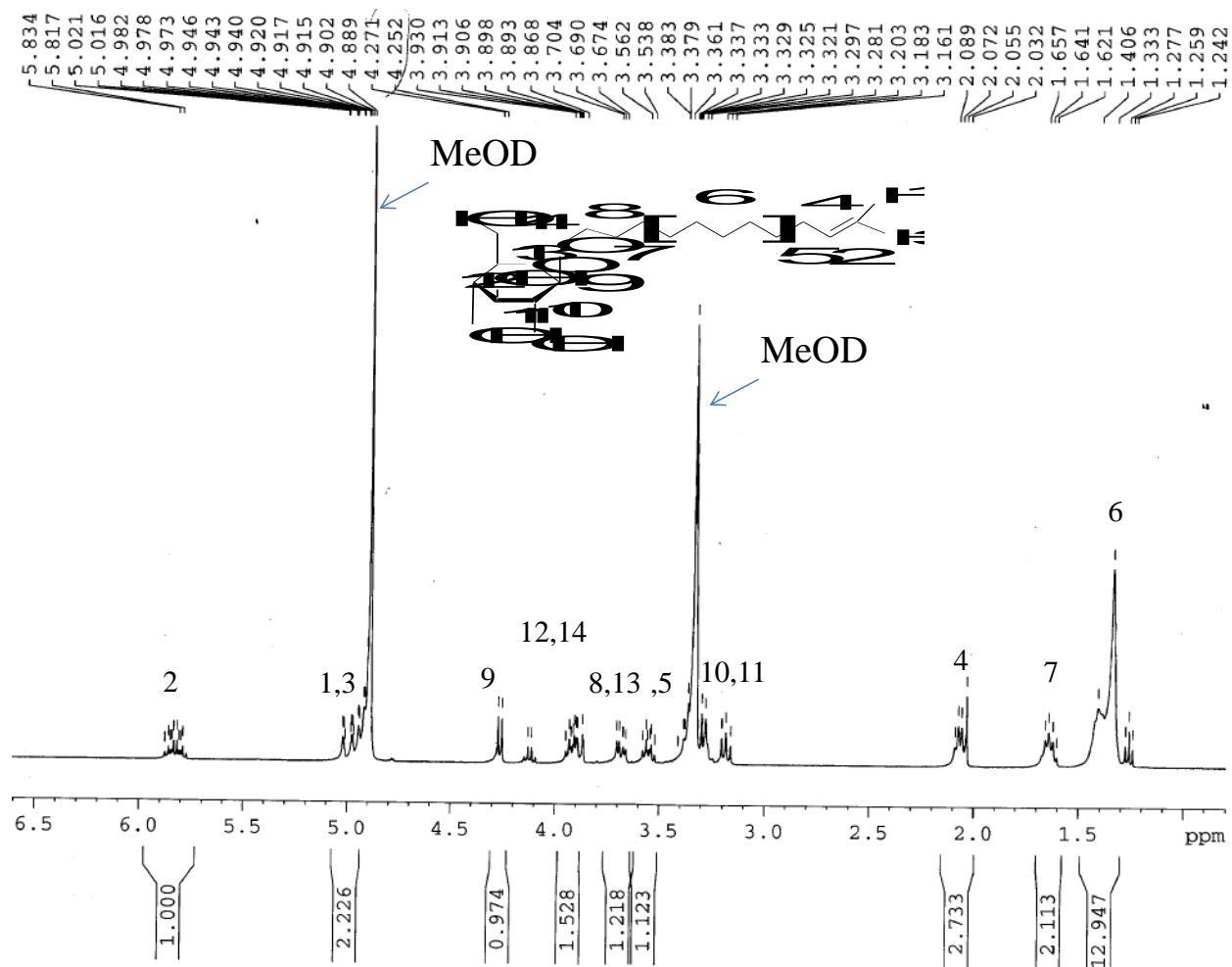
**Supporting Material for Chapter 3**



**Scheme B1** Synthesis scheme for poly(*n*-undecyl β-D-glucopyranoside 4,6-hydrogen phosphate, sodium salt **9**) (poly-β-SUGP), poly(*n*-undecyl β-D-glucopyranoside 6-hydrogen sulfate, monosodium salt **13**) (poly-β-SUGS), poly-(*n*-octyl β-D-glucopyranoside 4,6-hydrogen phosphate, sodium salt **8**), (poly-β-SOGP), poly(*n*-octyl β-D-glucopyranoside 6-hydrogen sulfate, monosodium salt **12**) (poly-β-SOGS).

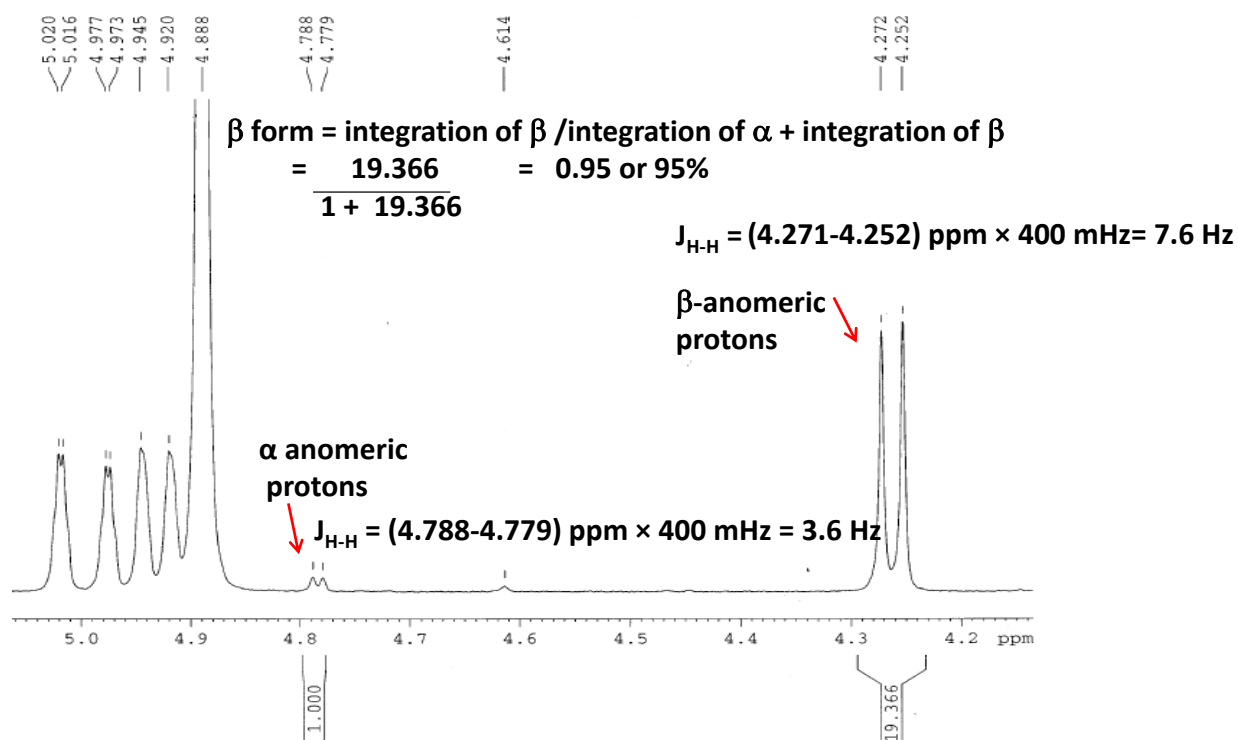


**Figure B1.** <sup>1</sup>H-NMR of **Compound 4**, *n*-octenyl β-D-glucopyranoside in MeOD

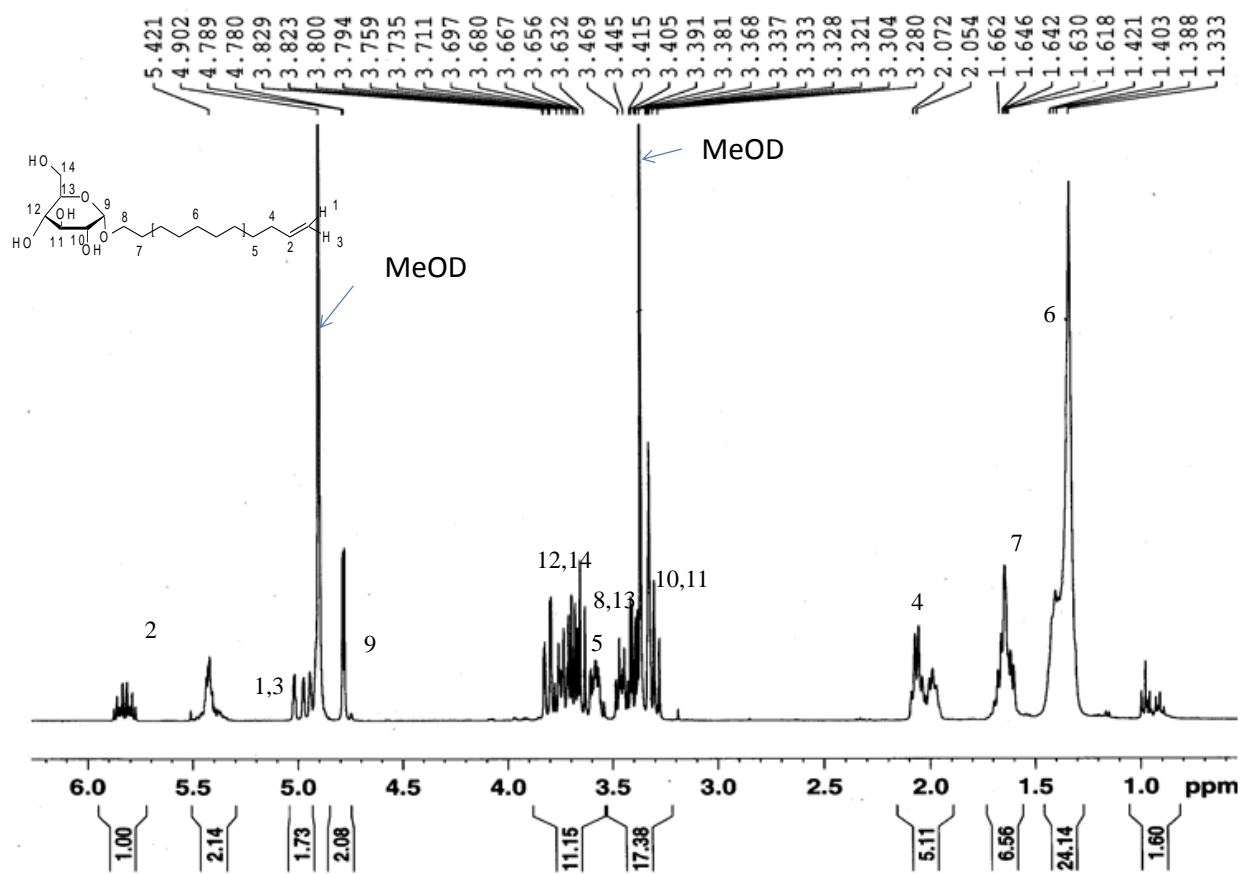


**Figure B2.**  $^1\text{H-NMR}$  of **Compound 5**, *n*-undecenyl  $\beta$ -D-glucopyranoside in MeOD

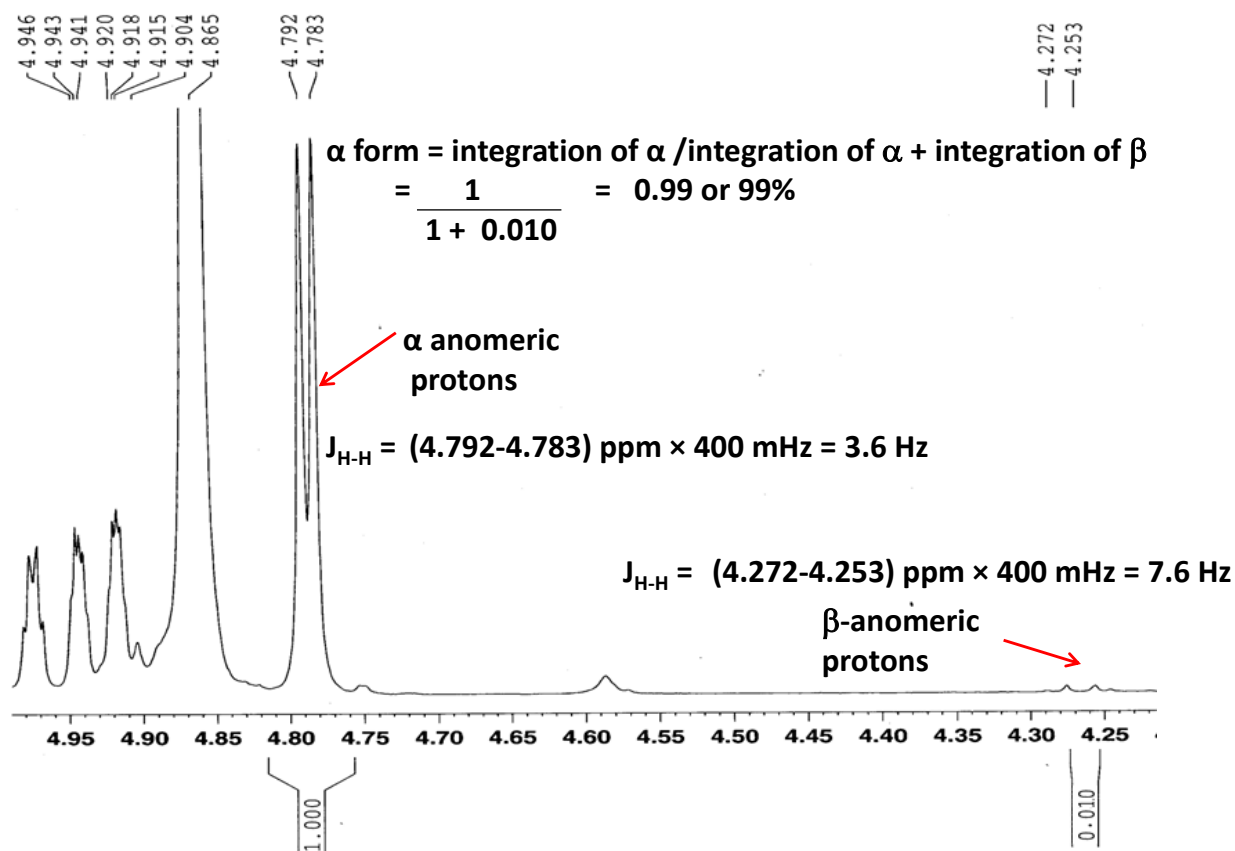




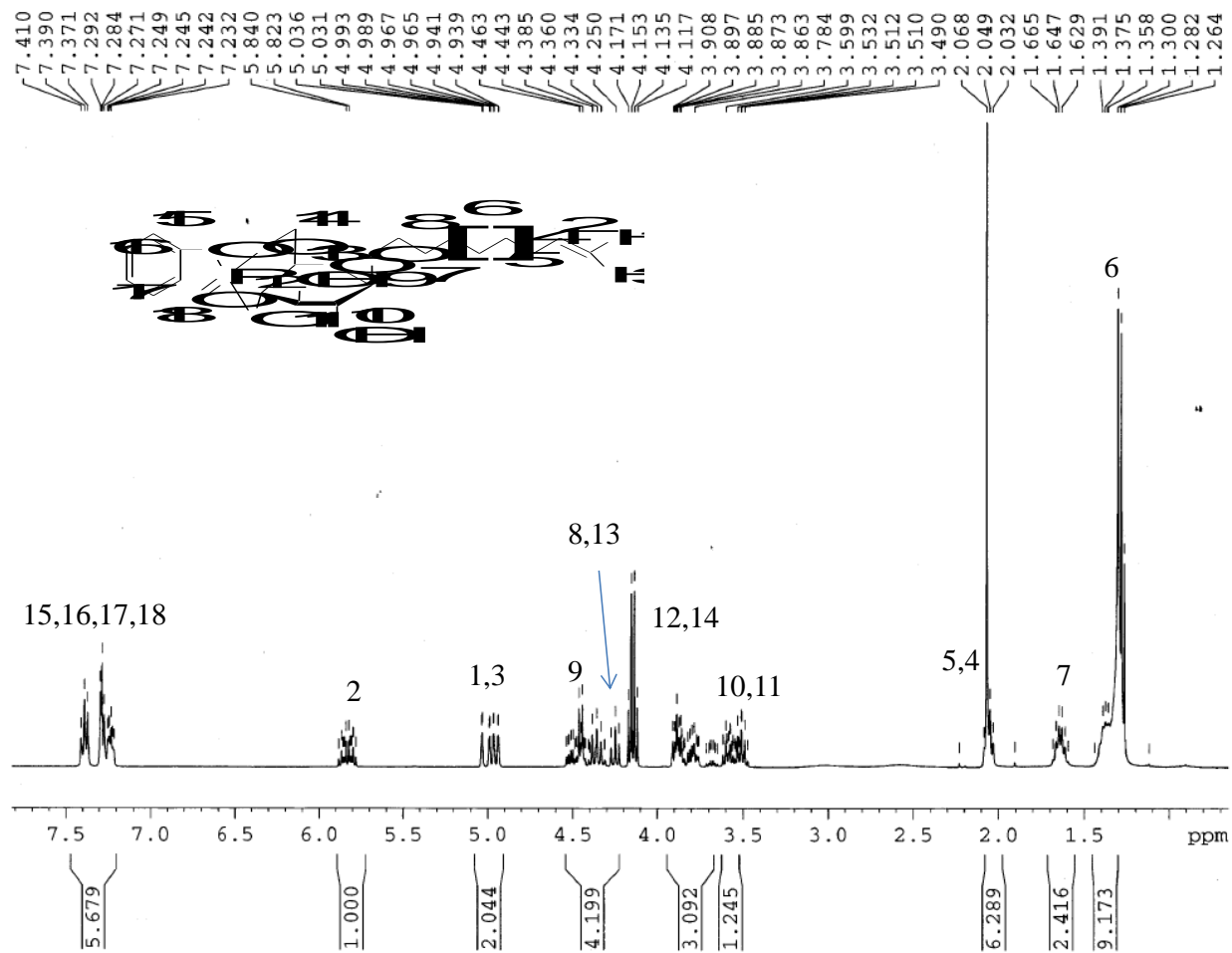
**Figure B3.**  $^1\text{H-NMR}$  of  $\alpha$  and  $\beta$  ratio of **Compound 5** *n*-undecenyl  $\beta$ -D-glucopyranoside



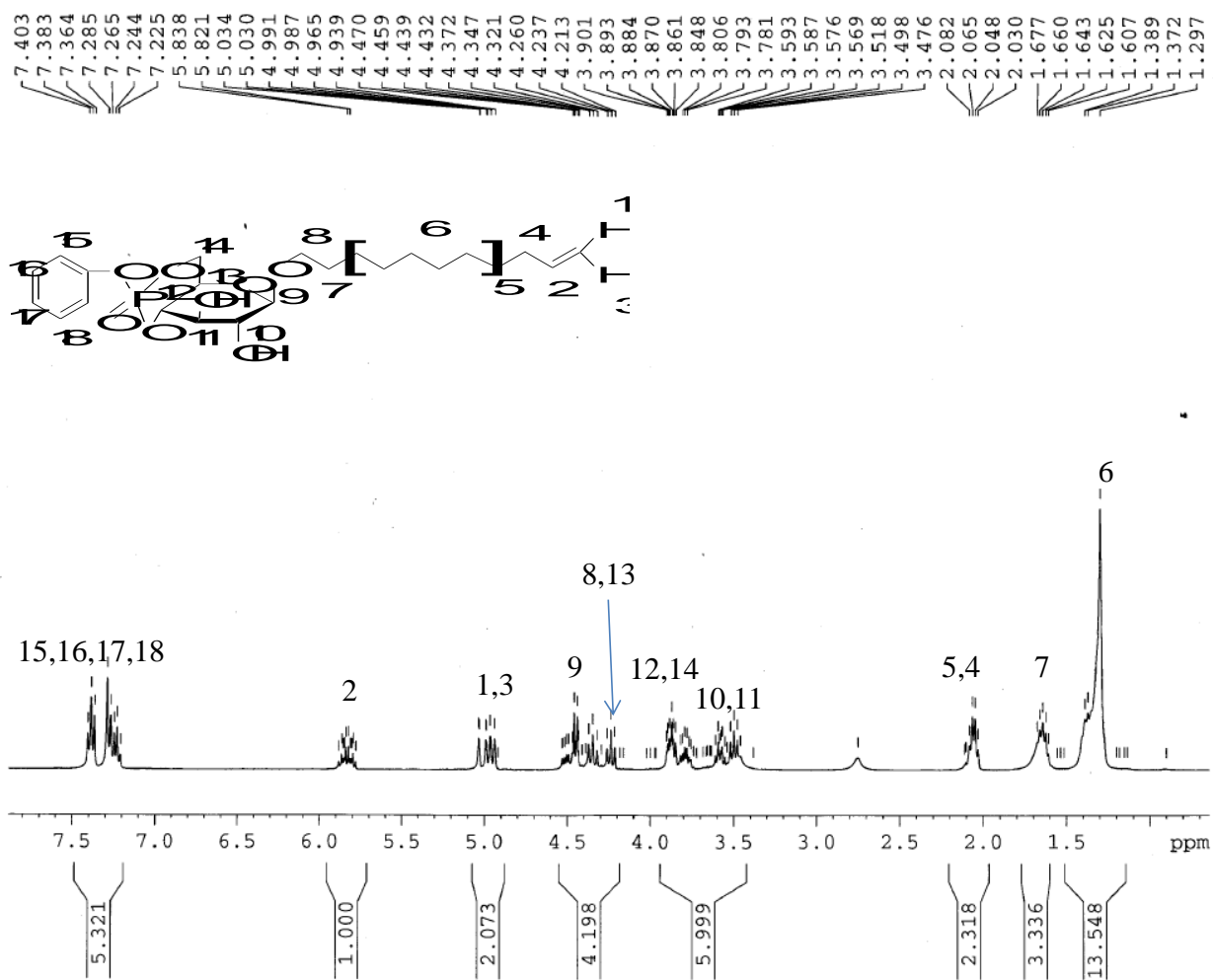
**Figure B4.** <sup>1</sup>H-NMR of **Compound 15** *n*-undecyl α-D-glucopyranoside in MeOD



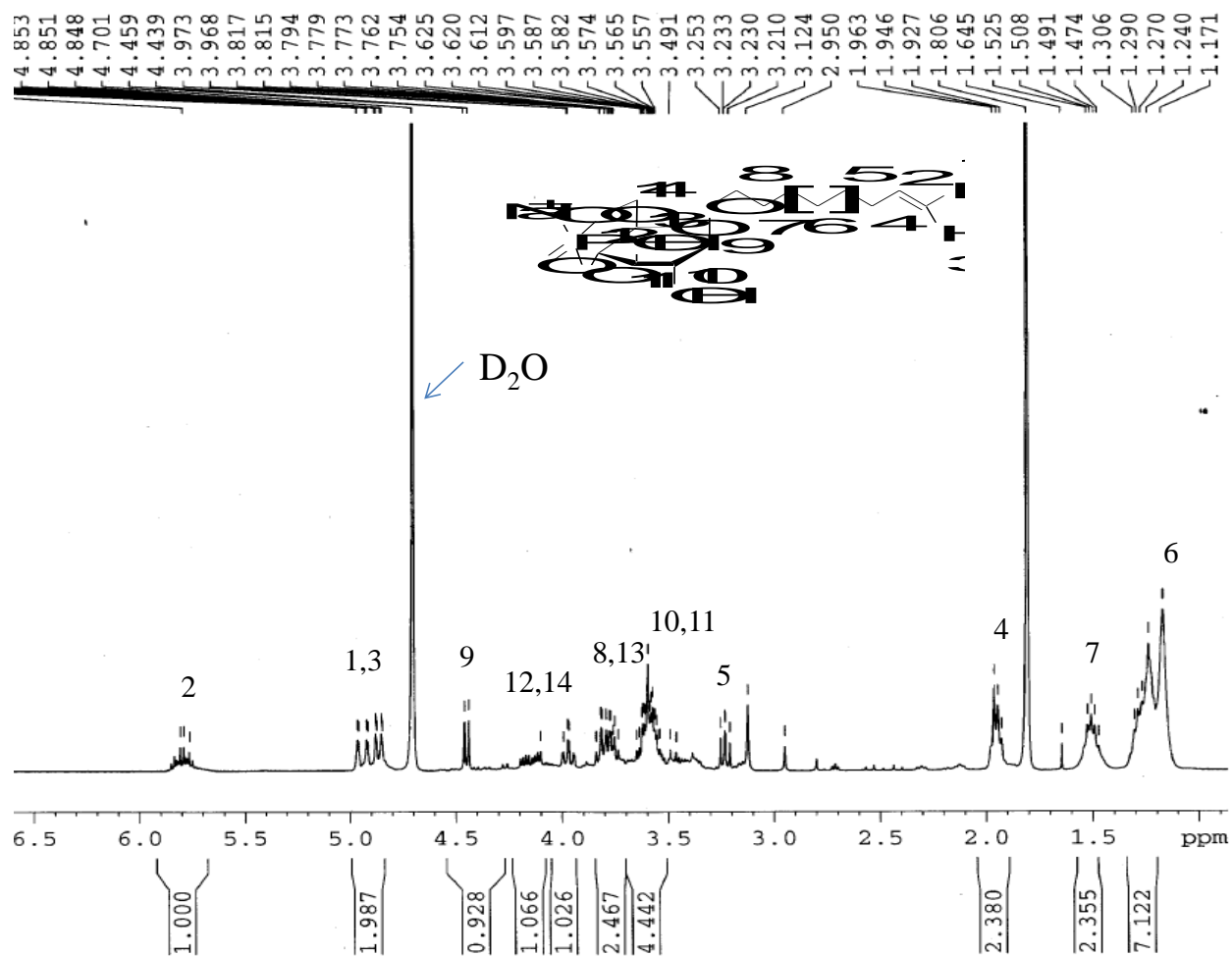
**Figure B5.**  $^1\text{H-NMR}$  of  $\alpha$  and  $\beta$  ratio of **Compound 15** *n*-undecenyl  $\alpha$ -D-glucopyranoside



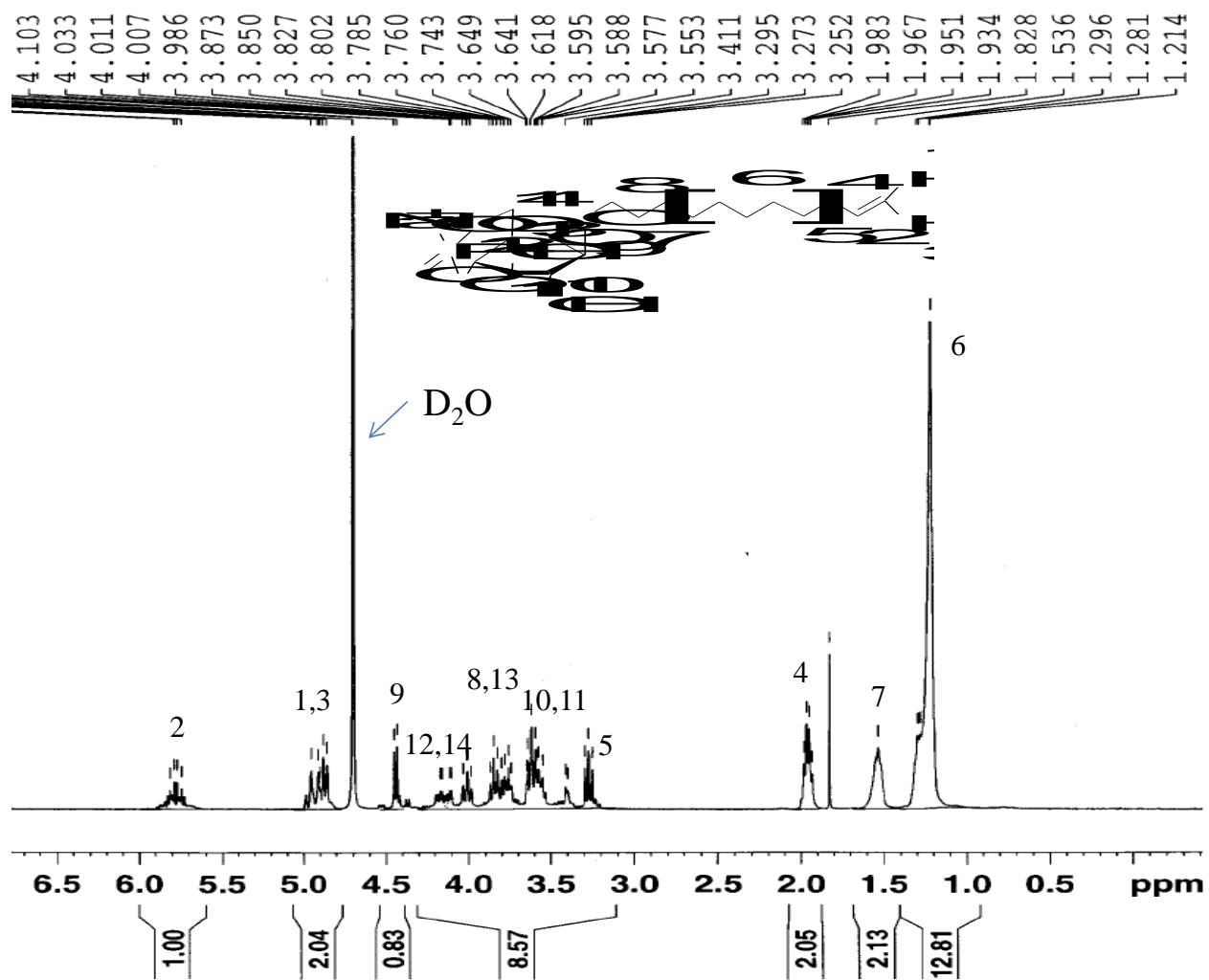
**Figure B6.** <sup>1</sup>H-NMR of **Compound 6**, *n*-octenyl β-D-glucopyranoside 4,6-phenyl phosphate in CDCl<sub>3</sub>



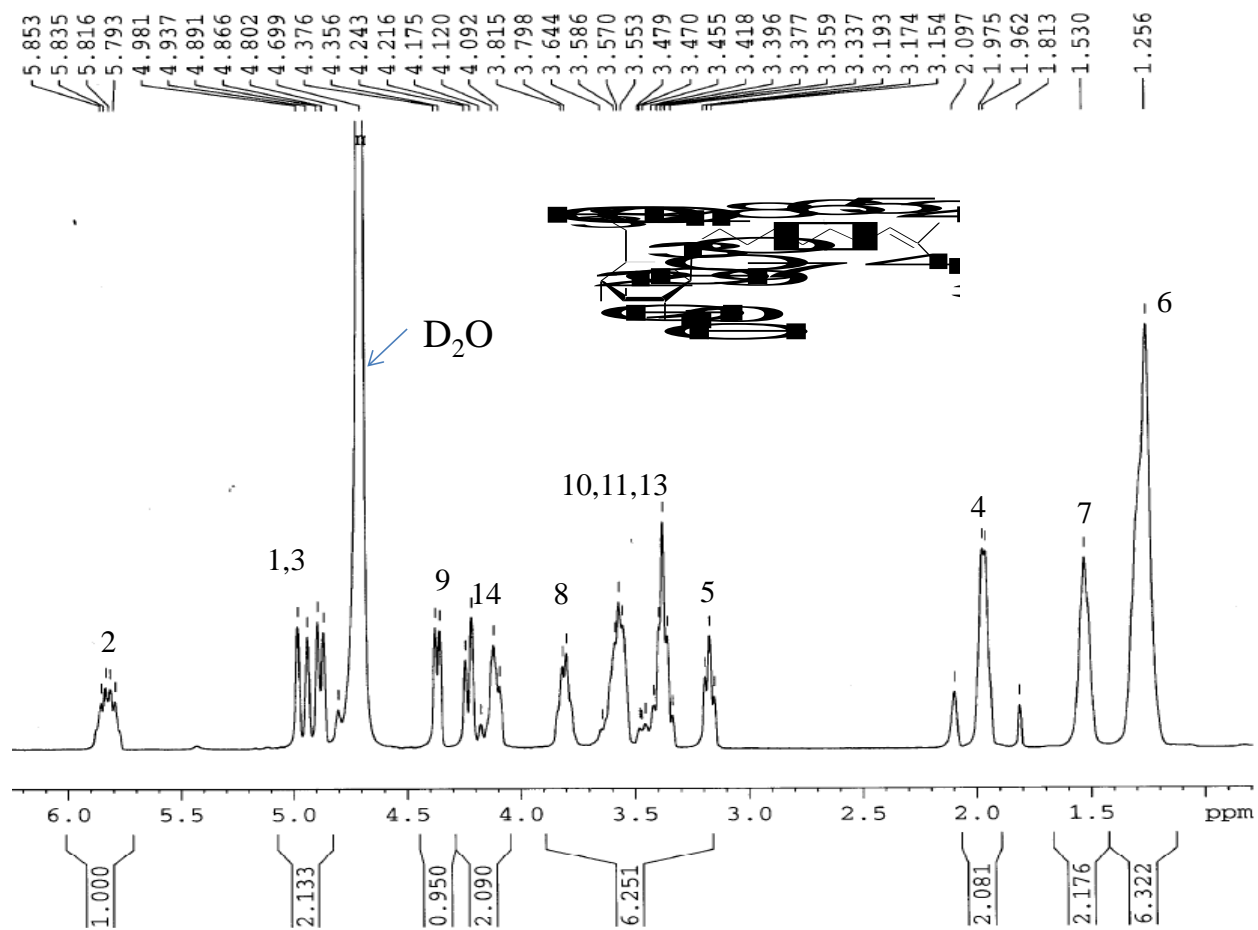
**Figure B7.**  $^1\text{H-NMR}$  of **Compound 7**, *n*-undecenyl  $\beta$ -D-glucopyranoside 4,6-phenyl phosphate in  $\text{CDCl}_3$



**Figure B8.** <sup>1</sup>H-NMR of **Final Product 8** *n*-octenyl β-D-glucopyranoside 4,6-hydrogen phosphate, sodium salt in D<sub>2</sub>O

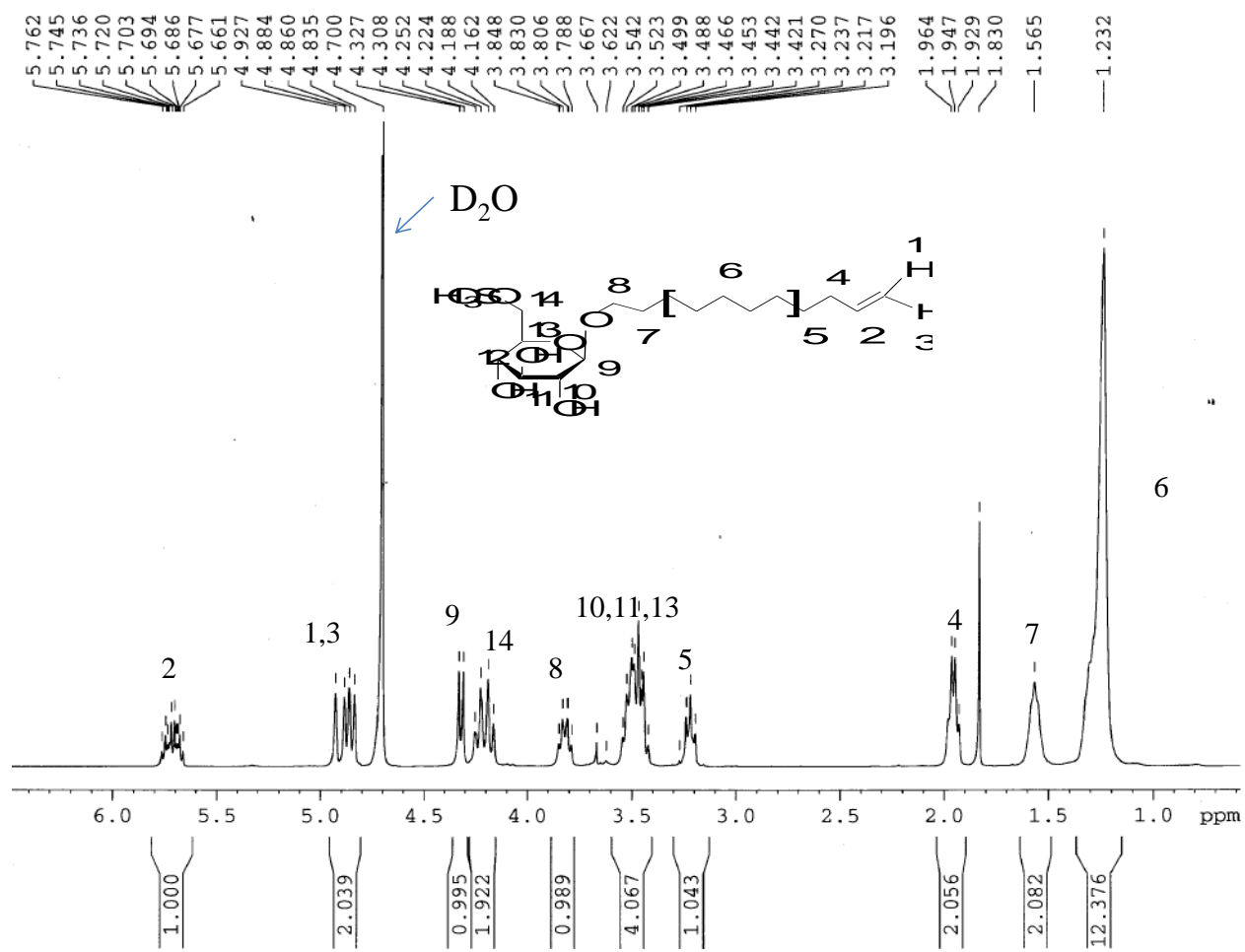


**Figure B9.**  $^1\text{H-NMR}$  of **Final Product 9** *n*-undecenyl  $\beta$ -D-glucopyranoside 4,6-hydrogen phosphate, sodium salt in  $\text{D}_2\text{O}$

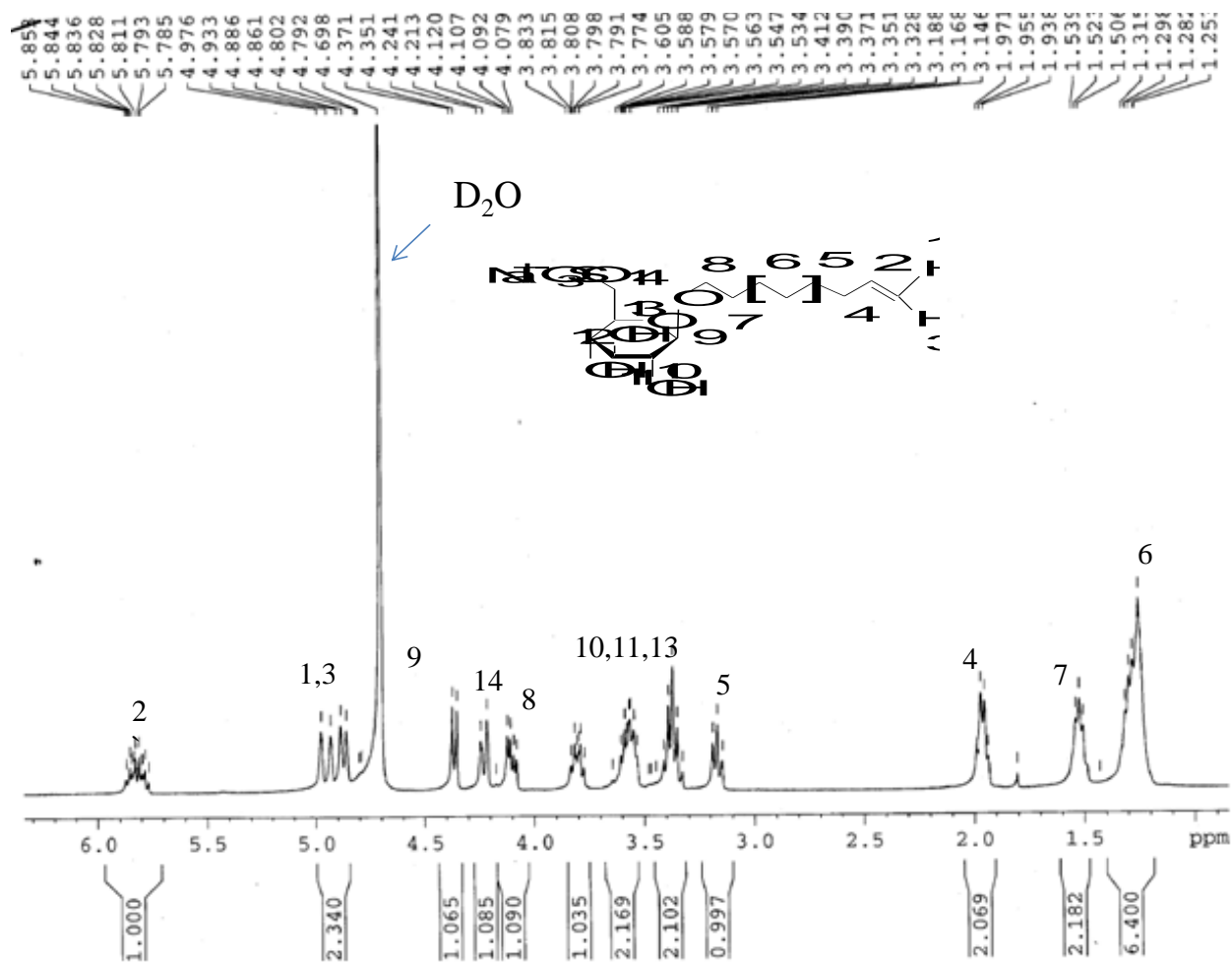


**Figure B10.**  $^1\text{H-NMR}$  of **Compound 10**, *n*-octenyl  $\beta$ -D-glucopyranoside 6-hydrogen sulfate in  $\text{D}_2\text{O}$

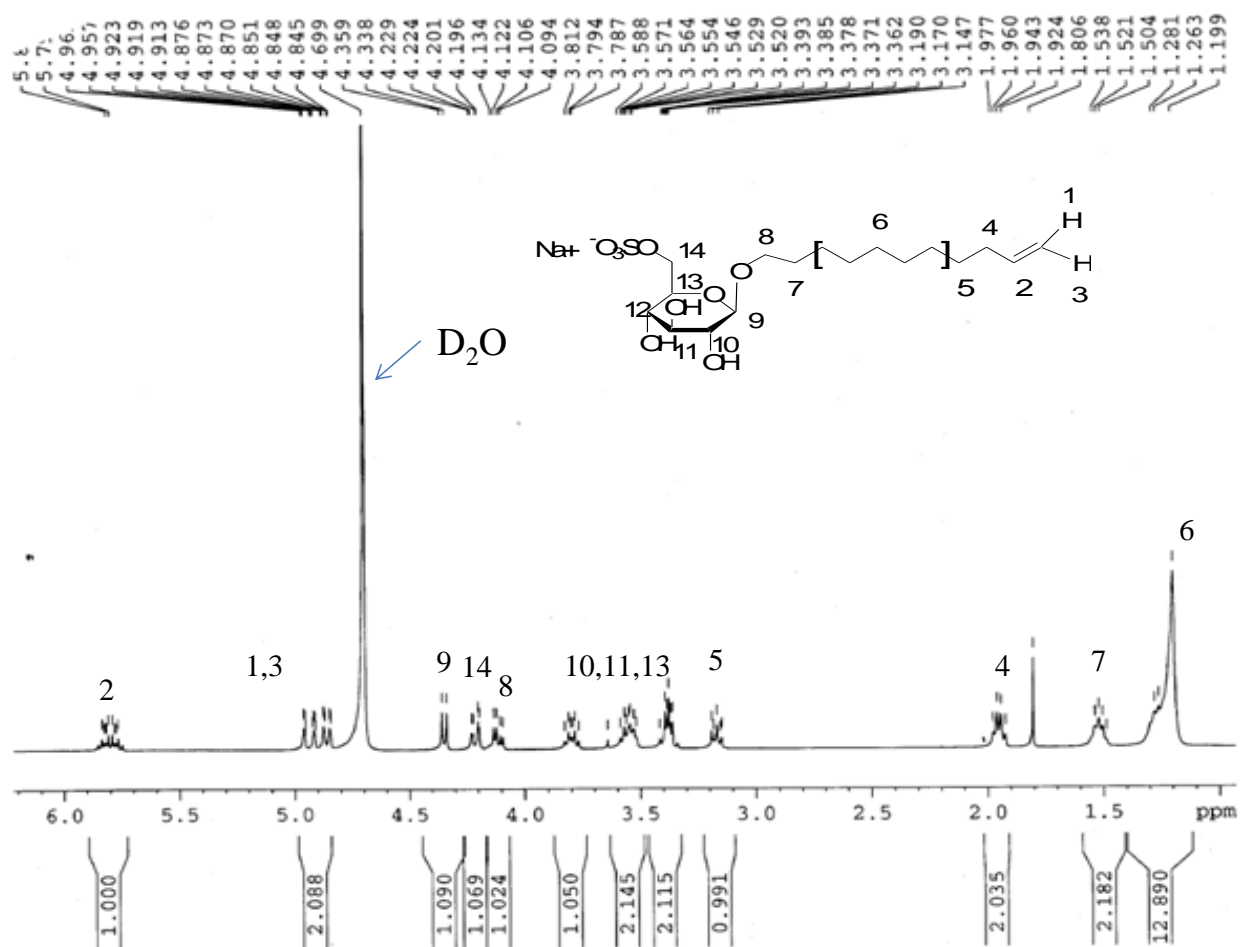




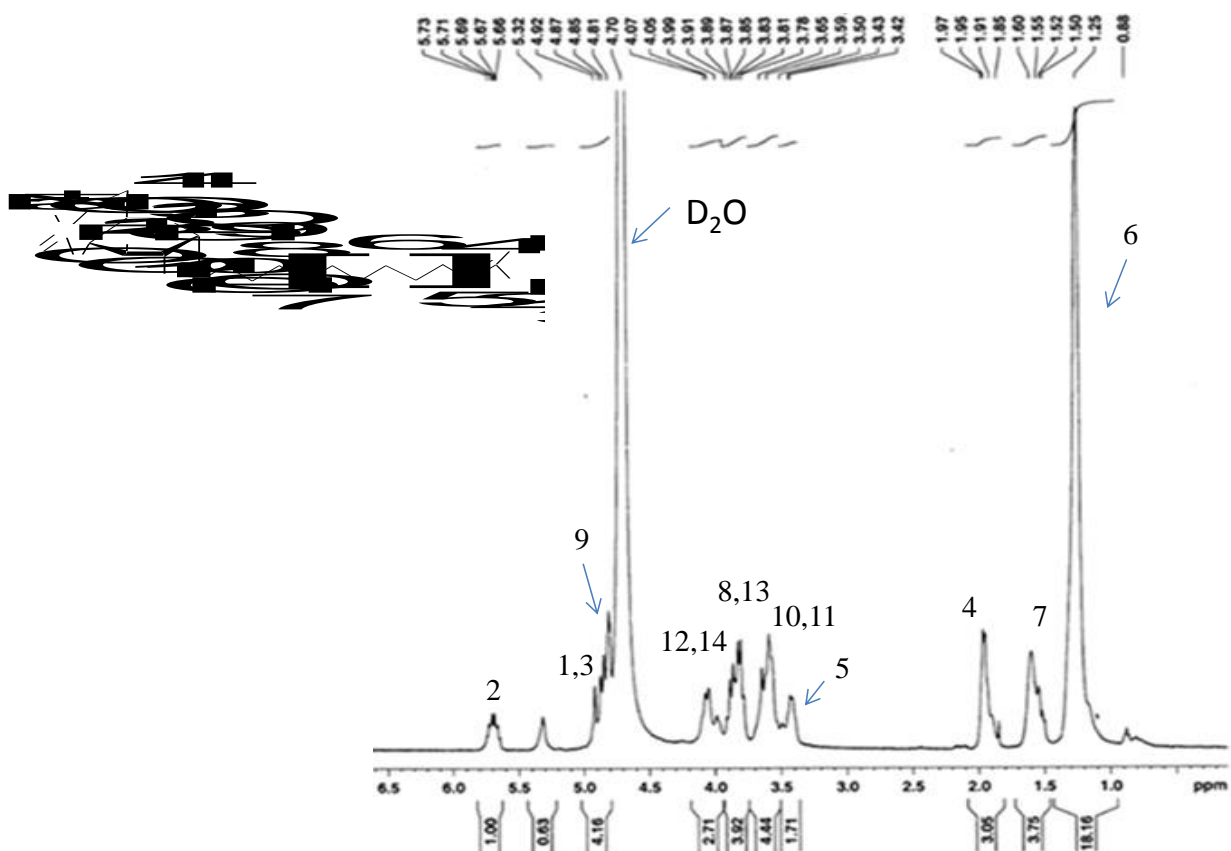
**Figure B11.**  $^1\text{H-NMR}$  of **Compound 11** *n*-undecenyl β-D-glucopyranoside 6-hydrogen sulfate in  $\text{D}_2\text{O}$



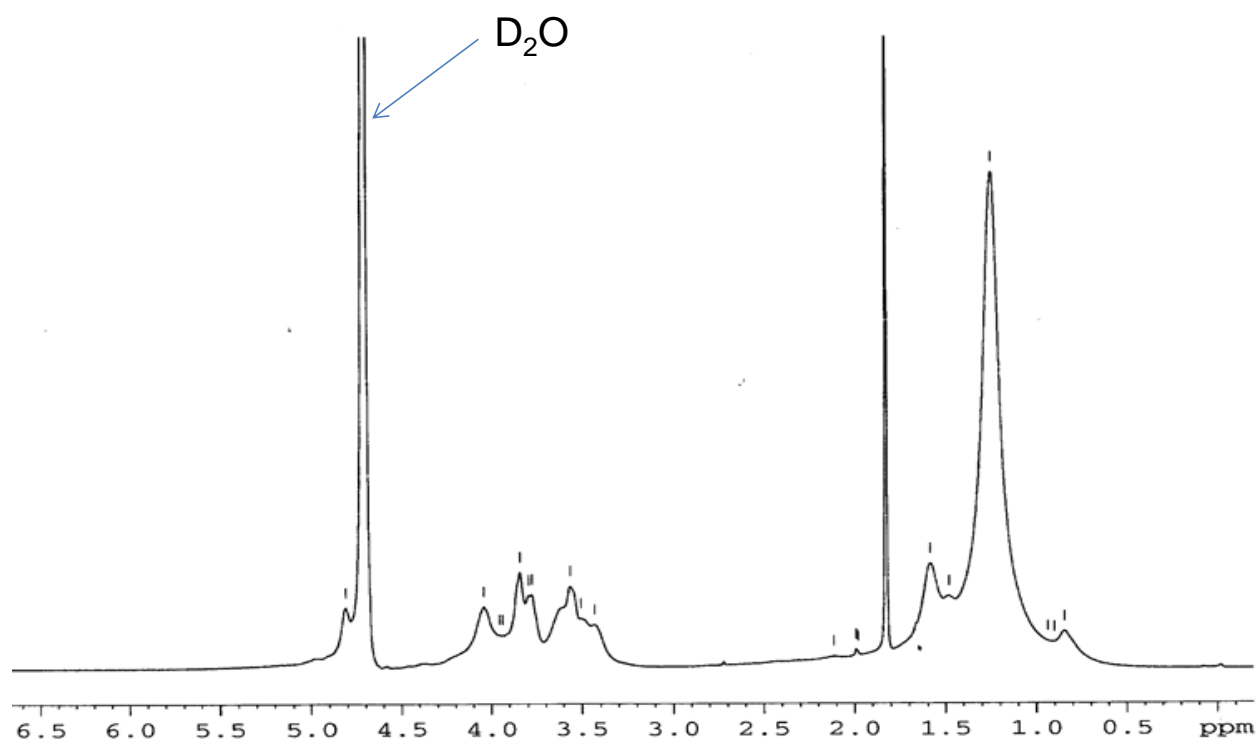
**Figure B12.**  $^1\text{H-NMR}$  of final product Compound 12, *n*-octenyl  $\beta$ -D-glucopyranoside 6-hydrogen sulfate, monosodium salt in  $\text{D}_2\text{O}$



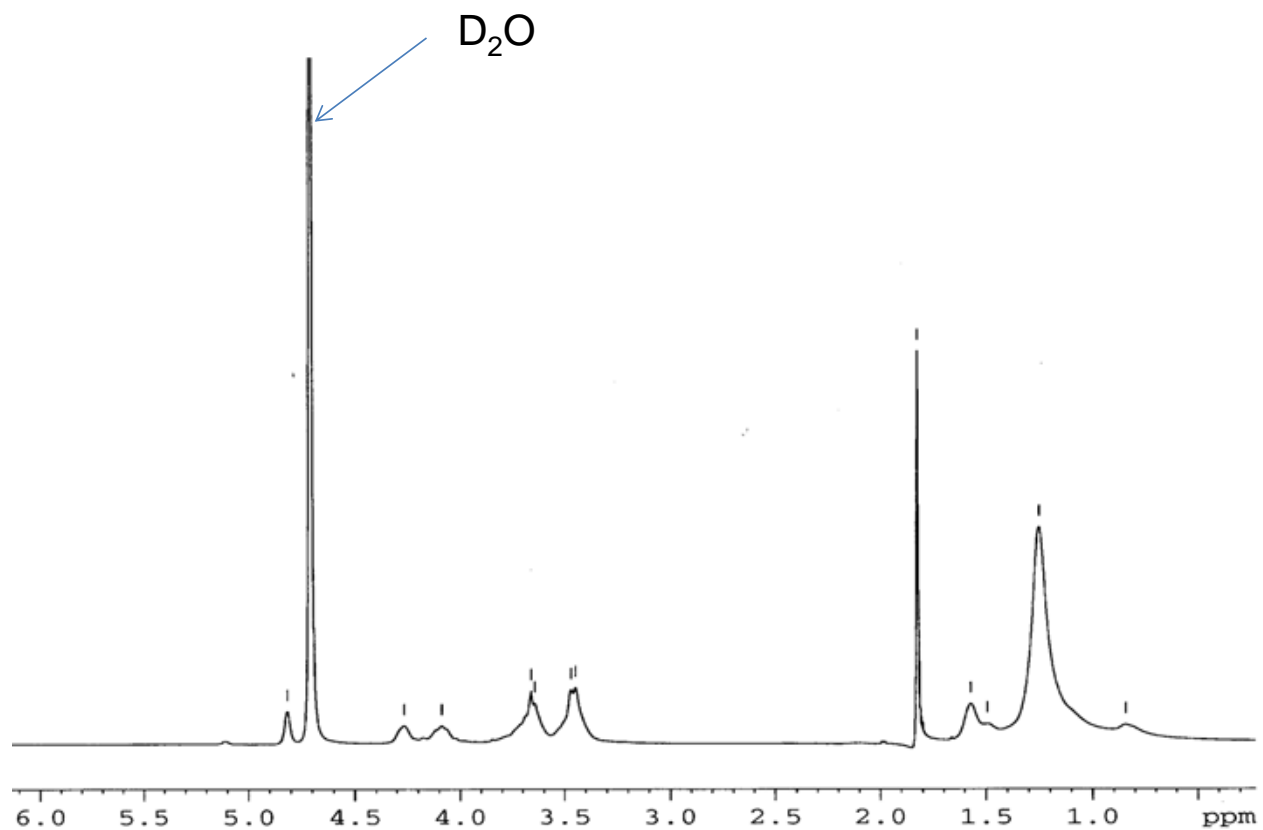
**Figure B13.**  $^1\text{H-NMR}$  of final product Compound 13,  $n$ -undecenyl  $\beta$ -D-glucopyranoside 6-hydrogen sulfate, monosodium salt in  $\text{D}_2\text{O}$



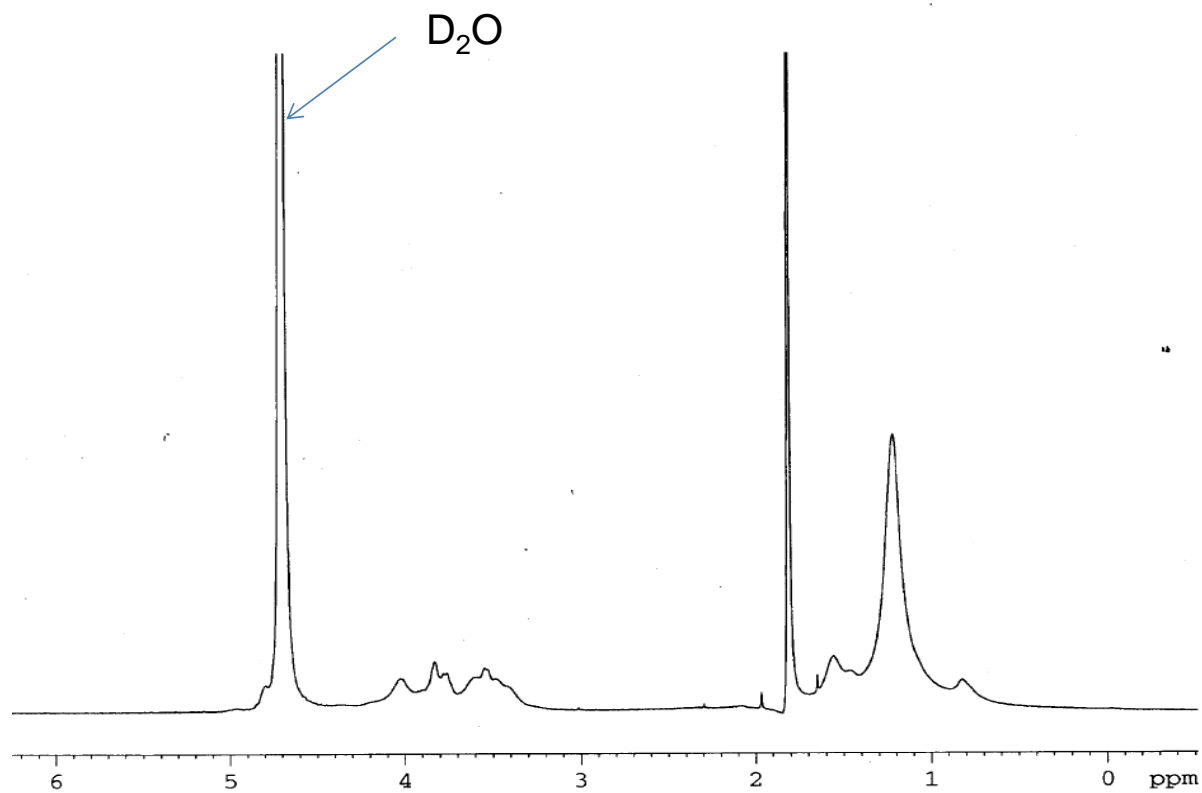
**Figure B14.**  $^1\text{H-NMR}$  of Compound 16, *n*-undecenyl  $\alpha$ -D-glucopyranoside 4,6-hydrogen phosphate, sodium salt in  $\text{D}_2\text{O}$



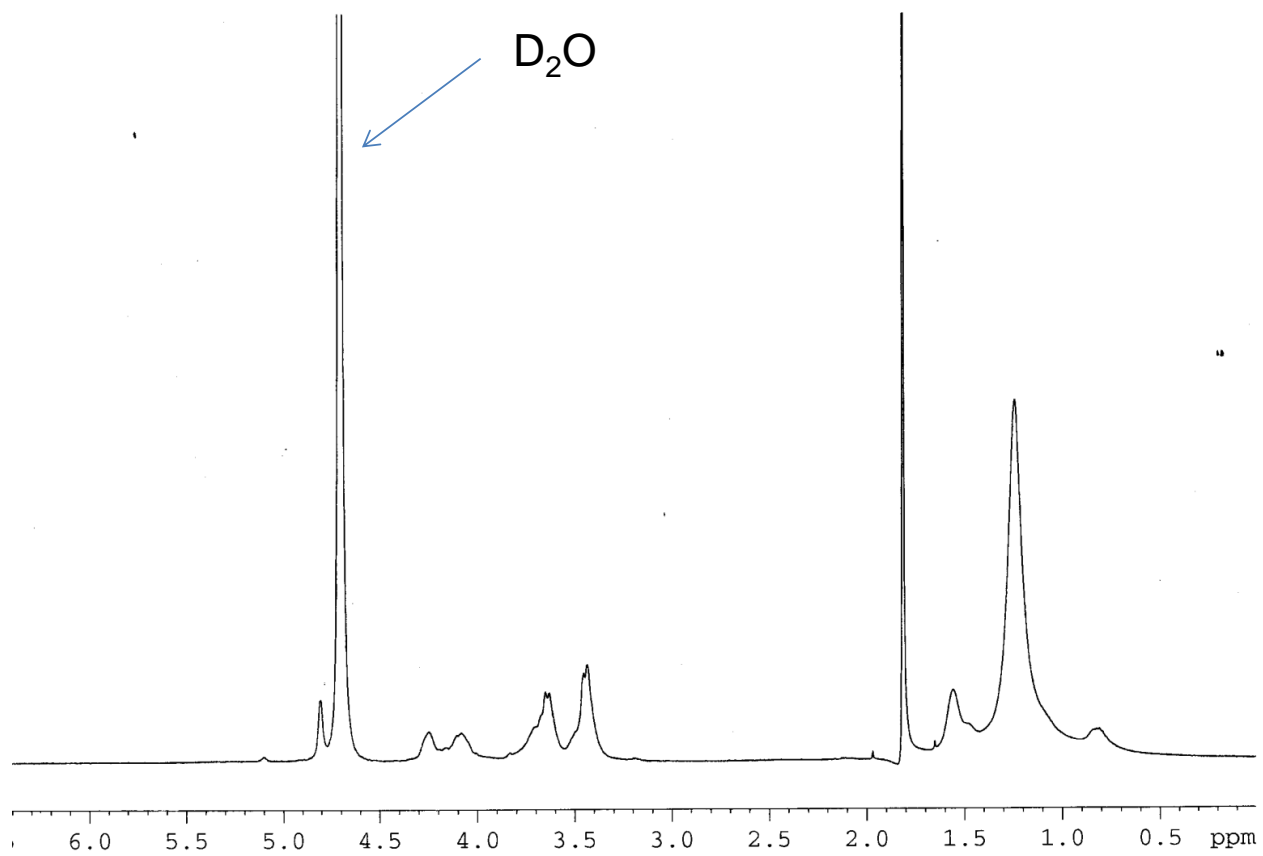
**Figure B15.**  $^1\text{H-NMR}$  of **Compound 17**, poly *n*-undecyl  $\beta$ -D-glucopyranoside 4,6-hydrogen phosphate, sodium salt in  $\text{D}_2\text{O}$



**Figure B16.**  $^1\text{H-NMR}$  of **Compound 18**, poly *n*-undecyl  $\beta$ -D-glucopyranoside 6-hydrogen sulfate, monosodium salt in  $\text{D}_2\text{O}$

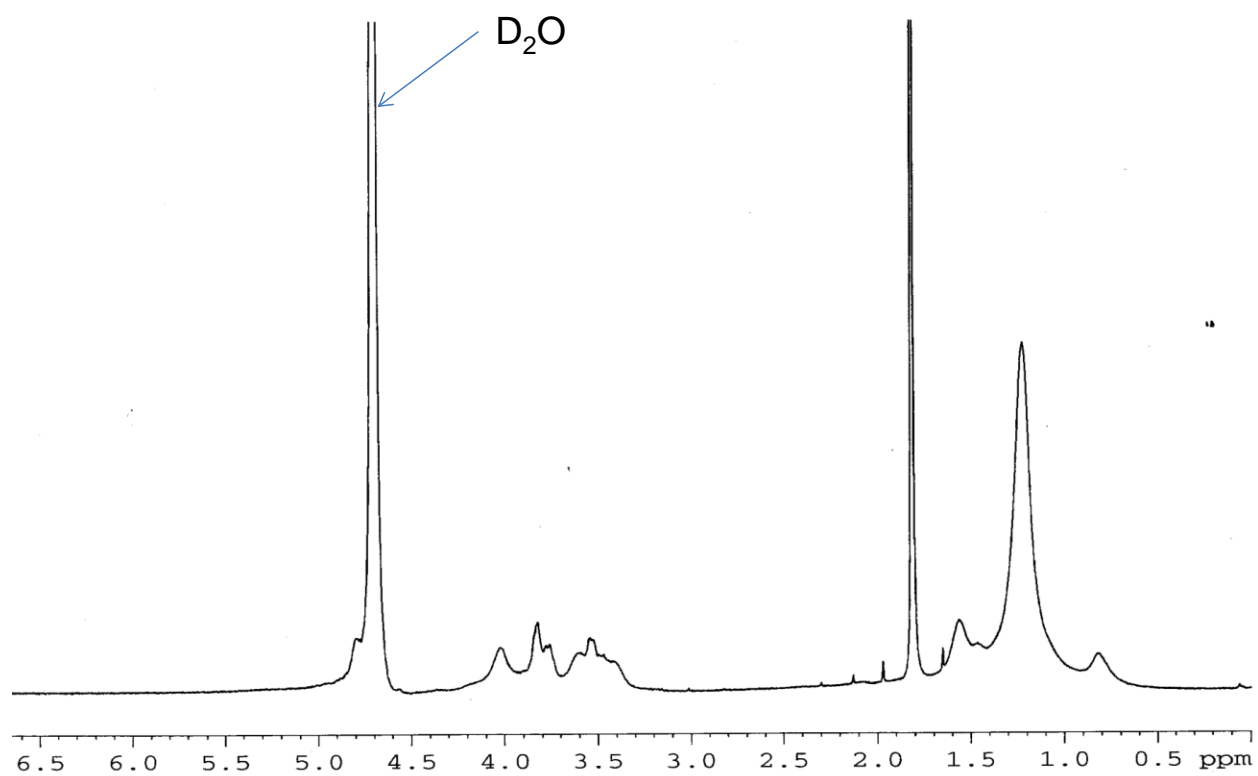


**Figure B17.**  $^1\text{H-NMR}$  of **Compound 19**, poly *n*-octyl  $\beta$ -D-glucopyranoside 4,6-hydrogen phosphate, sodium salt in  $\text{D}_2\text{O}$

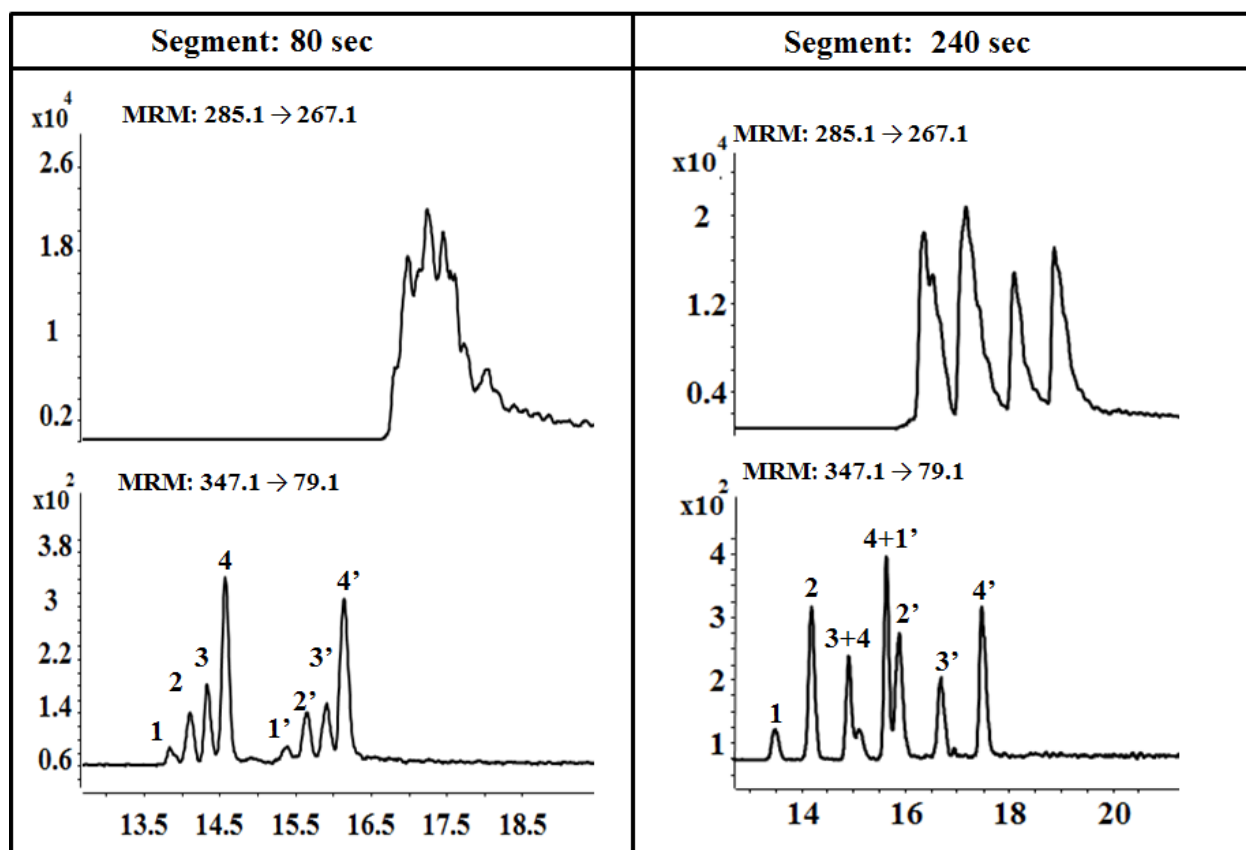


**Figure B18.**  $^1\text{H-NMR}$  of **Compound 20**, poly *n*-octyl  $\beta$ -D-glucopyranoside 6-hydrogen sulfate, monosodium salt in  $\text{D}_2\text{O}$



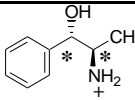
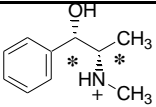
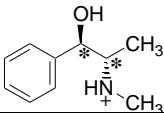
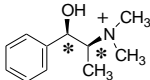
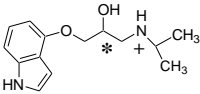
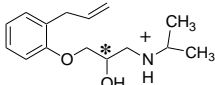
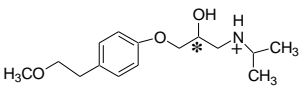
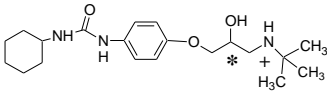
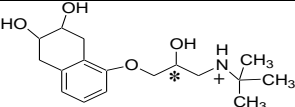
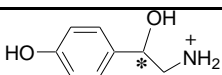
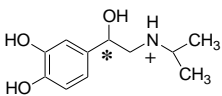
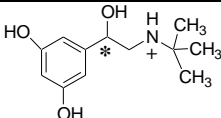
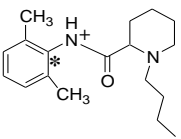
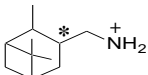
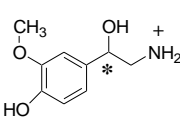


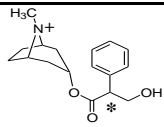
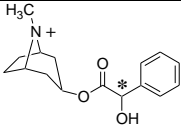
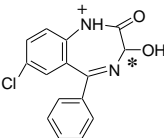
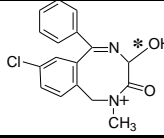
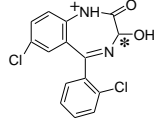
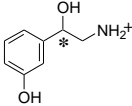
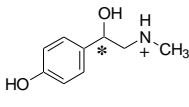
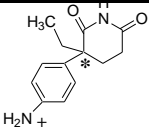
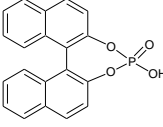
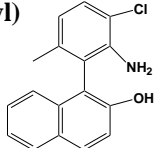
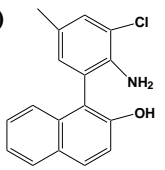
**Figure B19.**  $^1\text{H-NMR}$  of **Compound 21**, poly *n*-undecyl  $\alpha$ -D-glucopyranoside 4,6-hydrogen phosphate, sodium salt in  $\text{D}_2\text{O}$

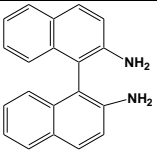
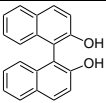
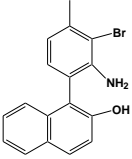
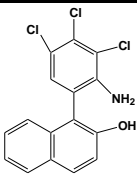
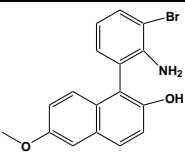


**Figure B20.** Optimization of spacer segments in Multiplexed MEKC-MS/MS

**Table B1.** Chiral separations of cationic compounds and binaphthyl derivatives

Analyte	$R_s$	$N_{avg}$	MRM transition
<b>Norephedrine</b> 	1.8	47000	152.2 → 117.0
<b>pseudoephedrine</b> 	2.4	87000	166.1 → 115.1
<b>ephedrine</b> 	1.6	46000	166.1 → 115.1
<b>methylephedrine</b> 	2.1	25000	180.2 → 147.2
<b>pindolol</b> 	0.5	6300	249.2 → 116.2
<b>alprenolol</b> 	0.5	6000	250.2 → 116.2
<b>metoprolol</b> 	0.4	3700	268.2 → 116.2
<b>talinolol</b> 	0.1	4800	364.3 → 308.3
<b>nadolol</b> 	$R_{s1}:3.5, R_{s2}: 1.8$	$N_{1avg}: 25000$ $N_{2avg}: 20000$	310.2 → 254.1
<b>octopamine</b> 	1.8	1400	154.1 → 136.1
<b>isoproterenol</b> 	2	2000	212.1 → 194.2
<b>terbutaline</b> 	2.1	2900	226.1 → 152.1
<b>bupivacaine</b> 	1.4	16000	289.2 → 140.2
<b>3-pinanemethylamine</b> 	0.3	21000	168.2 → 151.2
<b>normetanephrine</b> 	1.8	4000	184.1 → 166.1

<b>Atropine sulfate</b>				
		1.5	7200	290.2 → 124.2
<b>Homatropine</b>				
		5	1200	276.2 → 124.2
<b>Oxazepam</b>				
		0.1	1900	287.1 → 240.9
<b>temazepam</b>				
		0.3	2000	301.1 → 254.9
<b>Lorazepam</b>				
		0.7	1700	321.233.0 → 274.9
<b>Norphenylephrine</b>				
		2	1200	154.1 → 91.1
<b>Synepherine</b>				
		1.4	3300	168.1 → 77.1
<b>Aminogluthetimide</b>				
		0.3	1000	233.1 → 146.0
<b>1,1'-Binaphthyl-2,2'-diyl hydrogenphosphate</b>				
		9.4	6200	347.1 → 79.1
<b>1-(2-amino-3-chloro-6-methylphenyl)naphthalen-2-ol</b>				
		Rs <sub>1</sub> : 2.4, Rs <sub>2</sub> : 2.0	N <sub>1avg</sub> : 9000, N <sub>2avg</sub> : 19000	282.1 → 264.0
<b>1-(2-amino-3-chloro-5-methylphenyl)naphthalen-2-ol</b>				
		Rs <sub>1</sub> : 2.4, Rs <sub>2</sub> : 2.0	N <sub>1avg</sub> : 1000, N <sub>2avg</sub> : 18000	282.1 → 264.1

<b>1,1'-binaphthalene-2,2'-diamine</b> 	0.2	1200	283.1→266.1
<b>1,1'-Bi-2-naphthol</b> 	3.5	6000	285.1→267.1
<b>1-(2-amino-3-bromo-4-methylphenyl)naphthalen-2-ol</b> 	1.7	21000	326.0→308.0
<b>1-(2-amino-3,4,5-trichlorophenyl)naphthalen-2-ol</b> 	0.1	1400	336.0→318.0
<b>1-(2-amino-3-bromophenyl)-6-methoxynaphthalen-2-ol</b> 	1.9	36000	342.0→309.0